

1 **Answer to the reviewer 1 comment of NHESS-2018-319.**

2  
3 We acknowledge the reviewer for the fast and complete review of the paper. In the following we  
4 show the actions taken to improve the paper quality. The Author Replies (AR) to the Reviewer  
5 Comments (RC) are in blu.

6  
7 Before discussing in details the RCs, it's import to outline that the subject paper contained two  
8 typos. The first refers to the length scale of the background error matrix in the x and y directions  
9 that varies between 14 and 25 km and not , between 20 and 30 km, as erroneously reported in the  
10 manuscript. The second refers to the correct lightning number for each day are 82 331 for the 9  
11 September, 291 164 for the 10 September (170 000 is written into the manuscript) and 105 467 for  
12 the 16 September (60 000 written in the manuscript). Despite the typos, the results shown in the  
13 paper were obtained using the correct number of flashes and the correct length scales in the  
14 background error matrix.

15 In the first submission, we stressed the improvement given by the data assimilation at the local scale  
16 on the precipitation VSF (Very Short term Forecast, 0-3h). To highlight this point, we showed  
17 several ways to improve the forecast by the assimilation of lightning, radar data or both, as it's  
18 evident for the Serano case study, for which the radar assimilation impacted the forecast of the first  
19 phase (03-06 UTC) whereas lightning impacted the second one (18-21 UTC).

20 Notwithstanding, given the comments of reviewers 1 and 2 and the results section (Section 4)  
21 underwent a substantial rewriting. In particular, in the revised version of the paper, we deleted  
22 Section 4.1.2 (second phase of the Serano case study) and Section 4.2.1 (first case of the Livorno  
23 case study). The results of Section 4.2.1 are now shortly commented in Section 5 (Discussion and  
24 conclusions) to highlight that there is space for improvement. Following the comments of the  
25 reviewer #2, the scores of the phases commented in the paper were summarized in three tables  
26 (Tables: 4-6) for specific thresholds (1, 6, 10, 20, 30, 40 mm/3h and, for Livorno, also 50 mm/3h).  
27 This limited the number of precipitation thresholds considered but increased the readability of the  
28 paper.

29 The space gained by deleting the aforementioned sub-sections was used to extend the discussion  
30 about the adopted assimilation methodologies. In particular, we extended the section "Lightning  
31 data assimilation" to include a discussion on the useful comments raised by the reviewer 1; we  
32 extended the section "Radar data assimilation" to show an example of 3D-Var assimilation of the  
33 reflectivity factor (this should also answer to few comments of the reviewer 1).

34 Finally, we added supplemental material to the paper discussing the following two points: a) the  
35 relative contribution to the total water mass given by lightning and radar reflectivity factor data  
36 assimilation (Section S1); b) the sensitivity of the precipitation VSF to the nudging formulation  
37 (Sections S2). In addition, the supplemental material provides different plots of Figures 15-17  
38 (Section S3, as requested by reviewer 1) and the forward radar operator used in RAMS-3DVar  
39 (Section S4), as requested by the reviewer 3.

40 The important points considered in the supplemental material weren't included into the paper to  
41 avoid exceeding the length limit. However, the supplemental material is recalled in several parts of  
42 the paper to help the reader to consider it for reading.

43  
44

45 **Reviewer's preamble**

46 Summary: The authors utilize a cloud-scale functional relationship between lightning and water  
47 vapor mass mixing ratio published in the literature and applied it to a homegrown 3DVAR

48 framework at the convection-allowing scale to evaluate the analysis and short term forecast of two  
49 selected high impact weather events over Italy.

50  
51 Recommendation: reject and, eventually, re-submit.

52  
53 Main Comments:

54 While the manuscript could eventually offer some merit for this journal, I found the analysis  
55 generally very rudimentary with the authors going at length in describing in excruciating level of  
56 details individual figures/panels in a repetitive and redundant manner without distilling the content  
57 into concise arguments/hypotheses. Given its repetitive nature, the entire results section could, in  
58 fact, easily be condensed into a 2-3 pages. Most importantly, the manuscript (hereafter, m/s) lacks  
59 rigor and rationales for the set ups and methods put forth for each, respective DA approaches.  
60 Salient Major issues are itemized below.

61  
62 **RC(1).** As far as the scientific content is concerned, the core ideas and notions of this lightning  
63 data assimilation (LDA) method are conceptually similar to those from many existing studies,  
64 which fundamentally aim at promoting convective development through the introduction of latent  
65 heating within a prescribed neighborhood region/column centered at observed lightning locations.  
66 Past works from Benjamin et al. (2004), Alexander et al. (1999), Chang et al. (2001), Papadopoulos  
67 et al. (2005), Pessi and Businger (2009), have used empirical relationships between lightning-  
68 rainfall rates-latent heating or lightning- reflectivity rates-latent heating [e.g., in the HRRR].  
69 Following a similar idea, recent works such as Machand and Fuelberg (2014), Lynn et al. (2015),  
70 Lynn (2017), Fierro et al. (2012; 2014, 2015), Wang et al. (2017, 2018) proposed LDA means that  
71 essentially boost the local thermal buoyancy where lightning is observed. A very limited portion of  
72 these techniques, however, offer alternative approaches to address spurious convection (i.e.,  
73 removal) – which is a far more challenging problem to tackle. For completeness and given the  
74 relatively limited advances in LDA relative to radar DA, the authors should do a better job in  
75 discussing and including all the aforementioned references in their text. I was in fact astonished to  
76 notice that the integrity of the Results section in section 4 is completely devoid of references to  
77 previous works.

78 In particular, since they opted to borrow an LDA method from one of these investigators,  
79 comparisons with their study should be performed more systematically throughout the m/s. For  
80 instance, the works of Federico et al. 2017b is invoked when referring to multi-day forecast  
81 statistics using the Fierro et al. method without mentioning that, such a study, was already  
82 conducted by the same author over a larger domain and using nearly three times more forecast  
83 days/cases (Fierro et al. 2015 study). Given this omission, their study (Federico et al. 2017b)  
84 inadequately state that such multi-day statistics for this LDA have never been conducted. In a  
85 similar manner, it is of relevance to underline whenever appropriate that, in this work: (i) radial  
86 velocity is not included (specify why), (ii) only cloud-to-ground lightning data are considered and  
87 (iii) spurious convection is not addressed. In the light of (i) and (ii), one of the recent studies they  
88 cite (Fierro et al. 2016) not only assimilated level II radar data (radial velocity + reflectivity factor)  
89 but used total lightning data. This needs to be clearly stated, for completeness (Cf comment 3 below  
90 for rationales).

91  
92 **AR:** In the revised version of the paper we extended the discussion of the LDA in the introduction,  
93 in the data and method section and in the discussion of the results in order to include most of the  
94 mentioned references. The problem caused by the missed reference in Federico et al. (2017b) study  
95 was corrected in the reviewed manuscript.

96 Regarding the specific comment (i): it's worth mentioning that we are working on the assimilation  
97 of the radial velocity but the operator is not yet implemented in the 3D-Var. Besides, while the  
98 reflectivity factor measured by the radar network is operationally available, the radial velocity is not

99 operationally processed. Currently, it needs further research to manage some issues (complex  
100 orography, scan strategies optimized for rainfall estimation). For these reasons, we focused on the  
101 assimilation of the reflectivity factor. These motivations are discussed in the revised version of the  
102 paper in Section 3.3 by writing:

103  
104 “Radial velocity is not assimilated within the RAMS@ISAC model because it is not operationally  
105 processed, the scan strategy being optimized for QPE purposes. Furthermore, the implementation of  
106 a radial velocity data assimilation scheme is under development in RAMS-3DVAR and it is not  
107 currently available for testing. For these reasons, we didn’t consider the assimilation of this  
108 parameter.”

109  
110 Regarding point (ii) in the paper we wrote that total lightning is assimilated, not only CG. For the  
111 events analyzed in the paper the fraction of IC strokes to the total number of strokes detected by  
112 LINET is about 30% (22% on 09 September, 30% on 10 September and 35% on 16 November).  
113 There are cases when the IC strokes recorded by LINET are more than 50% of the total number of  
114 strokes over Italy. In general, the Section on LDA has been extended to consider this point and  
115 others; (iii) The spurious convection is not considered by the LDA but it is considered in the  
116 assimilation of radar reflectivity factor. We specified better this point in the revised version of the  
117 paper, but the comment is already present in the first submitted version.

118  
119 **RC (2).** In term of DA methodology, I found one major drawback, which is never discussed, nor  
120 evaluated. Given that both the LDA and their “RAD” experiment make adjustments to the relative  
121 humidity (RH) field, it is expected that both techniques will overlap in their adjustments over all the  
122 (many) grid points characterized by observed lightning flash rates exceeding zero. This is because  
123 changing RH is equivalent to adjusting Qv as  $RH \sim Qv/Qv\_saturation$ . A more self-consistent DA  
124 approach would adjust the pseudo- observations for the Qv or RH field in a manner that eliminates  
125 any possibility of overlap during the minimization. Toward that end, the authors should include  
126 soundings and/or horizontal cross sections of RH/Qv that shows, quantitatively, how the RH field is  
127 adjusted by each respective DA approach (radar vs lightning).

128  
129 Second, given that lightning is a cloud-scale observation, I cannot find any justifications for not  
130 conducting the 3DVAR analysis on the innermost, higher resolution domain. Instead, the method  
131 minimizes the cost function on the intermediate domain and, later, projects the innovations on the  
132 coarser-scale domain. This needs to be addressed.

133  
134 **AR:** First: we added a complete new section (Section S1 of the supplemental material) to address  
135 this point. In this section, we show the evolution of the accumulated precipitation and total water  
136 mass in the atmosphere (i.e. water vapour mass+mass of hydrometeors) as a function of time  
137 (including the spin-up period).

138

139 **Second:**

140 Data assimilation is not performed on domain D3 (R1) because the use of this domain is  
141 exceptional and we don’t have background error statistics for this grid.

142 The background error statistics for the domain D2 is computed by the NMC method, which, for this  
143 paper, is based on HyMeX-SOP1 simulations. The Appendix A and B of Federico (2013) show the  
144 details of the application of the method, which requires a large number of simulations (see Barker et

145 al., 2004 for the general discussion). These simulations are not available for the innermost grid of  
146 the Livorno case, which was introduced to better resolve the precipitation at the local scale and to  
147 show how precise can be the impact of lightning and radar data assimilation on the VSF. These  
148 motivations have been clarified in the revised version of the paper.

149 It is worth specifying that this limitation refers only to the assimilation of the radar reflectivity  
150 factor because flashes are assimilated by nudging. Nevertheless, we could not compare simulations  
151 with or without data assimilation for a specific domain assimilating lightning in the innermost  
152 domain and for this reason we assimilated flashes over the D2 only.

153 In the revised version of the paper, we specified better the role of the domain D3 and the reason for  
154 not assimilating lightning and radar reflectivity factor over the domain D3.

155 It is specified in section 3.1 (RAMS@ISAC and simulations set-up) as follows:

156 “The third domain covers the Tuscany Region, has 4/3 km horizontal resolution (R1), and it is used  
157 for Livorno to represent with higher spatial detail the precipitation field over Tuscany. The fine  
158 structures of the precipitation field are smeared out over Tuscany using only domains D1 and D2.  
159 The operational implementation of the RAMS@ISAC model uses the domains D1 and D2 and no  
160 refinements for specific areas of Italy are used because Italy is a complex orography country and  
161 grid refinements for a specific event can be done only a-posteriori, i.e. after the occurrence of the  
162 event.”

163

164 And few lines below:

165

166 “It is noted that data assimilation is performed over the domain D2 (R4) only, and the innovations  
167 are transferred to domain D3 (R1), for the Livorno case, by the two way-nesting. The domain D3 is  
168 used for the Livorno case to refine the resolution of the precipitation field over Tuscany and to  
169 show the spatial and temporal precision of the precipitation forecast over Tuscany using data  
170 assimilation. However, its usage is exceptional because, as stated above, Italy is a complex  
171 orography country and grid refinements over specific areas are used only after the occurrence of an  
172 event. For these reasons the domain D3 is usually not used in RAMS@ISAC and statistics about the  
173 background error aren’t available for this grid. The background error in RAMS-3DVar is computed  
174 by the NMC method (Parrish and Derber, 1992), which requires a number of simulations (at least  
175 two-weeks) verifying at the same time but starting with a lag of 12 h. These simulations are not  
176 performed in this paper and background error statistics for the domain D3 are not available.

177 Being lightning assimilated by nudging, they could be assimilated over the domain D3.  
178 Nevertheless, to preserve the rationale of the paper, i.e. comparing simulations with or without data  
179 assimilation for specific domains, we didn’t assimilate lightning over the domain D3.

180 Because lightning and radar cloud scale observations, their assimilation at higher horizontal  
181 resolution is foreseeable in future works.”

182

183 RC Third, the radius of influence/decorrelation length scale chosen for radar reflectivity factor (50  
184 km) is far too large for convective scale applications and would incur unrealistically large amount

185 of Qv mass added into the domain – which will undoubtedly yield to spin-up issues and the  
186 generation of convective-scale gravity waves that will degrade longer term ( $\geq 3$ h) solutions  
187 (please provide plot of perturbation pressure in your response). In that regard, the authors should  
188 indicate and contrast the total amount of Qv mass added by RAD and LIGHT.

189  
190 AR: The 50 km length is not a distance to spread the innovation introduced by the radar reflectivity  
191 factor data assimilation. It represents a search radius to compute the pseudo-profile of relative  
192 humidity used in 3D-Var. A discussion about this point was introduced in the new section on radar  
193 reflectivity factor data assimilation (Section 3.3).

194 In particular, we wrote:

195  
196 “It is important to point out that the 50 km length-scale of the above step doesn’t  
197 represent the horizontal correlation length-scale of the background error, which  
198 determines the horizontal spread of the innovations in the 3D-Var data assimilation (the  
199 latter length-scale is between 14 and 25 km depending on the level). The 50 km length-  
200 scale is used to set a square for computing the pseudo-profile of relative humidity (Eqn.  
201 (2)). This profile is given by a weighted average whose weights are determined by the  
202 agreement between the simulated and observed reflectivity factor. The larger the  
203 agreement the larger the weight. This distance seems appropriate because the spatial  
204 error of meteorological models in simulating meteorological features, for example fronts,  
205 can be of this order. The control simulation for the two events considered in this paper  
206 confirms this choice.”

207  
208 **RC (3).** In the context of forecast improvements, the Qv-based method they borrowed/adapted was  
209 scaled for total lightning data ( $> 50\%$  detection efficiency of intra-cloud [IC] flashes). I was  
210 surprised to find that absolutely no information on the detection efficiency and geolocation  
211 accuracy of the lightning network used (LINET) is provided in the text [no figures either]. Given  
212 the large area covered by this study, it is thus very likely that the geolocation accuracy of this  
213 network remains very poor for low amplitude flashes and for all flashes over oceanic regions. Given  
214 the low sferics amplitudes of IC flashes, the VLF portion of the sensor will miss nearly all these  
215 flashes, while the VHF portion only is able to detect some of the IC flashes within a few tens of  
216 kilometers away from the station [e.g., Rison, MacGorman works]. Thus, it is relevant to state and  
217 underscore that LINET only detects a very small portions of the total IC flashes in the study domain  
218 (likely  $< 5\%$ ). Motivation for scaling the F12 method for IC flashes (in lieu of cloud-to-ground  
219 [CG] flashes), lies in the well-documented finding that, in contrast to CGs, ICs are well correlated  
220 with thunderstorm kinematic and microphysical evolution (updraft strength, updraft volume,  
221 graupel mass etc, see Wiens et al. 2005, Schultz et al. 2011 among many others). CGs, on the other  
222 hand, were found to be correlated with the descent of reflectivity cores and the onset of the demise  
223 of the storm’s updraft core [MacGorman and Nielsen 1991, MacGorman et al. 1989, Rutledge and  
224 Lang’s seminal works etc]. Not surprisingly, ICs were found to lag CG by an average of 15 min  
225 [see one of the recent MacGorman study]. Moreover, Boccippio et al. 2001 and Medici et al. 2017  
226 found that in deep continental convection, IC flashes always outnumber CGs by a ratio sometime  
227 exceeding 10:1. Based on these facts, it becomes clear why the Fierro method emphasized the use  
228 of IC flashes [or total lightning] for their application. Further motivation arises from the recent  
229 successful launches of the GLM instrument aboard GEOS-16/17, which will provide continuous  
230 day/night coverage of total lightning at  $\sim 90\%$  detection efficiency (DE) over a large domain  
231 covering the Americas (Gurka et al. 2006; Goodman et al. 2012, 2013, Rudlosky et al. 2018). Note  
232 that GLM will provide flash extent information of lightning, while the metric derived from the  
233 (limited) point flash data in this study can only provide a very rough surrogate for CG flash location  
234 density at best. Similar space-borne technology to detect lightning have been developed by China  
235 (Feng-Yun-4, yang et al. 2016) with these data being assimilated in recent works by Wang et al.

236 (2017, 2018) – which were never referenced either. Apart from their propensity to detect total  
237 lightning at a high DE, the chief advantage of this technology lies in its ability to retrieve lightning  
238 over remote oceanic regions.

239  
240  
241 AR. LINET has been started and used operationally since 2004. Since then, more than 100  
242 publications provided evidence about both DE and location accuracy (LA). In particular, since the  
243 beginning in 2004 LINET exhibited a statistical average location accuracy of some 100 m. Because a  
244 minimum of 5 sensor reports are exploited for each stroke solution, the LA does not deteriorate  
245 within several 100 km from a sensor. Thus, the LA is excellent all over the present study region.

246 LINET Europe comprises more than 200 sensors and provides more extensive stroke data than any  
247 other VLF/LF system in the region.

248 LINET detects and records stroke signals down to currents of a few kA (CG normalization). This is  
249 the reason why LINET ranges are large enough to exploit  $\geq 5$  sensors for geolocation without  
250 reducing the typical baselines of 250-300 km. The resulting DE is good enough to detect any CG.  
251 Over the Mediterranean the stroke DE diminishes due to larger baselines. However, the flash  
252 detection is less sensitive because of the stronger strokes that characterize a flash.

253 Like any other VLF/LF system signals are recorded whether CG or IC. Thus, the detected IC portion  
254 is certainly not lower than in any other VLF/LF system. As a consequence, total lightning is  
255 reported at least as efficient than in any other VLF/LF system, and will be beneficial for the  
256 purposes in the present paper.

257 IC discrimination of LINET is based on TOA analysis. The advantage is a unique discrimination when  
258 the detection geometry is within certain ranges; the disadvantage is decreasing discrimination  
259 power when the distance to the closest sensor become too large, because of too small TOA  
260 differences between CG and IC at the same 2D location. Thus, over water far from land the  
261 identified IC fraction decreases, though total lightning counts remain relevant.

262 It is true that leader steps signify discharge processes (see, e.g., well-known LMA results).  
263 However, it is well-proven that VLF/LF detects pulses from IC activity that are very similar to CG  
264 strokes; this is why CG-IC discrimination is very challenging for VLF/LF systems. We think, though,  
265 that any VHF issue is not relevant here, because there is no large-scale VHF system that covers  
266 Italy and the surrounding sea with baselines of a few 10 km.

267 Observations from global networks or satellites may be a point of future concern, but do not  
268 represent any focus in the present paper; also, IC discrimination is either not yet possible or poor.  
269 It may be mentioned that GLM lightning data is not yet an issue; interestingly, Eumetsat/NASA on  
270 behalf of NOAA have selected LINET to carry out the first evaluation of the new lightning data  
271 source. This has been communicated in Science Team Meetings and conferences (see GLM Cal/Val  
272 2017 Ground Validation Field Campaign 2017).

273 The discussion about the LINET network has been extended in the revised version of the paper.

274  
275 RC (4) The following key information pertaining to the respective DA methods are missing/never  
276 discussed:

277 (a) What are the background/observation errors for reflectivity/lightning? (b) What statistics are  
278 used for model error?

279 AR. Lightnings are assimilated by nudging and no error is associated with them. The error matrix  
280 for model error has been clarified in the section on the radar reflectivity factor data assimilation  
281 (Section 3.3).  
282

283 RC (c) How is the adjoint for the lightning data assimilation operator derived?

284 AR. The derivation of the adjoint of lightning data assimilation was performed using two case  
285 studies of the HyMeX-SOP1 (unpublished work) as commented in Federico et al., (2017a). We  
286 commented about this point in the new section on lightning data assimilation. Also, the  
287 supplemental material (Section S2) shows the sensitivity of the rainfall VSF scores (POD and ETS)  
288 to the nudging formulation.  
289

290 RC (d) What assumptions are made for grid points with zero lightning or zero reflectivity  
291 observations ? Does the radar DA or LDA treat those as missing observations or equate those to the  
292 background values to reduce spread ?

293 AR. Lightning are assimilated by nudging and this comment doesn't apply. In the case of radar, grid  
294 points with zero reflectivity factor and zero simulated reflectivity factor are assumed missing  
295 observation, and the innovations can spread according to the background error matrix. This has  
296 been clarified in the revised version of the paper (Section 3.3).  
297

298 RC (e) What Gaussian decorrelation length scales are assumed for each observation? Please  
299 specify/justify/explain. How would the selection of a given length scale value, influence the results  
300 ?

301 AR. The observation error matrix for radar reflectivity is diagonal (this was already stated in the  
302 first submission of the paper). We acknowledge that the sensitivity tests proposed by the reviewer  
303 are interesting, nevertheless they are left for future studies. The importance of this point is discussed  
304 shortly in the revised version of the paper. We wrote:

305  
306 "The observation error matrix  $R$  in Eqn. (4) is diagonal and observations' errors are uncorrelated.  
307 This choice is partially justified by under sampling the radar reflectivity factor observation by  
308 choosing one point every five grid points in both horizontal directions of the radar observations  
309 Cartesian grid (Rohn et al., 2001). However, correlation observations errors have significant impact  
310 on the final analysis, as shown for example in Stewart et al. (2013), and different choices of the  
311 matrix  $R$  will be considered in future studies.  
312 The value of the elements on the diagonal of  $R$  depends on the vertical level and are  $1/4$  of the  
313 diagonal element of the  $B_z$  matrix at the corresponding height. By this choice, we give more credit  
314 to the observations than to the background and analyses strongly adjust the background towards  
315 observations."  
316

317 RC (f) Is spurious convection addresses by either DA method ? Please elaborate.

318 AR. Yes, in the radar reflectivity factor data assimilation, but not in lightning data assimilation. The  
319 point is already present in the discussion paper, but it has been clarified in the revised version of the  
320 paper in the section dedicated to the radar data assimilation (Section 3.3).  
321

322 RC (g) Does the variational minimization set use a multi-scale approach ? If yes, what influence  
323 radii are chosen and how many cycles ?

324 AR. We don't use the multi-scale approach. This has been clarified in the paper in the section  
325 dedicated to the radar data assimilation (Section 3.3).  
326

327 RC (5) Why did the authors not include the fractions skill score FSS as the main evaluation metric  
328 for their forecast? Several works have posited that, in contrast to ETS, FSS does not penalize

329 displacement errors as much and, arguably, FSS offers a more accurate measure of skill on  
330 convection-allowing grids (Mittermaier et al. 2013).

331 Additionally, more recent studies evaluating forecast performance have been making usage of the  
332 so-called performance diagrams, which conveniently merge several key contingency table elements  
333 into one single diagram (Roebber 2009). The authors should show such diagrams to provide a more  
334 complete and succinct view of the overall forecast performance of the case they selected.

335  
336 AR. Considering POD and ETS gives the possibility to show the many facets of a forecast, and this  
337 is important. These scores are also widely used in the bibliography and this make the results of this  
338 paper comparable with other papers. We, of course, acknowledge that there are other interesting  
339 measurements of the model performance, as FSS, that could be considered. Taking into  
340 consideration this comment and the comment of the reviewer 2 about the score we propose the  
341 following solution: we consider three neighborhood radii to take into account for displacement  
342 errors; nearest neighborhood (as in the first submission), 25 km and 50 km. We put the scores in  
343 three tables (Tables 4-6 of the revised paper) following a remark of the second reviewer.

344  
345 RC (6) The case studies selected are cherry-picked given the confession that CTRL generally failed  
346 to provide reasonable forecast estimates of precipitation for both cases herein. For good measure,  
347 fairness and to better underscore the performance of the DA method, the authors should show the  
348 results for one case in which CTRL did not perform well and contrast it to one case where CTRL  
349 did preform reasonably well.

350  
351 AR. The events were selected because they were missed by several forecasts and, for this reason,  
352 they are challenging. Moreover, they had important consequences because nine people died and  
353 damage to properties was extensive. We stressed this point in the introduction by writing:

354  
355 “The forecast of severe events at the local scale still remains a challenge because of the multitude  
356 of physical processes involved over a wide range of scales (Stensrud et al., 2009). The Serano case,  
357 being localized in space, poses challenges in forecasting the exact position and timing of  
358 convection initiation; the Livorno event involves the interaction between a high impact storm with  
359 the complex orography of Italy, which is difficult to simulate at the local scale. For the above  
360 reasons the forecast of both events was challenging, as confirmed by the poor forecast of  
361 RAMS@ISAC. The difficulty to forecast timely and accurately the precipitation fields of the two  
362 events is the reason for choosing them as test cases.”

363  
364 RC (7) The authors omit to mention that the degradation of the forecast at  $\geq 3$ h is mainly due to  
365 saturation of the model solution by errors and biases within the initial / boundary conditions derived  
366 from large scale models or re-analysis datasets. This needs to be shown for both cases, especially  
367 given the unrealistically large (50 km) decorrelation length scale used for radar reflectivity factor.

368  
369 AR. Agreed, we considered this point in the revised version of the paper. However, the model  
370 errors play also a role in the degradation of the forecast in addition to IC/BC. Again 50 km is not  
371 the decorrelation length scale for radar reflectivity factor.

372 Section 5 (Discussion and Conclusions) was updated by adding the following statements:

373 “Another important point to study is how long the innovations introduced by data assimilation  
374 lasts in the model forecast. While in this study we consider the VSF at 3h, future studies must  
375 explore longer time ranges. This kind of study was performed for lightning data assimilation  
376 (Fierro et al., 2015; Federico et al., 2017b; Lynn et al. 2015 among others) and for radar data  
377 assimilation (Hu et al. 2006; Jones et al. 2014, among others), using a rationale similar to that used  
378 in this paper.



379 In general, the performance of the forecast and the impact of lightning and radar data assimilation  
380 decrease with forecasting time because of the propagation of boundary conditions inside the  
381 domain and because of model errors. Improving the data assimilation system also contributes to a  
382 longer resilience of model performance. The studies cited above showed that lightning and radar  
383 data assimilation can have an impact up to 24h depending on several factors (model, data  
384 assimilation, quality of the data, meteorological conditions, initial and boundary conditions).  
385 A study considering both radar reflectivity factor and lightning should be performed to understand  
386 the resilience of the innovations introduced by data assimilation. ”

387  
388 RC (8) Title: Revise to include that: (i) primarily CG flashes are assimilated and (2) the model  
389 vehicle is RAMS.

390  
391 AR. We included in the title that RAMS@ISAC is the model vehicle. As stated above, the IC  
392 flashes for the case studies considered in this paper is about 30%, which is not a small fraction of  
393 the total lightning. The discussion on the method assimilating lightning has been widened to  
394 consider this and other points. Considering the comments of the reviewer 3 we decided to include  
395 the word “preliminary” to the paper title. The new title is:

397 **“Preliminary results of the impact of lightning and radar data assimilation on the very short**  
398 **term rainfall forecasts of RAMS@ISAC: application to two case studies in Italy”**

399  
400 RC Because these issues are collectively substantial and would require thorough rewriting of the  
401 manuscript in many places, I opted not to dwell on editorial comments for the time being.  
402 Additionally, the level of English remains, in my view, unacceptable for publication.

403  
404 AR. We revised the English of the paper, also according to the comments of the reviewer 2 in the  
405 PDF file. The copy-editing service of the journal will also improve the quality of the English.

406  
407 RC Figures:

408 Figures 5, 6, 8, 12a, 13a, 14a, 15a, 16a, 17a, 18a: The use of colored dots makes it very difficult to  
409 effectively compare the observations with those of the simulations: For consistency, either both sets  
410 of plots should show colored dots or shaded contours. For lightning, the authors should effectively  
411 show the gridded lightning data that were used to create the Qv or RH pseudo-observations.

412  
413 AR. Agreed. It is always difficult to choose the right representation of the precipitation field when  
414 comparing model output with raingauges. We acknowledge that the solution suggested by the  
415 reviewer is a good one, however we also like our representation because: a) rainfall at the  
416 raingauges is not interpolated, avoiding errors introduced by the interpolation process; b) the  
417 rainfall predicted by the model shown as a field gives the possibility to see the behavior of the  
418 model also in parts uncovered by raingauges. We propose the following solution: a) redrawing the  
419 RAMS@ISAC rainfall field changing the colorbar to match exactly the raingauges colorbar; b)  
420 adding the representation suggested by the reviewer as supplemental material to the paper  
421 (Figures S3-S5 of the supplemental material); c) recalling the supplemental material when  
422 discussing the second VSF of Livorno to highlight the wet frequency bias when assimilating radar  
423 reflectivity factor (see Figure S5 of the supplemental material).

424 Ok for the Figures about lightning. They have been redrawn according to the reviewer remark.

425

426

427 RC Additional comments:

428 General comment: What is the main rationale for using a model that is marginally known by the  
429 community (RAMS) versus a more commonly used, battle tested, publicly available model such as  
430 WRF-ARW ? The authors not only seem to re-invent the wheel here but render any potential future  
431 work dedicated to reproducibility of the results - to the least - very challenging.

432  
433 AR. RAMS@ISAC is used/maintained/developed at ISAC-CNR since several years (and it is also  
434 operational over Italy since 2000, in different versions/adaptations etc), and it is important for us to  
435 test our tool for challenging cases, as those considered in this work.

436 Also, we are WRF users too (see, for example, Avolio and Federico, 2018) and for the cases of this  
437 paper no substantial differences were found for the performance of WRF and RAMS@ISAC  
438 models (using the same initial and dynamic boundary conditions). The performance of the WRF  
439 model for the Livorno case is shown, for example, in Ricciardelli et al. (2018). The reviewer can  
440 verify that the comments given in this paper about the performance of RAMS@ISAC for the most  
441 intense phase of the Livorno case can also be applied to the WRF model (see specifically their  
442 Figures 11 and 12 for the most intense phases in Livorno). It has to be noted that Ricciardelli et al.  
443 (2018) used ECMWF IC/BC, which are different from that used in this paper. So, the results of this  
444 paper could be even more valuable because they are “more general” and not linked to the specific  
445 modelling tool.

446  
447 To clarify this point we added the following sentence in Section 4.2.3:  
448 “Considering the evolution of CTRL rainfall forecast for the two VSF of Livorno, we concluded that  
449 CTRL was able to predict abundant rain over Livorno, but the rainfall forecast was delayed  
450 compared to the real occurrence. A similar behaviour was found in Ricciardelli et al. (2018) using  
451 the WRF model, showing that the results of this paper for Livorno are likely not tied to the specific  
452 model used.”

453  
454  
455 RC (1) Bottom, page 2: what are “conventional data” ? Why are radial velocity data not used ? Line  
456 70: the main advantage of using 3DVAR vs 4DVAR, EnKF or hybrid methods lies in their already  
457 low computational burden. Thus, I do not agree with this justification. Also, variables are not  
458 “perturbed”; but adjusted by VAR methods.

459  
460 AR. See reply to the RC on the same topic, i.e., assimilation of Doppler velocity. We changed the  
461 paper according to the reviewer suggestion for the other parts of the comment.

462  
463 RC (2) Pages 3 and 4: Please refer to Major Comments 1 and 3. Lines 105: Given that “Federico et  
464 al. (2017a) implemented the methodology of Fierro et al. (2012) ...”, how come on line 112 “We  
465 use the method of Federico et al. (2017a) to assimilate lightning...” ? Please revise accordingly.

466 AR. Ok for this comment. We added the reference to Fierro et al. (2012). The comment of line 112  
467 come from the fact that we intended to cite the adaptation of the methodology, that is discussed in  
468 Federico et al. (2017a). We clarified that conventional data are SYNOP and RAOB.

469  
470 RC (3) Line 124: c.f. end of Major Comment 1.  
471 AR. We wrote “total lightning”.

472  
473 RC (4) Line 240: RAMS used diagnostic relationships (vs explicit) to forecast lightning as it does  
474 not explicitly solves for the 3D electric field. Line 243: “Fourth”

475 AR. For the first comment we wrote: “Second, it predicts the occurrence of lightning following the  
476 diagnostic methodology of Dahl et al. (2012),...”

477  
478 RC (5) Line 290: Delete equation set as these are considered basic/common knowledge.

479 AR. In some papers, where we omitted the equations, we had the opposite comment. However, for  
480 this paper, to reduce length and to give more space to the important points raised by the reviewers  
481 the equations were deleted.

482  
483 RC (6) Section 3.2, lines 300-312: Explicitly state and indicate that equation (2) is from Fierro et al.  
484 (2012, 2015) and not from Federico et al. Line 305: Please explain the rationales behind the choices  
485 of these constants: In particular, how are the forecast metrics affected for a 20% change in A, which  
486 has been shown to exhibit the most notable influence on the forced convection?

487 AR. Ok for the reference. The functional form is of the same as in Fierro et al. (2012, 2015), but the  
488 coefficients were adapted to RAMS@ISAC as shown in Federico et al (2017a). In Federico et al.  
489 (2017a) it is clearly stated that the method is that of Fierro et al. (2012), the only difference being  
490 the adaptation to RAMS@ISAC model. A sensitivity test to the nudging formulation is shown in  
491 the supplemental material (Section S2).

492  
493 RC (7) Line 316-317: c.f. Major Comment 2.

494 AR. We clarified better the ability of LINET to detect both IC and CG.

495  
496 RC (8) End of page 11: c.f. Major Comment 2

497 AR. Not applicable to the revised version.

498  
499 RC (9) Line 356: do the authors refer to the LFC or the LCL, (which may I add is an idea borrowed  
500 from Marchand and Fuelberg 2014 and Fierro et al. 2016). What is the top of the adjustment layer  
501 for lightning? Please elaborate.

502 AR. It is the LCL. The idea is of Caumont et al. (2010), we didn't add the reference to this point of  
503 the paper because the whole methodology is taken from Caumont et al. (2010), already cited  
504 several times. The top adjustment for lightning is -25°C. However, this is already stated in the  
505 paper (Lines 314-315 "The check and eventual substitution of the water vapor is performed every  
506 five minutes and it is made only in the charging zone (0 °C, -25°C).").

507  
508 RC (10) Line 410 and elsewhere. This is similar to the results of Fierro et al. 2016. C.f. Major  
509 Comment 1. Please establish comparisons with previous works throughout the manuscript.

510 AR. We integrated better the results of this paper with those of previous works.

511  
512 RC (11) Line 669: This statement is incorrect. The DE of ground based sensors levels off very  
513 rapidly with distance from land. This is where space-borne lightning detection systems such as the  
514 GLM or Feng Yun-4 can fill the gap.

515 AR. Ok, however the good coverage of the LINET network for some important areas, as between  
516 Corsica and Italian mainland (both Liguria and Tuscany) makes this point "less problematic" for the  
517 Livorno case, while the Serano event occurred over the Italian mainland.

518  
519 RC (12) Lines 716-725: c.f. Major Comment 1.

520 AR We added the references. (Fierro et al., 2015; Federico et al., 2017b; Lynn et al. 2015, Hu et al.,  
521 2006; Jones et al., 2014).

522  
523  
524 REFERENCES (it misses some references given by the reviewer)

525  
526 Alexander, G. D., Weinman, J. A., Karyampoudi, V. M., Olson, W. S., and Lee, A. C. L.: The effect of  
527 assimilating rain rates derived from satellites and lightning on forecasts of the 1993 superstorm,  
528 Mon. Weather Rev., 127, 1433–1457, 1999.

529

530 Avolio, E., Federico, S.: WRF simulations for a heavy rainfall event in southern Italy: Verification and  
531 sensitivity tests, *Atmospheric Research*, Volume 209, 2018, Pages 14-35, ISSN 0169-8095,  
532 <https://doi.org/10.1016/j.atmosres.2018.03.009>.  
533

534 Barker, D.M., Huang, W., Guo, Y.-R., and Xiao, Q.N.: A Three-Dimensional Variational Data  
535 Assimilation System For MM5: Implementation And Initial Results, *Monthly Weather Review*, 132,  
536 897-914, 2004.

537 Benjamin, S. G., and Coauthors, 2004: An hourly assimilation– forecast cycle: The RUC. *Mon. Wea.*  
538 *Rev.*, 132, 495–518, doi:10.1175/1520-0493(2004)132,0495:AHACTR.2.0.CO;2.

539 Boccippio, D. J., K. L. Cummins, H. J. Christian, and S. J. Goodman, 2001: Combined satellite- and  
540 surface-based estimation of the intracloud–cloud-to-ground lightning ratio over the continental  
541 United States. *Mon. Wea. Rev.*, 129, 108–122, doi:10.1175/1520-  
542 0493(2001)129,0108:CSASBE.2.0.CO;2

543 Caumont, O., Ducrocq, V., Wattrelot, E., Jaubert, G., and Pradier-Vabre, S.: 1D+3DVar assimilation  
544 of radar reflectivity data: a proof of concept, *Tellus A: Dynamic Meteorology and*  
545 *Oceanography*, 62:2, 173-187, [https://www.tandfonline.com/doi/abs/10.1111/j.1600-  
546 0870.2009.00430.x](https://www.tandfonline.com/doi/abs/10.1111/j.1600-0870.2009.00430.x), 2010.

547 Chang, D. E., Weinman, J. A., Morales, C. A., and Olson, W. S.: The effect of spaceborn microwave  
548 and ground-based continuous lightning measurements on forecasts of the 1998 Groundhog Day  
549 storm, *Mon. Weather Rev.*, 129, 1809–1833, 2001.

550 Federico, S., Petracca, M., Panegrossi, G., and Dietrich, S.: Improvement of RAMS precipitation  
551 forecast at the short-range through lightning data assimilation, *Nat. Hazards Earth Syst. Sci.*, 17,  
552 61–76, <https://doi.org/10.5194/nhess-17-61-2017>, 2017a.

553 Federico, S., Petracca, M., Panegrossi, G., Transerici, C., and Dietrich, S.: Impact of the assimilation  
554 of lightning data on the precipitation forecast at different forecast ranges. *Adv. Sci. Res.*, 14, 187–  
555 194, 2017b.

556 Federico, S.: Implementation of a 3D-Var system for atmospheric profiling data assimilation into  
557 the RAMS model: Initial results, *Atmospheric Measurement Techniques*, 6(12), 3563-3576, 2013.

558 Fierro, A. O., Mansell, E., Ziegler, C., and MacGorman, D.: Application of a lightning data  
559 assimilation technique in the WRFARW model at cloud-resolving scales for the tornado outbreak  
560 of 24 May 2011, *Mon. Weather Rev.*, 140, 2609–2627, 2012

561 Fierro, A. O., J. Gao, C. Ziegler, E. R. Mansell, D. R. MacGorman, and S. Dembek, 2014: Evaluation  
562 of a cloud scale lightning data assimilation technique and a 3DVAR method for the analysis and  
563 short-term forecast of the 29 June 2012 derecho event. *Mon. Wea. Rev.*, 142, 183–202,  
564 doi:10.1175/MWR-D-13-00142.1..

565 Fierro, A. O., A. J. Clark, E. R. Mansell, D. R. MacGorman, S. Dembek, and C. Ziegler, 2015: Impact  
566 of storm-scale lightning data assimilation on WRF-ARW precipitation forecasts during the 2013  
567 warm season over the contiguous United States. *Mon. Wea. Rev.*, 143, 757–777,  
568 doi:<https://doi.org/10.1175/MWR-D-14-00183.1>.

569 Fierro, A.O., Gao, I., Ziegler, C. L., Calhoun, K. M., Mansell, E. R., and MacGorman, D.  
570 R.: Assimilation of Flash Extent Data in the Variational Framework at Convection-Allowing Scales:  
571 Proof-of-Concept and Evaluation for the Short-Term Forecast of the 24 May 2011 Tornado  
572 Outbreak. *Mon. Wea. Rev.*, 144, 4373–4393, <https://doi.org/10.1175/MWR-D-16-0053.1>, 2016.

573 Goodman, S. J., and Coauthors, 2013: The GOES-R Geostationary Lightning Mapper (GLM). *Atmos.*  
574 *Res.*, 125–126, 34–49, doi:10.1016/j.atmosres.2013.01.006.

575 Hu, M., M. Xue, and K. Brewster, 2006: 3DVAR and cloud analysis with WSR-88D level-II data for  
576 the prediction of the Fort Worth, Texas, tornadic thunderstorms. Part I: Cloud analysis and its  
577 impact. *Mon. Wea. Rev.*, 134, 675–698, doi:10.1175/MWR3092.1.

578 Jones, T. A., J. A. Otkin, D. J. Stensrud, and K. Knopfmeier, 2014: Forecast evaluation of an  
579 observing system simulation experiment assimilating both radar and satellite data. *Mon. Wea.*  
580 *Rev.*, 142, 107–124, doi:10.1175/MWR-D-13-00151.1.

581

582 Lynn, B. H., G. Kelman, and G. Ellrod, 2015: An evaluation of the efficacy of using observed  
583 lightning to improve convective lightning forecasts. *Wea. Forecasting*, 30, 405–423 doi:10.1175/  
584 WAF-D-13-00028.1 .

585 MacGorman, D. W. Burgess, V. Mazur, W. D. Rust, W. L. Taylor, and B. C. Johnson, 1989: Lightning  
586 rates relative to tornadic storm evolution on 22 May 1981. *J. Atmos. Sci.*, 46, 221–251,  
587 doi:10.1175/1520-0469(1989)046<0221:LRRRTS.2.0.CO;2.

588 MacGorman, W. D. Rust, P. Krehbiel, W. Rison, E. Bruning, and K. Wiens, 2005: The electrical  
589 structure of two supercell storms during STEPS. *Mon. Wea. Rev.*, 133, 2583–2607,  
590 doi:10.1175/MWR2994.1.

591 MacGorman, I. R. Apostolakopoulos, N. R. Lund, N. W. S. Demetriades, M. J. Murphy, and P. R.  
592 Krehbiel, 2011: The timing of cloud-to-ground lightning relative to total lightning activity. *Mon.*  
593 *Wea. Rev.*, 139, 3871–3886, doi:10.1175/MWR-D-11-00047.1

594 Mittermaier, M., N. Roberts, and S. A. Thompson, 2013: A long-term assessment of precipitation  
595 forecast skill using the Fractions Skill Score. *Meteor. Appl.*, 20, 176–186,  
596 doi:<https://doi.org/10.1002/met.296>.

597 Papadopoulos, A., Chronis, T. G., and Anagnostou, E. N.: Improving convective precipitation  
598 forecasting through assimilation of regional lightning measurements in a mesoscale model, *Mon.*  
599 *Weather Rev.*, 133, 1961–1977, 2005.

600 Parrish, D.F., and Derber, J.C.: The National Meteorological Center’s Spectral Statistical  
601 Interpolation analysis system, *Monthly Weather Review*, 120, 1747-1763, 1992.

602 Pessi, A. T., and S. Businger, 2009: The impact of lightning data assimilation on a winter storm  
603 simulation over the North Pacific Ocean. *Mon. Wea. Rev.*, 137, 3177–3195, doi:10.1175/  
604 2009MWR2765.1

605 Ricciardelli, E.; Di Paola, F.; Gentile, S.; Cersosimo, A.; Cimini, D.; Gallucci, D.; Gerald, E.; Larosa, S.;  
606 Nilo, S.T.; Ripepi, E.; Romano, F.; Viggiano, M. Analysis of Livorno Heavy Rainfall Event: Examples  
607 of Satellite-Based Observation Techniques in Support of Numerical Weather Prediction. *Remote*  
608 *Sens.* 2018, 10, 1549.

609  
610 Rohn, M., Kelly, G., Saunders, R. W.: Impact of a New Cloud Motion Wind Product from Meteosat  
611 on NWP Analyses and Forecasts, *Monthly Weather Review*, 129, 2392-2403, 2001.

612 Stensrud, D.J., M. Xue, L.J. Wicker, K.E. Kelleher, M.P. Foster, J.T. Schaefer, R.S. Schneider, S.G.  
613 Benjamin, S.S. Weygandt, J.T. Ferree, and J.P. Tuell, 2009: Convective-Scale Warn-on-Forecast  
614 System. *Bull. Amer. Meteor. Soc.*, 90, 1487–1500, <https://doi.org/10.1175/2009BAMS2795.1>

615 Stewart, L. M., Dance, S. L., Nichols, N. K.: Data assimilation with correlated observation errors:  
616 experiments with a 1-D shallow water model, *Tellus A: Dynamic Meteorology and Oceanography*,  
617 65:1, 2013, DOI: 10.3402/tellusa.v65i0.19546

618  
619 Wiens, K. C., S. A. Rutledge, and S. A. Tessendorf, 2005: The 29 June 2000 supercell observed  
620 during STEPS. Part II: Lightning and charge structure. *J. Atmos. Sci.*, 62, 4151–4177,  
621 doi:10.1175/JAS3615.1

622  
623  
624  
625  
626  
627  
628  
629  
630  
631  
632  
633  
634  
635  
636  
637

638 **Answer to the reviewer #2 comments on NHESS-2018-319.**

639

640 We acknowledge the reviewer for the useful comments on the paper, both in the general comments  
641 section and in the pdf file. Our answers are in red. The Author Replies (AR) to the Reviewer  
642 Comments (RC) are in blue.

643 AR: Before discussing in details the RCs, it's import to outline that the subject paper contained  
644 two typos. The first refers to the length scale of the background error matrix in the x and y  
645 directions that varies between 14 and 25 km and not , between 20 and 30 km, as erroneously  
646 reported in the manuscript. The second refers to the correct lightning number for each day  
647 are 82 331 for the 9 September, 291 164 for the 10 September (170 000 is written into the  
648 manuscript) and 105 467 for the 16 September (60 000 written in the manuscript). Despite  
649 the typos, the results shown in the paper were obtained using the correct number of flashes  
650 and the correct length scales in the background error matrix.

651

652 RC: Extracted from the general comments:

653 This manuscript addresses an interesting and challenging topic, moreover represents a  
654 substantial contribution to the understanding of natural hazards and their consequences  
655 matching the scope of NHESS. However, the scientific and presentation quality are poor,  
656 above all because the results are presented in a "repetitive and heavy" manner and the  
657 English language needs a deep revision.

658 Specific comments: please see the notes on the pdf for each section and also for each figure's  
659 caption, moreover please deeply motivate the reason why: a) radial velocity is not  
660 assimilated: the operator is not implemented or the data are not available?; b) data  
661 assimilation is performed in the domain D02 only; c) you used a background error matrix of  
662 fall 2012 for case studies of late summer 2017. Technical corrections: please see the notes on  
663 the pdf for each section and also for each figure's caption.

664 AR: Comment "...in a repetitive and heavy manner". In the first submission of the paper we  
665 stressed the important improvement given by the data assimilation at the local scale on the  
666 precipitation VSF (Very Short term Forecast, 0-3h). To highlight this point, we showed the  
667 many ways in which the forecast is improved by the assimilation of lightning, radar or both  
668 data. For example, the two stages of the Serano case show that the radar (first phase 03-06  
669 UTC on 16 September) or lightning (second phase of the event, 18-21 UTC on 16 September)  
670 were the key observation to assimilate in order to improve the precipitation VSF. Also, other  
671 stages had specific aspects that we discussed.

672 Our attempt, however, was not successful, considering the comments of reviewer #1 and  
673 reviewer #2 and the results section (Section 4) underwent a substantial rewriting. In  
674 particular, in the revised version of the paper, we deleted Section 4.1.2 (second phase of the  
675 Serano case) and Section 4.2.1 (first case of the Livorno case). The results of Section 4.2.1 are  
676 shortly commented in Section 5 (Discussion and conclusions) to highlight that there is space  
677 for improvement. Following the comments of the reviewer #2, the scores of the phases  
678 discussed into the paper have been put in three tables (Tables: 4-6) for specific thresholds (1,  
679 6, 10, 20, 30, 40 mm/3h and, for Livorno, also 50 mm/3h) and, following the remarks of the  
680 reviewer #1, different neighborhood radii have been used to compute ETS and POD scores.

681 The space gained by deleting the two sub-sections stated above and by other corrections was  
682 used to extend the discussion about the methods of assimilating lightning and radar in the 3D-  
683 Var model. These sections should be clear in the revised version of the paper.

684 Finally, to avoid the repetitive discussion, we added supplemental material to this paper to  
685 show how lightning and radar data assimilation works together, presenting the evolution of  
686 the total water averaged for all VFS of the two cases and including in this discussion the  
687 assimilation stage (Section S1).

688 The supplemental material shows also sensitivity tests of the precipitation scores (POD and  
689 ETS) to the nudging formulation (Section S2). Section S2 requested new simulations with  
690 different model settings (see Table S1 in the supplemental material).

691 Also, the supplemental material contains some plots requested by the reviewer #1 and the  
692 formula used to compute the reflectivity factor (dBz) of RAMS@ISAC requested by reviewer  
693 #3.

694 We didn't include the supplemental material in the paper, as stated in the discussion phase of  
695 this paper, to avoid excessive length. However, the paper has few references to the  
696 supplemental material to help readers to decide if they are interested to this material.

697 "...the English language needs a deep revision". We revised the English of the paper, also  
698 according to the remarks of the reviewer #2 in the PDF file. Also, the copy-editing service of  
699 the journal will improve the quality of the English before the eventual publication of the  
700 paper.

701

702 AR: Specific question a) We are working on the assimilation of the radial velocity but the  
703 operator is not yet implemented in the 3D-Var. Also, while the reflectivity factor measured by  
704 the radar network is operationally available, the product of radial velocity is under  
705 development. At the moment, it needs further research to solve some issues (complex  
706 orography, operations of the radars not optimal for the Doppler retrieval and others). For  
707 these reasons, the attention was on the assimilation of radar reflectivity factor. These  
708 motivations are discussed in the revised version of the paper in Section 3.3 by writing:

709

710 "Radial velocity is not assimilated within the RAMS@ISAC model because it is not operationally  
711 processed, the scan strategy being optimized for QPE purposes. Furthermore, the implementation of  
712 a radial velocity data assimilation scheme is under development in RAMS-3DVAR and it is not  
713 currently available for testing. For these reasons, we didn't consider the assimilation of this  
714 parameter."

715

716 Specific question b) Data assimilation is not performed on domain D3 (R1) because the use of  
717 this domain is exceptional and we don't have background error statistics for this grid.  
718 Background error statistics for the domain D2 are computed by the NMC method, which, for  
719 this paper, is based on HyMeX-SOP1 simulations. The Appendix A and B of Federico (2013)



720 shows the details of the application of the method, which requires a number of simulations  
721 (see Barker et al., 2004 for the general discussion). These simulations are not available for the  
722 innermost grid of the Livorno case, which was introduced to better resolve the precipitation  
723 at the local scale and to show how precise can be the impact of lightning and radar data  
724 assimilation on the VSF. These motivations are clarified in the revised version of the paper.

725 Of course, this limitation is only for radar reflectivity factor because flashes are assimilated by  
726 nudging. Nevertheless, we couldn't compare simulations with or without data assimilation for  
727 a specific domain assimilating lightning in the innermost domain and, for this reason, we  
728 assimilated flashes over the domain D2 only.

729 In the revised version of the paper we specified better the role of the domain D3 and the  
730 reason for not assimilating lightning and radar reflectivity factor over the domain D3.

731 We wrote in section 3.1 (RAMS@ISAC and simulations set-up)

732

733 "The third domain covers the Tuscany Region, has 4/3 km horizontal resolution (R1), and it is  
734 used for Livorno to represent with higher spatial detail the precipitation field over Tuscany  
735 and to show better the precision of the rainfall VSF using data assimilation at the local scale.  
736 The fine structures of the precipitation field are smeared out over Tuscany using only  
737 domains D1 and D2. The operational implementation of the RAMS@ISAC model uses the  
738 domains D1 and D2 and no refinement for specific areas of Italy are used because Italy is a  
739 complex orography country and grid refinements for a specific event can be done only a-  
740 posteriori, i.e. after the occurrence of the event."

741

742 And few lines below:

743

744 "It is noted that data assimilation is performed over the domain D2 (R4) only, and the  
745 innovations are transferred to domain D3 (R1), for the Livorno case, by the two way-nesting.  
746 The domain D3 is used for the Livorno case to refine the resolution of the precipitation field  
747 over Tuscany and to show the spatial and temporal precision of the precipitation forecast  
748 over Tuscany using data assimilation. However, its usage is exceptional because, as stated  
749 above, Italy is a complex orography country and grid refinements for specific areas are used  
750 only after the occurrence of an event. For these reasons the domain D3 is usually not used in  
751 RAMS@ISAC and statistics about the background error aren't available for this grid. The  
752 background error in RAMS-3DVar is computed by the NMC method (Parrish and Derber,  
753 1992), which requires a number of simulations (at least two-weeks) verifying at the same  
754 time but starting with a lag of 12 h. These simulations are not performed in this paper and  
755 background error statistics for the domain D3 are not available.

756 Being lightning assimilated by nudging, they could be assimilated over the domain D3.  
757 Nevertheless, to preserve the rationale of the paper, i.e. comparing simulation with or without  
758 data assimilation for specific domains, we didn't assimilate lightning over the domain D3.

759 Being lightning and radar cloud scale observations, their assimilation at higher horizontal  
760 resolution is foreseeable in future works. “

761

762 Specific questions c) We chose the background error matrix computed for HyMeX-SOP1  
763 because the period was characterized by several convective events over Italy, as documented  
764 in Ferretti et al., (2014), while the period preceding the convective events of this paper was  
765 characterized by fair weather, typical of the summer Mediterranean season. For this reason,  
766 we believe that the matrix for the HyMeX-SOP1 is more representative of convective events  
767 compared to the matrix computed for the period of the storms occurrence. We wrote to  
768 comment on this point:

769

770 “The background error matrix is computed using the NMC method (Parrish and Derber, 1992;  
771 Barker et al. 2004) applied to the HyMeX-SOP1 (Hydrological cycle in the Mediterranean  
772 Experiment – First Special Observing Period occurred in the period 6 September-6 November  
773 2012; Ducroq et al., 2014). This choice is motivated by the fact that HyMeX-SOP1 contains  
774 several heavy precipitation events over Italy and the background error matrix is  
775 representative of the convective environment of the cases considered in this paper. In  
776 particular, 10 out of 20 declared IOP (Intense Observing Period) of HyMeX-SOP1 occurred in  
777 Italy (Ferretti et al., 2014). On the contrary, the period of September 2017, especially before  
778 the events selected in this study was characterized by fair and stable weather conditions over  
779 Italy and the background error matrix for September 2017 is less representative of the  
780 convective environments that characterise the events of this paper.”

781

782 RC: PDF file with technical corrections:

783

784 AR: Considering the pdf file, all corrections were accepted. There are, however, few points that  
785 need a short discussion. They are listed below.

786 Elements of novelty of the paper: we highlighted better the elements of novelty of this paper in the  
787 introduction. We wrote:

788

789 “This paper presents for the first time the assimilation of the radar reflectivity factor in the  
790 RAMS@ISAC model and shows how the assimilation of the radar reflectivity factor works together  
791 with lightning data assimilation. Also, this paper shows how accurate in space and time can be the  
792 forecast of the precipitation field using cloud scale observations over complex terrain, contributing  
793 in this way to a number of works on the same subject.”

794

795 Comment on Line 276: The frequency bias was not shown to keep the discussion concise. However,  
796 was important to point out that the model has a wet bias, especially when assimilating radar

797 reflectivity factor. For this purpose, we introduced the score that was used to highlight that the  
798 model has a wet bias, nevertheless we didn't show any figure to keep the discussion more concise.  
799 In the revised version of the paper the wet bias of the model is highlighted better and a discussion  
800 on how to reduce the wet bias is added in the "Discussion and conclusions" section (Section 5).

801 In particular in the "Discussion and Conclusions" section we wrote:

802 "The wet bias of RAD and RADLI forecast is the main drawback of the results of this paper. To  
803 reduce the moisture added by radar and lightning data assimilation further research is needed and  
804 different approaches are possible (Fierro et al., 2016). In particular: a) assimilating for a shorter  
805 time period (0-6h in this paper); b) reducing the length-scales of the 3D-Var in the horizontal  
806 directions to limit the spreading of the innovations or assuming an innovation equal to zero for  
807 grid points without lightning and with zero reflectivity factor observed and simulated; c) reducing  
808 the amount of water vapour added to the model (for example reducing the values of A and B  
809 constants for lightning data assimilation or relaxing the request of saturation when radar  
810 reflectivity is observed in areas where the model has zero reflectivity); d) adding moisture to a  
811 shallower vertical level.

812 It is also noted that a combination of heating and moistening could provide the same buoyancy  
813 with less water vapour addition (Marchand and Fulberg, 2014)."

814

815 While in the supplemental material (Section S2) we wrote:

816 "It is finally noted that RAD and RADLI have high POD values for all thresholds, nevertheless their  
817 ETS is below that of LIGHT and SAT up to 32 mm/3h (RADLI) and 42 mm/3h (RAD). This behavior is  
818 caused by the larger number of false alarms given by assimilating radar reflectivity factor  
819 compared to simulations assimilating lightning. This result shows again that RAD and RADLI  
820 configurations have a wet frequency bias. In particular, the frequency bias of RAD and RADLI  
821 configuration is about 3 between 20 and 40 mm/3h."

822

823 Line 306: There was a typing error into equation 2 (equation 1 in the revised version of the paper).  
824 The correct equation is:

825

$$826 \quad q_v = Aq_s + Bq_s \tanh(CX)(1 - \tanh(Dq_g^t))$$

827

828 and  $q_s$  is in the last term. We also note that the number of lightning assimilated by the model is  
829 larger than that reported in the first submission of the paper for both cases for a mistake we did in  
830 checking the numbers. The correct number of assimilated flashes is reported at the start of this  
831 answer. The results, however, were obtained using the correct number of flashes.

832

833 Line 314: “The check and eventual substitution of the water vapor is performed every five minutes  
834 and it is made only in the charging zone (0 °C, -25°C).” To better explain this choice, we  
835 reformulated the sentence adding references to the charging zone:

836

837 “The check and eventual substitution of the water vapor is performed every five minutes and it is  
838 made within the mixed phase layer zone (0 °C, -25°C), wherein electrification processes are the  
839 most active (Takahashi 1978, Emersic and Saunders, 2010; Fierro et al., 2015).”  
840

841 Line 314: the comment is: could you add some more details about this quality control?

842 We added two references. We wrote:

843 “The processing chain aims at identifying most of the uncertainty sources as clutter, partial beam  
844 blocking and beam broadening. The radar observations are processed according to nine steps  
845 detailed in Vulpiani et al. (2014), Petracca et al. (2018) and references therein.”

846

847

#### 848 References

849

850 Barker, D.M., Huang, W., Guo, Y.-R., and Xiao, Q.N.: A Three-Dimensional Variational  
851 Data Assimilation System For MMS: Implementation And Initial Results, *Monthly Weather*  
852 *Review*, 132, 897-914, 2004.

853 Ducrocq, V., Braud, I., Davolio, S., Ferretti, R., Flamant, C., Jansa, A., Kalthoff, N.,  
854 Richard, E., Taupier-Letage, I., Ayrat, P.-A., Belamari, S., Berne, A., Borga, M.,  
855 Boudevillain, B., Bock, O., Boichard, J.-L., Bouin, M.-N., Bousquet, O., Bouvier, C.,  
856 Chiggiato, J., Cimini, D., Corsmeier, U., Coppola, L., Cocquerez, P., Defer, E., Delanoë,  
857 J., Di Girolamo, P., Doerenbecher, A., Drobinski, P., Dufournet, Y., Fourrié, N.,  
858 Gourley, J.J., Labatut, L., Lambert, D., Le Coz, J., Marzano, F.S., Molinié, G., Montani,  
859 A., Nord, G., Nuret, M., Ramage, K., Rison, W., Roussot, O., Said, F., Schwarzenboeck,  
860 A., Testor, P., Van Baelen, J., Vincendon, B., Aran, M., and Tamayo, J.: HYMEX-SOP1  
861 The Field Campaign Dedicated to Heavy Precipitation and Flash Flooding in the  
862 Northwestern Mediterranean. *Bull. Amer. Meteor. Soc.*, 95, 1083-  
863 1100, <https://doi.org/10.1175/BAMS-D-12-00244.1>, 2014.

864

865 Emersic, C., and C. P. R. Saunders, 2010: Further laboratory investigations into the  
866 relative diffusional growth rate theory of thunderstorm electrification. *Atmos. Res.*, 98,  
867 327-340, doi:<https://doi.org/10.1016/j.atmosres.2010.07.011>.

868

869 Federico, S.: Implementation of a 3D-Var system for atmospheric profiling data  
870 assimilation into the RAMS model: Initial results, *Atmospheric Measurement Techniques*,  
871 6(12), 3563-3576, 2013.

872 Ferretti, R., Pichelli, E., Gentile, S., Maiello, I., Cimini, D., Davolio, S., Miglietta, M. M.,  
873 Panegrossi, G., Baldini, L., Pasi, F., Marzano, F. S., Zinzi, A., Mariani, S., Casaioli, M.,  
874 Bartolini, G., Loglisci, N., Montani, A., Marsigli, C., Manzato, A., Pucillo, A., Ferrario, M. E.,  
875 Colaiuda, V., and Rotunno, R.: Overview of the first HyMeX Special Observation Period

876 over Italy: observations and model results, *Hydrol. Earth Syst. Sci.*, 18, 1953–1977,  
877 <https://doi.org/10.5194/hess-18-1953-2014>, 2014.

878 Fierro, A. O., A. J. Clark, E. R. Mansell, D. R. MacGorman, S. Dembek, and C. Ziegler,  
879 2015: Impact of storm-scale lightning data assimilation on WRF-ARW precipitation  
880 forecasts during the 2013 warm season over the contiguous United States. *Mon. Wea.*  
881 *Rev.*, 143, 757–777, doi:<https://doi.org/10.1175/MWR-D-14-00183.1>.

882 Fierro, A.O., Gao, L., Ziegler, C. L., Calhoun, K. M., Mansell, E. R., and MacGorman, D.  
883 R.: [Assimilation of Flash Extent Data in the Variational Framework at Convection-](#)  
884 [Allowing Scales: Proof-of-Concept and Evaluation for the Short-Term Forecast of the 24](#)  
885 [May 2011 Tornado Outbreak](#). *Mon. Wea. Rev.*, 144, 4373–  
886 4393, <https://doi.org/10.1175/MWR-D-16-0053.1>, 2016.

887 Marchand, M., and H. Fuelberg, 2014: Assimilation of lightning data using a nudging  
888 method involving low-level warming. *Mon. Wea. Rev.*, 142, 4850–4871,  
889 doi:10.1175/MWR-D-14-00076.1.

890 Parrish, D.F., and Derber, J.C.: The National Meteorological Center’s Spectral Statistical  
891 Interpolation analysis system, *Monthly Weather Review*, 120, 1747–1763, 1992.

892 Petracca, M., L.P. D’Adderio, F. Porcù, G. Vulpiani, S. Sebastianelli, and S. Puca, 2018: V  
893 alidation of GPM Dual-Frequency Precipitation Radar (DPR) rainfall products over  
894 Italy. *J. Hydrometeor.*, 19, 907–925, <https://doi.org/10.1175/JHM-D-17-0144.1>

895 Takahashi, T., 1978: Riming electrification as a charge generation mechanism in  
896 thunderstorms. *J. Atmos. Sci.*, 35, 1536–1548, doi:<https://doi.org/10.1175/1520>  
897 [0469\(1978\)035<1536:REAACG>2.0.CO;2](https://doi.org/10.1175/15200469(1978)035<1536:REAACG>2.0.CO;2).

898

899 Vulpiani, G., A. Rinollo, S. Puca, and M. Montopoli, 2014: A quality-based approach for  
900 radar rain field reconstruction and the H-SAF precipitation products validation. *Proc.*  
901 *Eighth European Radar Conf.*, Garmish-Partenkirchen, Germany, ERAD, Abstract 220, 6  
902 pp., [http://www.pa.op.dlr.de/erad2014/programme/](http://www.pa.op.dlr.de/erad2014/programme/ExtendedAbstracts/220_Vulpiani.pdf)  
903 [ExtendedAbstracts/220\\_Vulpiani.pdf](http://www.pa.op.dlr.de/erad2014/programme/ExtendedAbstracts/220_Vulpiani.pdf) (last access January 2019).

904

905

906

907

908

909

910

911

912

913

914

915

916

917

918

919

920

921

922

923  
924  
925 **ANSWER to the Reviewer #3**  
926  
927 Review of the manuscript  
928 „The impact of lightning and radar data assimilation on the performance of very short  
929 term rainfall forecasts for two case studies in Italy”  
930 by  
931 Stefano Federicio, Rosa Claudia Torcasio, Elenio Aviolo, Olivier Caumont, Mario  
932 Montopoli, Luca Baldini, Gianfranco Vulpiani and Stefano Dietrich  
933 The study discusses the impact of the assimilation of lightning and radar reflectivity data  
934 on the performance of very short-range rainfall forecasts for two convective case studies  
935 in Italy. They showed that especially the combined assimilation of both observation types  
936 has a clear and positive impact on the forecast performance.  
937 The manuscript is interesting and tackles a very important subject, since the forecast of  
938 severe precipitation is still a major weakness of current forecast systems. However, you  
939 have to provide more information on how the two observation types are assimilated. The  
940 equations and the text you provide are not enough to convince the reader that the  
941 methodology with all its coefficients is scientifically justified. Furthermore, I am concerned  
942 about the coarse vertical resolution you applied for the simulations.  
943 Therefore, major revisions of the methodology section are necessary before I can suggest  
944 the publication of the manuscript.  
945 In the following, I spilt my judgement into major and minor comments.  
946

947 We acknowledge the reviewer for the useful comments on the paper, both in the general comments  
948 section and in the pdf file. Our answers are in red. The Author Replies (AR) to the Reviewer  
949 Comments (RC) are in blue.

950 AR: Before discussing in details the RCs, it's import to outline that the subject paper contained  
951 two typos. The first refers to the length scale of the background error matrix in the x and y  
952 directions that varies between 14 and 25 km and not , between 20 and 30 km, as erroneously  
953 reported in the manuscript. The second refers to the correct lightning number for each day  
954 are 82 331 for the 9 September, 291 164 for the 10 September (170 000 is written into the  
955 manuscript) and 105 467 for the 16 September (60 000 written in the manuscript). Despite  
956 the typos, the results shown in the paper were obtained using the correct number of flashes  
957 and the correct length scales in the background error matrix.  
958

959 We acknowledge the reviewer for the interesting remarks, which helped to improve the  
960 paper. In general, we note that both lightning and radar reflectivity factor data assimilation  
961 sections have been expanded, as requested by the reviewer, and the “Data and  
962 Methods” section should be much clearer in the revised version of the paper. In the  
963 following there are important points raised by the reviewer (the choice of the background  
964 error matrix, or superobs for example), which we can only comment without performing  
965 again the simulations. Because they are important for the data assimilation system and  
966 we can only comment on them, we prefer to add the word “preliminary” to the title of the  
967 paper. In this way we highlight that important points of the physical options of the  
968 software are still to be fully tested.  
969

970 The new title proposed is: "Preliminary results of the impact of lightning and radar  
971 reflectivity factor data assimilation on the very short term rainfall forecasts of  
972 RAMS@ISAC: application to two case studies in Italy"

973  
974 The revised paper has supplemental material where we investigate the following two  
975 points: a) the relative contribution of lightning and radar data assimilation to the behavior  
976 of total water mass in the simulation; b) the sensitivity of the rainfall VSF to lightning data  
977 formulation.

978  
979 **RC: Major comments**

980 - You show the horizontal dimensions and resolutions of your domains. However, for the  
981 vertical dimension you only write that it covers the troposphere and the lower  
982 stratosphere. How many levels do you use up to which height? How many of these levels  
983 are in the boundary layer? These are important information strongly influencing your  
984 results. This needs to be mentioned in the text. I found the total number of vertical levels  
985 and the model top height in the table you provide. However, to my opinion a horizontal  
986 resolution of 1 km combined with only 36 levels up to more than 22 km height is way too  
987 coarse to adequately describe the developing processes.

988  
989 AR: The set-up of the RAMS@ISAC in this paper is the same as the operational setting,  
990 with the exception of the usage of domain D3 for the Livorno flood. In the operational  
991 setting a compromise must be chosen between the grid resolution and the computational  
992 time. While a future release of the operational setting will use more vertical levels (42), for  
993 the current year we are still using 36 levels. Among them 10 are below 1 km, 15 below 2  
994 km and 18 below 3 km. The level 21 is at 5200 m in the terrain following coordinates used  
995 by RAMS. Above 6 km the model levels are more than 1000 m apart, with a maximum of  
996 1200 m for the vertical layer at the model top.

997 Of course more vertical levels are useful to resolve important processes in the vertical as,  
998 as in cases of fronts, Planetary Boundary Layer processes, clouds etc., nevertheless a  
999 compromise between vertical resolution and computing time is necessary. Note, also,  
1000 that this vertical grid was used with success in several heavy precipitation events over  
1001 Italy. We wrote (Section 3.1):

1002  
1003 "The resolutions and the extensions of the grids in the vertical direction is the same for the  
1004 three domains. The vertical grid covers the troposphere and the lower stratosphere.  
1005 Vertical levels have different spacings and are more packed close to the ground. Among  
1006 the 36 levels used in this paper 10 are below 1 km, 15 below 2 km and 18 below 3 km.  
1007 The first vertical level is at 24 m above the surface in the terrain following coordinates used  
1008 by RAMS@ISAC, the level 21 is at 5200 m. Above 6 km the model levels are about 1000  
1009 m apart, with a maximum of 1200 m for the vertical layer at the model top."

1010  
1011 RC: You write that the R10 simulation is applied as lateral boundary condition for the  
1012 inner domain simulations and that you use assimilation in the inner domains. O.k. so far –  
1013 but do you adjust the lateral boundaries provided by R10 to the new situation after the  
1014 assimilation? If not they may negatively influence your forecast. If you think that this is not  
1015 necessary for your short-term forecasts, this has to be mentioned in the text.

1016  
1017 AR: This point is related with the operational setting of RAMS@ISAC. Updating the R10  
1018 domain to the new situation after data assimilation is beneficial for the simulation.

1019 Nevertheless, this would require additional simulations of the R10 model increasing the  
1020 computing time for the whole chain. We added the following comment (in Section 3.1):  
1021 “The R10 run is not updated after the acquisition of new data by the analysis system and  
1022 this is a limitation of the results shown in this paper.”

1023  
1024 RC: The description of the lightning data assimilation is too short. The reader has no  
1025 chance to understand equation (2) with all its coefficients without further explanation. In  
1026 the text, you mention graupel mixing ratio  $q_g$ , but the equation only contains  $q_s$ . What is  
1027  $q_s$  or should it be  $q_g$ ? The way you present it sounds like “Voodoo”.

1028  
1029 AR: Lightning section was mostly rewritten in the revised version of the paper and  
1030 extended to consider this and other comments of the reviewers. In the revised version of  
1031 the paper it should be more readable. The correct form of Equation (2) (Eqn. (1) in the  
1032 revised version of the paper is):

$$q_s = Aq_s + Bq_s \tanh(CX)(1 - \tanh(Dq_s^a))$$

1033  
1034  
1035 and now  $q_g$  is present.

1036  
1037 RC: How do the assimilation system deals with sharp gradients along the vertical profile  
1038 when you only adjust the profile in a certain height region?

1039  
1040 AR: Lightning data assimilation as well as radar data assimilation can produce sharp  
1041 gradients in the vertical directions. For lightning data assimilation a nudging is performed  
1042 to avoid a direct insertion of the data in the model, while in the case of radar the data are  
1043 directly introduced in RAMS@ISAC. Nevertheless, our experience with RAMS@ISAC  
1044 shows that, at least for the setting of this paper, the sharp gradients introduced in the  
1045 model do not produce incorrect results or blowing up of the model. We highlighted this  
1046 point into the paper (Section 3.3):

1047 “Lightning and radar data assimilation may produce sharp gradients in vertical direction  
1048 caused by the addition of water vapour to specific layers. In the case of lightning, the  
1049 water vapour is added by nudging to reduce the sharp gradients. However, radar data  
1050 assimilation, which accounts for the largest mass of water added to RAMS@ISAC (see  
1051 Section S.1 of the supplemental material), directly inserts the water vapour into the  
1052 model. Our experience with RAMS@ISAC, however, shows that results are reliable and  
1053 the sudden addition of water vapour doesn’t cause shocks to the model simulation,  
1054 despite the notable gradients of specific humidity.”

1055  
1056 RC: You only adjust  $q_v$ ? How do you make sure that this results in more precipitation? Do  
1057 you tune this with the coefficients? If yes – you have to include the information in the text.

1058 AR: The increase/decrease of the water vapour depends on the data assimilation.  
1059 Lightning can only increase the water vapour while radar can increase or decrease the  
1060 water vapour. However, if the added/removed water vapour determines more/less  
1061 precipitation depends on the physical and dynamical processes occurring in  
1062 RAMS@ISAC and no specific tuning is done. The only exception is that if, after the data  
1063 assimilation, the model is oversaturated, the water vapour is reduced to the saturated  
1064 value (at the RAMS@ISAC temperature).

1065 We added the following sentence at the end of Section 3.3 “Data and Methods”: “It is  
1066 finally noted that the data assimilation increase/decrease the water vapour into the model  
1067 depending on the cases. The eventual increase/decrease of the forecasted rainfall



1068 depends on the physical and dynamical processes occurring into the meteorological  
1069 model, without any specific tuning.”

1070  
1071 RC: I understand why you reduce the resolution of the radar data. But is a pure sampling  
1072 the best method? Usually one uses a kind of “super obbing” to avoid the implementation  
1073 of errors (e.g. by insects) or extremes. Please comment on this and add explanation why  
1074 you choose sampling.

1075  
1076 AR: This is an aspect that need to be improved in future version of the software. Using  
1077 superobs does a better job compared to the sampling of the data for the reasons stated  
1078 by the reviewer and superobs improve the performance of the data assimilation. The only  
1079 point that favours the sampling method compared to superobs is that the latter could  
1080 increase the correlation among the observations’ errors. We highlighted the point in  
1081 Section 3.3 by writing:

1082 “It is important to note the pure sampling of the data could result in implementation of  
1083 errors (for example reflectivity given by insects or birds) or extremes. Creating  
1084 superobservations would reduce this problem, the main drawback being the missing of  
1085 very localised phenomena. While the aim of this paper is to present the update of the  
1086 data assimilation system of RAMS@ISAC and its application to two challenging cases,  
1087 the problem of using superobservations will be considered in future studies because it  
1088 impacts the results.”

1089  
1090 RC: The error value of 1 to 3 dBz seems to be too small, making the system very sensitive  
1091 to the radar data. Especially when combining this with a pure sampling of the radar data  
1092 sounds dangerous to me. Please explain why you use this error value.

1093  
1094 AR: The choice of a small error for the reflectivity factor is motivated by two reasons: a)  
1095 the data are carefully checked by the Civil protection Department; b) the performance of  
1096 the control simulation, not assimilating any data, is rather poor for the case studies.  
1097 Nevertheless, the choice could not be optimal for other cases. We highlighted this point  
1098 in Section 3.3 by writing:

1099 “The error of radar data is assumed small (1dBz) for two reasons: a) reflectivity data are  
1100 carefully checked by the Civil Protection Department; b) the performance of the control  
1101 simulation, not assimilating any data, is rather poor for the case studies. This setting,  
1102 however, could not be optimal for cases when the control forecast performs better and  
1103 different choices should be done for those cases.”

1104  
1105 RC: You mention that cross correlations between the variables are neglected in this  
1106 study. Do you neglect them in the observation operator only or in the assimilation  
1107 system? Every assimilation system needs cross correlations between the variables e.g. to  
1108 spread the information of the observations horizontally and vertically.

1109  
1110 AR: The expression we used is not correct. We neglect cross correlations among different  
1111 variables. In the current form, the data assimilation system uses the variables: (u=zonal  
1112 velocity, v=meridional velocity, T=temperature, q=water vapor mixing ratio). For the  
1113 results of this paper we neglected cross correlations in the **B** matrix among different  
1114 variables (specifically (u,q), (v,q) (T,q)), while we maintained the error correlations among  
1115 different levels and in the horizontal plane of q to spread the innovations in the vertical  
1116 and horizontal directions (the latter being shown in Figure 14b of the revised paper). This

1117 is a point that need to be improved in future versions of the software, by considering also  
1118 cross correlations among different variables. We will precise better this point adding the  
1119 following sentence (Section 3.3):  
1120 “Cross correlations among different variables of the data assimilation system are  
1121 neglected in this study and the application of the RAMS-3DVar affects the water vapour  
1122 mixing ratio only. Cross correlations among different variables can improve the  
1123 performance of data assimilation system, and an example of their impact in the RAMS-  
1124 3DVar is shown in Federico (2013). Nevertheless, the impact the cross correlations  
1125 among different variables of the 3D-Var in the precipitation VSF will be explored in future  
1126 works.”.

1127  
1128 RC: - Mention not only that the forward operator for reflectivity is from the WSM6 scheme  
1129 of WRF – also mention the equation of the forward operator.

1130  
1131 AR: We added the expression of the forward radar operator in the supplemental material  
1132 (Section S4) to avoid excessive paper length. A reference was put into the paper to the  
1133 reference material (Section 3.3).

1134  
1135  
1136 **RC: Minor comments**

1137 - Although the text is well readable, the language can be improved. Although, I am not a  
1138 native speaker, I stumbled over several things. Here some examples:

1139 - Page 4, line 113: ... case studies occurred in September 2017 ...

1140 - Page 5, line 135: ... developed to the lee ...

1141 - Page 5, line 151: Also notable is the feeding ...

1142 - Page 5, line 158: ... is also clearly seen in the radar ...

1143 - Page 5, line 163: ... can be noted over central-northern Italy.

1144 - Page 6, line 165: ... cloud system was active for several ...

1145 - Page 6, line 168: ... were recorder during the day; ...

1146 - Page 6, line 170: ... from 00 UTC ...

1147 - Page 6, line 186: ... occurred within a few hours.

1148 - Page 6, line 192: illustrated better than represented? [We chose illustrated.](#)

1149 - Page 6, line 195: ... interaction between the air-masses and the Western Alps  
1150 generated a depression ...

1151 - Page 7, line 197: ... it is noted that divergent ...

1152 - Page 7, line 198: ... it is apparent that the equivalent ... [We wrote “it is evident the  
1153 equivalent...”](#)

1154 - Page 7, line 201: ... low pressure system ...[Not applicable in the revised version of the  
1155 paper.](#)

1156 - Page 7, line 204: From a synoptic point of view, ...

1157 - Page 7, line 206: ... more intense than the Serano case ...

1158 - Page 7, line 211: ... recorded over Italy, following ...

1159 - Page 7, line 213: ... for the Serano case.

1160 - Page 7, line 215: ... it is well evident that the cloud system ...

1161  
1162 [AR: All the above points were corrected, with the exceptions indicated in blu.](#)

1163  
1164 RC: Abstract: Lines 29 to 31. Do you need this sentence? To my opinion, the sentence  
1165 above is enough.

1166  
1167 AR: Deleted.  
1168  
1169 RC: Abstract: Merge lines 32 to 34 with the paragraph above.  
1170  
1171 AR: Done.  
1172  
1173 RC: Mention once in the text why you use the term “reflectivity factor” instead of  
1174 reflectivity.  
1175  
1176 AR: Ok. We added the following footnote to express the point, the first time the term  
1177 “reflectivity factor” is introduced in the paper (excluding the abstract). “Throughout the  
1178 paper we use the expression radar reflectivity factor, which is the quantity provided by  
1179 the radar (and expressed in  $\text{mm}^6\text{m}^{-3}$  or dBz) after conversion from the received power.  
1180 The radar reflectivity factor is different from reflectivity and is obtained in the special case  
1181 of Rayleigh approximation. Reflectivity is not the quantity that radars usually provide and  
1182 display on their screens although most of people refer to it.”  
1183  
1184 RC: For me “Probability of detection” and “Hit rate” is the same. What you defined with  
1185 Hit rate is the so-called “Hit score” e.g. following  
1186 <https://iri.columbia.edu/~jhansen/mason11july.pdf>  
1187  
1188 AR: Thank you for noting this point. We used the definition of the Wilks book (Chapter 7).  
1189 However, in the revised version of the paper only the POD is considered. Following the  
1190 remarks of the reviewer#1 we deleted the equations for the scores. This helped to have a  
1191 shorter paper. Also the scores were put in tables (not graphs), following a comment of  
1192 reviewer #2. Graphs of the scores are presented in the supplemental material (Section  
1193 S2).  
1194  
1195 RC: Translate the acronym “GPROF”  
1196  
1197 AR: It stands for Goddard Profiling Algorithm (added into the paper).  
1198  
1199 RC: Before you start to discuss the result, mention once how you name your different  
1200 experiments. It gets clear during the reading, but if you mention it once, you do not need  
1201 to repeat it later during the manuscript.  
1202  
1203 AR: Thanks for noting this point (also requested by reviewer#2). We did it at the start of  
1204 Section 4 (results). We also added a table (Table 3) to better clarify the point. Also the  
1205 supplemental material of the paper has a table (Table S1) specifying the types of  
1206 simulations considered.  
1207  
1208 RC: Page 19, line 570: you mean LIGHT instead of FLASH?  
1209 AR: Yes. It was an error. Corrected.  
1210  
1211 RC: Page 22, lines 673 to 677: You mention that reflectivity data assimilation helps to  
1212 better

1213 represent light precipitation events and lightning data helps to represent strong events.  
1214 One abstract later (lines 684 to 686) you argue the other way round. So, the influence of  
1215 the different observation types also depend on the situation.

1216 AR: Thanks for noting the point. We added the following sentence: "These results show  
1217 also that the influence of different observations depends on the meteorological situation."  
1218

1219  
1220 RC: Page 23, line 702: Start a new paragraph and sentence after the promising results  
1221 and the drawbacks.

1222 AR: Done.

1223  
1224 RC: What do you think is the reason for the increased false alarm rate in the RADLI  
1225 forecasts? How do you think you can improve the situation in future versions of the  
1226 system?

1227 AR: The reason for having more false alarms in RADLI forecasts compared to other  
1228 configurations is the larger amount of water vapour added to this kind of simulation, a  
1229 direct consequence of the addition of water vapour given by both radar and lightning. In  
1230 the supplemental material of this paper the evolution of the water vapour mass is  
1231 presented, including the assimilation stage. Results, as expected, show the largest  
1232 amount of water (not only in the vapour form) added to RADLI by data assimilation.  
1233 Possible ways to decrease false alarms in future versions of the software are shortly  
1234 introduced in Section 5 (Conclusion and discussion). We wrote: "To reduce the moisture  
1235 added by radar and lightning data assimilation further research is needed and different  
1236 approaches are possible (Fierro et al., 2016). In particular: a) assimilating for a shorter  
1237 time (0-6h in this paper); b) reducing the length-scales of the 3D-Var in the horizontal  
1238 directions to limit the spreading of the innovations or assuming an innovation equal to  
1239 zero for grid points without lightning and with zero reflectivity factor; c) reducing the  
1240 amount of water vapour added to the model (for example reducing the values of A and B  
1241 constants for lightning data assimilation or relaxing the request of saturation when radar  
1242 reflectivity is observed in areas where the model has zero reflectivity); d) adding moisture  
1243 to a shallower vertical layer.

1244 It is also noted that a combination of heating and moistening could provide the same  
1245 buoyancy with less water vapour addition (Marchand and Fulberg, 2014) and this  
1246 approach could be used in future studies."  
1247

1248  
1249 RC: Figures: Increase the sizes of the figures. You have space on the page to do this. If  
1250 not put only two instead of three Figures on one page as done for Figures 10 to 12 on  
1251 page 37.

1252  
1253 AR: We enlarged the figures in the revised version of the paper. We will consider this  
1254 point when revising the proofs of the paper, if accepted for publication.  
1255

1256

## 1257 References

1258  
1259 Federico, S.: Implementation of a 3D-Var system for atmospheric profiling data  
1260 assimilation into the RAMS model: Initial results, Atmospheric Measurement Techniques,  
1261 6(12),3563-3576,2013.  
1262

1263 Fierro, A. O., Mansell, E., Ziegler, C., and MacGorman, D.: Application  
1264 of a lightning data assimilation technique in the WRFARW model at  
1265 cloud-resolving scales for the tornado outbreak of 24 May 2011, Mon.  
1266 Weather Rev., 140, 2609&#8211;2627, 2012.  
1267  
1268 Fierro, A.O., Gao, I., Ziegler, C. L., Calhoun, K. M., Mansell, E. R.,  
1269 and MacGorman, D. R.: Assimilation of Flash Extent Data in the Variational  
1270 Framework at Convection-Allowing Scales: Proof-of-Concept and Evaluation  
1271 for the Short-Term Forecast of the 24 May 2011 Tornado Outbreak. Mon. Wea.  
1272 Rev., 144, 4373&#8211;4393, <https://doi.org/10.1175/MWR-D-16-0053.1>, 2016.  
1273  
1274 Marchand, M., and H. Fuelberg, 2014: Assimilation of lightning data  
1275 using a nudging method involving low-level warming. Mon. Wea. Rev., 142,  
1276 4850&#8211;4871, [doi:10.1175/MWR-D-14-00076.1](https://doi.org/10.1175/MWR-D-14-00076.1)  
1277  
1278 D. S. Wilks, Statistical Methods in the Atmospheric Sciences,  
1279 Academic Press, New York, NY, USA, 2006  
1280  
1281  
1282  
1283  
1284  
1285  
1286  
1287  
1288  
1289  
1290  
1291  
1292  
1293  
1294  
1295  
1296  
1297  
1298  
1299  
1300  
1301  
1302  
1303  
1304  
1305  
1306  
1307  
1308  
1309  
1310  
1311

1312 LIST OF THE MAJOR CHANGES MADE IN THE PAPER  
1313  
1314 -The Title was changed.  
1315  
1316 -The introduction was partially rewritten, especially in the part considering lightning data  
1317 assimilation.  
1318  
1319 -Section 3.1 had major revisions to specify the vertical grid of RAMS@ISAC model and to clarify the  
1320 role of domain D3 in the simulations of the Livorno case study.  
1321  
1322 -Section 3.2 underwent a substantial rewriting to clarify better how the radar reflectivity factor  
1323 data assimilation is performed. An example of analysis is introduced and all the details of the 3D-  
1324 Var setting have been hopefully clarified.  
1325  
1326 -Section 3.3 underwent a substantial rewriting to clarify better how lightning data assimilation  
1327 works. A sensitivity experiment to the formulation of lightning data assimilation was added in the  
1328 supplemental material.  
1329  
1330 -Section 4 underwent major revision. Three VSF are considered (revised version) instead of five  
1331 (first submission) to reduce the length of the paper and to avoid repetitive comments. Scores  
1332 were computed for three neighborhood radii and were put in tables (Table 4-6) according to  
1333 reviewers' comments.  
1334  
1335 -We added supplemental material to the paper. Specifically, in this supplement we study: a) the  
1336 relative contribution to the total water mass given by lightning and radar reflectivity factor data  
1337 assimilation (Section S.1); b) the sensitivity of the precipitation VSF to the nudging formulation  
1338 (Section S2). Also, the supplemental material gives different plots of Figures 15-17 (Section S3) and  
1339 the forward radar operator used in RAMS-3DVar (Section S4).  
1340  
1341 -Discussion and conclusions were changed according to the major revision.  
1342  
1343  
1344  
1345  
1346  
1347  
1348  
1349  
1350  
1351  
1352  
1353  
1354  
1355

Formattato: Colore carattere: Testo 1

Formattato: Inglese (Regno Unito)

1356 Preliminary results of the impact of lightning and radar reflectivity factor data  
1357 assimilation on the very short term rainfall forecasts of RAMS@ISAC: application to  
1358 two case studies in Italy

Formattato: Tipo di carattere: Grassetto, Inglese americano

Formattato: Tipo di carattere: Grassetto, Inglese americano

1359  
1360 Stefano Federico<sup>1</sup>, Rosa Claudia Torcasio<sup>1</sup>, Elenio Avolio<sup>2</sup>, Olivier Caumont<sup>3</sup>, Mario Montopoli<sup>1</sup>,  
1361 Luca Baldini<sup>1</sup>, Gianfranco Vulpiani<sup>4</sup>, Stefano Dietrich<sup>1</sup>

Eliminato: The impact of lightning and radar data assimilation on the performance of very short term rainfall forecast for two case studies in Italy

Eliminato: <sup>2</sup>

- 1362
- 1363 1. ISAC-CNR, via del Fosso del Cavaliere 100, Rome, Italy
  - 1364 2. ISAC-CNR, zona Industriale comparto 15, 88046 Lamezia Terme, Italy
  - 1365 3. CNRM UMR 3589, University of Toulouse, Météo-France, CNRS, 42 avenue G. Coriolis,  
1366 31057 Toulouse, France
  - 1367 4. Dipartimento Protezione Civile Nazionale Ufficio III - Attività Tecnico Scientifiche per la  
1368 Previsione e Prevenzione dei Rischi, 00189 Rome

Formattato: Inglese (Regno Unito)

1369 **Abstract**  
1370

1371 In this paper, we study the impact of lightning and radar reflectivity factor data assimilation on the  
1372 precipitation VSF (Very Short-term Forecast, 3 hours in this study) for two relevant case studies  
1373 occurred in Italy. The first case refers to a moderate and localised rainfall over central Italy  
1374 occurred on 16 September 2017. The second case, occurred on 9 and 10 September 2017, was  
1375 very intense and caused damages in several geographical areas, especially in Livorno (Tuscany)  
1376 where nine people died.

Eliminato: the

Eliminato: C

Eliminato: happened

Eliminato: ,

Eliminato: occurred

Eliminato: causing

Eliminato: 9

Eliminato: lost their life

1377 The first case study was missed by several operational forecasts (from both public and private  
1378 sectors), including that performed by the model used in this paper, while the Livorno case was  
1379 partially predicted by operational models.

1380 We use the RAMS@ISAC model (Regional Atmospheric Modelling System at Institute for  
1381 Atmospheric Sciences and Climate of the Italian National Research Council), whose 3D-Var  
1382 extension to the assimilation of RADAR reflectivity factor is shown in this paper for the first time.

1383 Results for the two cases show that the assimilation of lightning and radar reflectivity factor,  
1384 especially when used together, have a significant and positive impact on the precipitation  
1385 forecast. For specific time intervals, the data assimilation is of practical importance for civil  
1386 protection purposes because changes a missed forecast of intense precipitation ( $\geq 40$  mm/3h) in a  
1387 correct one.

Eliminato: The improvement compared to the control model, not assimilating lightning and radar reflectivity factor, is systematic because occurs for all the Very Short-term Forecast (VSF, 3h) of the events considered.

Eliminato: it transforms

Eliminato: >

Eliminato: forecast

Formattato: Interlinea: multipla 1.15 ri

Eliminato:

Eliminato: in the forecast assimilating both types of data

Eliminato: ¶

1388 While there is an improvement of the rainfall VSF thanks to lightning and radar reflectivity factor  
1389 data assimilation, its usefulness is partially reduced by the increase of the false alarms, especially  
1390 when both data area assimilated.

1391 **Keywords:** data assimilation, lightning, radar reflectivity factor, RAMS@ISAC.

Formattato: Tipo di carattere: Non Grassetto

Formattato: Tipo di carattere: Non Grassetto

1392  
1393 **1. Introduction**

1416 Initial conditions of numerical weather prediction (NWP) models are a key point for a good  
 1417 forecast (Stensrud and Fritsch, 1994; Alexander et al., 1999). Nowadays limited area models are  
 1418 operational at the resolution of few kilometres (< 5 km) and data assimilation of non-conventional  
 1419 observations, as lightning or radar data, is crucial to correctly represent the state of the  
 1420 atmosphere at local scale (Weisman et al., 1997; Weygandt et al., 2008). This is especially  
 1421 important over the sea, where the absence of local observations and model deficiencies can  
 1422 misrepresent convection.

1423 The assimilation of radar reflectivity factor<sup>1</sup> is useful to improve the weather forecast, considering  
 1424 the high repetition rate (asynoptic data) and the high spatial resolution (local scale) of the radar  
 1425 data.

1426 First attempts to assimilate radar reflectivity factor are reported in Sun and Crook (1997, 1998),  
 1427 who expanded VDRAS (Variational Doppler Radar Analysis System) to include microphysical  
 1428 retrieval. Following these studies, several systems to assimilate radar observations, both Doppler  
 1429 velocity and reflectivity factor, were developed (Xue et al., 2003; Zhao et al., 2006; Xu et al., 2010).  
 1430 All these studies showed the stability and robustness of assimilating radar observations as well as  
 1431 the improvement of weather forecast.

1432 Radar data are also assimilated in WRF (Weather Research and Forecasting model, Skamarock et  
 1433 al., 2008; Barker et al., 2012) both using 3DVar (Xiao et al., 2005, 2007; Barker et al., 2004) and  
 1434 4DVar (Wang et al., 2013; Sun and Wang, 2012). The capability to assimilate radar data into WRF  
 1435 was recently applied to a heavy rainfall event over Central Italy by Maiello et al. (2014). They  
 1436 showed a notable and positive impact of the radar data assimilation on the precipitation forecast,  
 1437 also when radar data were assimilated together with conventional data (SYNOP and RAOB).

1438 In addition to direct methods, which assimilate the radar reflectivity factor adjusting the  
 1439 hydrometeor contents, there are indirect methods adjusting other variables. In particular, the  
 1440 method of Caumont et al. (2010) acts on the relative humidity field. It consists of two different  
 1441 steps: a 1D retrieval of relative humidity (pseudo-profile), which depends on the radar reflectivity  
 1442 factor observations, followed by 3D-Var assimilation of the pseudo-profile. This method has the  
 1443 advantage to reduce the computational cost at the kilometeric scale.

<sup>1</sup> Throughout the paper we use the expression radar reflectivity factor, which is the quantity provided by the radar (and expressed in mm<sup>6</sup>m<sup>-3</sup> or dBz) after conversion from the received power. The radar reflectivity factor is different from reflectivity and is obtained in the special case of Rayleigh scattering. Reflectivity is not the quantity that radars usually provide and display on their screens although most of people refer to it.

Formattato: Inglese (Regno Unito)

Eliminato: asynoptic local observati

Eliminato: s

Formattato: Inglese (Regno Unito)

Formattato: Inglese (Regno Unito)

Eliminato: the

Eliminato: important

Eliminato: because, being the reflectivity factor related to both the hydrometeors types and size, it can add information and eventually change the weather forecast. This is particularly important

Eliminato: The f

Eliminato: the

Eliminato: an

Eliminato: to the

Eliminato: model

Eliminato: approaches

Eliminato: are

Eliminato: those

Eliminato: , which assimilate

Eliminato: directly perturbing

Eliminato: predicted by the forecast models

Eliminato: that aim

Eliminato: at modifying

Eliminato: proposed

Eliminato: by

Eliminato: filed

Eliminato: , though less direct than perturbing hydrometeors,

Eliminato: , and to avoid questionable assumptions of the direct methods

Formattato: Inglese americano

Formattato: Apice

Formattato: Apice

Formattato: Inglese (Regno Unito)

Formattato: Inglese (Regno Unito)

Formattato: Inglese (Regno Unito)

Formattato: Inglese (Regno Unito)



1472 The choice of updating the moisture field directly is motivated by its greater impact on analyses  
 1473 and forecasts in comparison to that of hydrometeor-related quantities (e.g., Fabry and Sun, 2010).  
 1474 Caumont et al. (2010) showed that the method improved the weather prediction of a heavy  
 1475 precipitation event in southern France and of a eight-day long assimilation cycle experiment.  
 1476 The method was applied in other studies (Wattrelot et al., 2014, using AEROME model; Ridal and  
 1477 Dalbom, 2017; using HARMONIE model), or modified using 4D-Var in place of 3D-Var (Ikuta and  
 1478 Honda, 2011; using JNoVa model) showing its capability to improve the weather forecast. The  
 1479 method is also used in the operational context (Wattrelot et al., 2014).  
 1480 Flashes are another important source of asynoptic data due to their ability to locate precisely the  
 1481 convection with few temporal gaps (Mansell et al., 2007). In the last two decades, there have been  
 1482 attempts to assimilate lightning into meteorological models both at low horizontal resolution,  
 1483 which need a cumulus parameterization scheme to simulate convection, and at convection  
 1484 permitting scales.  
 1485 The first attempts to assimilate lightning in NWP models were based on relationships between  
 1486 lightning and rainfall rate estimated by microwave sensors on board polar satellites (Alexander et  
 1487 al., 1999; Chang et al., 2001; Jones and Macpherson, 1997; Pessi and Businger, 2009). In this  
 1488 approach, the rainfall rate was computed as a function of lightning observations and then  
 1489 transformed into latent heat, which was assimilated. The results of these studies showed a  
 1490 positive impact of lightning data assimilation on the forecast up to 24h also for fields at the large  
 1491 scale, as sea-level pressure.  
 1492 The study of Papadopoulos et al. (2005) used lightning to locate convection and the model water  
 1493 vapour profile was nudged towards vertical profiles recorded during convective events.  
 1494 Mansell et al. (2007) modified the Kain-Fritsch (Kain and Fritsch, 1993) cumulus convective scheme  
 1495 to force convection when/where flashes are observed while the convective scheme was not  
 1496 activated in the model simulation, demonstrating the potential of lightning to improve the  
 1497 convection forecast. A similar approach was introduced by Giannaros et al. (2016) into WRF  
 1498 showing the positive impact of lightning data assimilation on the precipitation forecast up to 24h  
 1499 for eight convective events occurred over Greece.  
 1500 Fierro et al. (2012) introduced a methodology to assimilate lightning at convection permitting  
 1501 scales by modifying the water vapour mixing ratio simulated by the WRF according to a function  
 1502 depending on the flash-rate and on the simulated graupel mixing ratio. The water vapour could be  
 1503 assimilated by nudging (Fierro et al., 2012) or 3D-Var (Fierro e al., 2016).

- Eliminato:** was able to improve
- Eliminato:** for
- Eliminato:** a case of
- Eliminato:** for
- Eliminato:** 6; Muller et al., 2017
- Eliminato:** in all cases
- Eliminato:** Lightning
- Eliminato:** as well as, availability in real time thanks to the low bandwidth required for data transfer
- Eliminato:** For these reasons, i
- Eliminato:** numerical weather prediction
- Eliminato:** (NWP)
- Formattato:** Inglese (Regno Unito)
- Formattato:** Inglese (Regno Unito)
- Eliminato:** , encouraging further researches
- Formattato:** Tipo di carattere: (Predefinito) Calibri, 12 pt, Colore carattere: Nero, Inglese (Regno Unito), Bordo: : (Nessun bordo)
- Formattato:** Bordo: Superiore: (Nessun bordo), Inferiore: (Nessun bordo), A sinistra: (Nessun bordo), A destra: (Nessun bordo), Tra : (Nessun bordo), Barra : (Nessun bordo)
- Formattato:** Tipo di carattere: (Predefinito) Calibri, 12 pt, Colore carattere: Nero, Inglese (Regno Unito), Bordo: : (Nessun bordo)
- Formattato:** Inglese (Regno Unito)
- Eliminato:** correctly locate
- Formattato:** Inglese (Regno Unito)
- Formattato:** Inglese (Regno Unito)
- Eliminato:** the
- Eliminato:** model
- Eliminato:** the
- Eliminato:** model

1522 Qie et al. (2014), using WRF, extended the methodology of Fierro et al. (2012) to assimilate ice  
1523 crystals, graupel and snow, showing promising results for deep convective events in China.

1524 Fierro et al. (2015) studied the performance of the Fierro et al. (2012) method for 67 days  
1525 spanning the 2013 warm season over the CONUS giving a statistically robust estimation of the  
1526 performance of the method. The computationally inexpensive lightning data assimilation method  
1527 improved considerably the short-term ( $\leq 6h$ ) precipitation forecast of high impact weather.

1528 Lynn et al. (2015) and Lynn (2017) also applied the method of Fierro et al. (2012) to boost the local  
1529 thermal buoyancy where/when lightning is observed. Results show that lightning data assimilation  
1530 improved lightning forecast. Importantly, Lynn et al. (2015) offer an approach to address spurious  
1531 convection (i.e., convection removal), which is a far more challenging problem to tackle.

1532 Federico et al. (2017a) implemented the methodology of Fierro et al. (2012) in RAMS@ISAC  
1533 model, showing the systematic and significant improvement of the precipitation forecast at the  
1534 very short range (3h) for twenty case studies occurred over Italy; the impact of lightning data  
1535 assimilation for longer time ranges (6h-24h; Federico et al., 2017b) showed considerable impact  
1536 on the 6h precipitation forecast, with smaller (negligible) effects at 12 h (24 h).

1537 In this paper, we study the impact of radar reflectivity factor and lightning data assimilation on the  
1538 very short term (3h) rainfall prediction for two case studies over Italy. We use the method of  
1539 Fierro et al. (2012) to assimilate lightning and the method of Caumont et al. (2010) to assimilate  
1540 the radar reflectivity factor. The case studies occurred in September 2017. The first case, hereafter  
1541 also referred to as Serano, occurred on 16 September, was characterized by moderate-intense and  
1542 localized rainfall. The second case, hereafter also referred to as Livorno, occurred on 09-10  
1543 September, was characterized by deep convection and very intense precipitation in several parts  
1544 of Italy. Even if the Livorno case occurred before the Serano case, we reverse the chronological  
1545 order in the discussion, ordering the event from the less intense to the most intense.

1546 The forecast of severe events at the local scale still remains a challenge because of the multitude  
1547 of physical processes involved over a wide range of scales (Stensrud et al., 2009). The Serano case  
1548 study, being localized in space, poses challenges in forecasting the exact position and timing of  
1549 convection initiation; the Livorno event involves the interaction between a high impact storm and  
1550 the complex orography of Italy, which is difficult to simulate at the local scale. For the above  
1551 reasons the forecast of both events was challenging, as confirmed by the poor forecast of  
1552 RAMS@ISAC. The difficulty to forecast timely and accurately the precipitation field is the reason  
1553 for choosing them as test cases.

Formattato: Inglese americano

Formattato: Inglese americano

Formattato: Inglese americano

Eliminato: obtaining the

Eliminato: a

Eliminato: the

Eliminato: observations

Eliminato: of

Eliminato: Federico

Eliminato: 7a

Eliminato: on

Eliminato: named

Eliminato: case

Eliminato: named

Eliminato: case

Eliminato: will

Eliminato: occurrence

Eliminato: ¶

T

Eliminato:

Eliminato: was missed by the control forecast, not assimilating radar reflectivity factor and lightning

Eliminato: .

Eliminato: T

Eliminato: was partially predicted by the control forecast, which missed the abundant precipitation over Central Italy (see Section 4), and predicted the intense precipitation over Livorno delayed compared to the observations

Eliminato:

1580 This paper presents for the first time the assimilation of the total lightning (intra cloud + cloud to  
1581 ground) and radar reflectivity factor in RAMS@ISAC model and shows how the assimilation of the  
1582 radar reflectivity factor works together with total lightning data assimilation. Also, this paper shows  
1583 how accurate in space and time can be the forecast of the precipitation field using cloud scale  
1584 observations over complex terrain, contributing in this way to a number of works on the same  
1585 subject.

1586 The paper is organized as follows: Section 2 gives details on the synoptic environment of the case  
1587 studies showing daily precipitation, lightning and radar observations; Section 3 gives details on the  
1588 meteorological model, lightning and radar data assimilation; Section 4 shows the results for three  
1589 very short-term forecast (VSF), one for Serano and two for Livorno; Discussion and conclusions are  
1590 given in Section 5. This paper has additional material where we discuss: a) how lightning and radar  
1591 reflectivity factors data assimilation adjust the total water field; b) the sensitivity of the results to  
1592 the choice of key parameters of lightning data assimilation.

1593

## 1594 2. The case studies

### 1595 2.1 The 16 September 2017 (Serano) case study

1596 During the 16 September 2017, Italy was under the influence of a cyclone that developed to the lee  
1597 of the Alps. The storm crossed Italy from NW to SE leaving light precipitation over most of the  
1598 peninsula with moderate rainfall over Central Italy. Figure 1 shows the precipitation recorded by  
1599 the Italian raingauge network on 16 September 2017. Light precipitation ( $\leq 5$  mm/day) is reported  
1600 by 1018 raingauges out of the 1666 stations measuring precipitation ( $\geq 0.2$  mm/day) on this day.  
1601 Fourteen stations over Central Italy recorded more than 50 mm/day. The maximum precipitation  
1602 was 90 mm/day in Città di Castello (Umbria Region, Figure 1). Because the meteorological radar  
1603 closest to the maximum precipitation is over mount Serano (Figure 1), hereafter this event will be  
1604 referred to as Serano.

1605 The synoptic condition during the event is shown in Figure 2. At 500 hPa (Figure 2a) a trough,  
1606 elongated in the SW-NE direction, extends over Western Europe and air masses are advected from  
1607 SW towards western Alps. The interaction between the airflow and the Alps generates a low  
1608 pressure to the lee of the Alps over Northern Italy.

1609 The analysis at the surface (Figure 2b) shows the meteorological front represented by the  
1610 equivalent potential temperature gradient between air masses advected over the Mediterranean

**Eliminato:** With respect to previous works, this study investigates the benefits brought by the combined use of radar and lightning observations into RAMS@ISAC, paving the way to systematic improvements of weather forecasts. ¶

**Eliminato:** is

**Eliminato:** , for specific times,

**Eliminato:** five

**Eliminato:** two

**Eliminato:** three

**Eliminato:** the whole Italian country w

**Eliminato:** on

**Eliminato:**

**Eliminato:** A I

**Eliminato:** below

**Formattato:** Inglese (Regno Unito)

**Eliminato:** and 6 stations more than 60 mm/day

**Formattato:** Colore carattere: Testo 1

**Eliminato:** on this day

**Formattato:** Colore carattere: Testo 1

**Formattato:** Colore carattere: Testo 1

**Eliminato:** mountain

**Formattato:** Colore carattere: Testo 1

**Formattato:** Colore carattere: Testo 1

**Eliminato:** o

**Formattato:** Colore carattere: Testo 1

**Eliminato:** the

**Eliminato:** the

**Eliminato:** , at low levels, on the lee

**Eliminato:** situation

1633 Sea from NW and air masses advected from the South over the Tyrrhenian Sea, **Notable is the**  
 1634 feeding of warm unstable air masses towards Central Italy.

1635 Infrared satellite images (Figure 3), from 00 UTC on 16 September to 00 UTC on 17 September,  
 1636 show the cold front structure moving slowly from NW **to** SE. Interestingly, at 00 UTC on 16  
 1637 September, it is apparent **the** well-defined cloud system over Central Italy (red circle of Figure 3a),  
 1638 which **caused** most of the daily precipitation observed between 43.50 **N** and 45.0 N in the six-  
 1639 hours **00 UTC-06 UTC** on 16 September,

1640 The well-defined cloud system over Central Italy is also **evident** in the radar Constant Altitude Plan  
 1641 Position Indicator (CAPPI) at 3 km above sea level at 02 UTC on 16 September (Figure 4). This  
 1642 CAPPI is formed by interpolating all the available data from the federated Italian radar network  
 1643 coordinated by the Department of Civil Protection (twenty-two radars, see Section 3.3 for their  
 1644 positions) and it is also referred **to** as the national radar composite (hereafter also mosaic). Several  
 1645 convective cells exceeding 35 dBz can be noted **over** central-northern Italy. Importantly, the cloud  
 1646 system over Central Italy shown by the satellite infrared channel at 00 UTC (Figure 3a) and that of  
 1647 the **radar** at 02 UTC have **similar positions, showing that** the cloud system **was active** for several  
 1648 hours over Central Italy,

1649 Figure 5 shows lightning recorded by the LINET network (Betz et al., 2009) on 16 September 2017.  
 1650 More than **105.000** flashes were recorded **during the day**; most of them occurred during the  
 1651 afternoon and evening, **but** a secondary maximum occurred **in the night, from 00 UTC to 06 UTC**.  
 1652 In this **phase**, more than **3000** flashes were observed **over** Central Italy.

1653

1654 **2.2 The 09-10 September 2017 (Livorno) case study**

1655 During the days 09 and 10 September 2017, Italy was hit by a severe storm characterised by  
 1656 intense and widespread rainfall over the country. **Figure 6a shows the precipitation on 09**  
 1657 **September recorded by the Italian raingauge network. Rainfall was intense over the Alps, where**  
 1658 **the maximum daily precipitation was observed (193 mm/day) and over Liguria, with precipitation**  
 1659 **of the order of 30-50 mm/day. One station over Tuscany reported 90 mm/day, showing that**  
 1660 **intense precipitation already started over the Region. The intensity of the storm on 09 September**  
 1661 **was high because 20 raingauges reported more than 100 mm/day and 70 raingauges more than 60**  
 1662 **mm/day, and, in most cases, this precipitation occurred within few hours.**

1663 The following day (see Figure 6b) had higher rainfall. Precipitation occurred mainly over Central  
 1664 Italy, especially over Lazio, and over Northern Italy, in particular the North-East. In Tuscany, the

**Eliminato:** , as a consequence of the pressure pattern that forms over the area

**Eliminato:** It is also n

**Eliminato:** 2017

**Eliminato:** towards

**Eliminato:** a

**Eliminato:** produced

**Eliminato:** between

**Eliminato:** C and

**Eliminato:** 2017

**Eliminato:** clear

**Eliminato:** n

**Eliminato:** on

**Eliminato:** CAPPI

**Eliminato:** a

**Eliminato:** and

**Eliminato:** insisted

**Eliminato:** (00-06 UTC)

**Eliminato:** 60

**Eliminato:** for

**Eliminato:** whole

**Eliminato:** (the peak of more than 8000 flashes in one hour was at 22 UTC),

**Eliminato:**

**Eliminato:** during

**Eliminato:** on 16 September

**Eliminato:** form

**Eliminato:** phase

**Eliminato:** 2

**Eliminato:** in

**Eliminato:** (see the green-blue dots in Figure 5)

**Eliminato:** From lightning observations, it follows that the storm had two main phases over Central Italy: the first one occurred during the night (00-06 UTC) and was characterised by the most intense rainfall; the second started after 18 UTC. In Section 4 one VSF for each phase will be considered.¶

**Eliminato:** Damages to property were reported in several parts of Italy, while nine people died around Livorno, in Tuscany for causes related to the storm. ¶

**Eliminato:** more

**Eliminato:** in

**Eliminato:** For example, the precipitation over Tuscany fell in the last 6 h of the day.

**Formattato:** Inglese (Regno Unito)

1708 two stations close to the sea, in the Livorno area, recorded about 150 mm/day mostly fallen in the  
 1709 hours between 00 and 06 UTC. The rainfall on 10 September was abundant: and 60 raingauges  
 1710 recorded more than 100 mm/day.  
 1711 Synoptic conditions leading to this storm are shown in Figure 7. At 500 hPa (Figure 7a) a trough  
 1712 extends from Northern Europe towards the Mediterranean. The interaction between the air-  
 1713 masses and Western Alps generated a depression to the lee of the Alps, which crossed the whole  
 1714 peninsula from NW to SE. It is noted the divergent flow over Central and Northern Italy favouring  
 1715 upward motions.  
 1716 At the surface, Figure 7b, it is evident the equivalent temperature gradient over the western  
 1717 Mediterranean caused by the contrast between air masses pre-existing over the sea and air  
 1718 masses advected from France towards the Mediterranean. The pressure field at the surface  
 1719 advects air masses from the South over the Tyrrhenian Sea. These warm and humid air masses  
 1720 feed the cyclone during its development.  
 1721 From a synoptic point of view, Livorno and Serano cases are similar and represent two cyclones  
 1722 developing to the lee of the Alps (Buzzi and Tibaldi, 1978). However, the Livorno case is more  
 1723 intense than Serano as shown by the larger rainfall occurred in the former case,  
 1724 The notable intensity of the Livorno case is confirmed by lightning observations (Figure 8). During  
 1725 the evening on 9 September (after 18 UTC) about 38.000 flashes were recorded by LINET. On 10  
 1726 September about 290.000 flashes were recorded over Italy, following the movement of the storm  
 1727 propagating from NW to SE. So, more than 300.000 flashes were recorded from 18 UTC on 09  
 1728 September to 00 UTC on 11 September, which are more than three times those recorded for  
 1729 Serano.  
 1730 Thermal infrared satellite images (channel, 10.8 micron; Figure 9) show the extension of the cloud  
 1731 coverage every 12 hours. It is well evident the cloud system associated with the cold front over  
 1732 Europe. More specifically, the satellite image at 00 UTC shows the cloud system over Livorno area  
 1733 (red circle in Figure 9b), before the main precipitation event over Tuscany (00-06 UTC), while  
 1734 Figure 9c shows the cloud system over Central Italy (orange circle), at the end of the period of  
 1735 intense precipitation over Lazio (06-12 UTC).  
 1736 We conclude the synoptic analysis of the case study with two CAPPI at 3 km observed by the radar  
 1737 network of the Department of Civil Protection. The CAPPI in Figure 10a, at 00 UTC on 10  
 1738 September, shows the cloud system over Tuscany with reflectivity factor up to 40 dBz. Other

- Eliminato: 256 stations out of 2065 stations reported more than 60 mm/day,
- Eliminato: of which
- Eliminato: represented
- Eliminato: by the situation at 00 UTC on 10 September, shown
- Eliminato: , when the storm was already producing precipitation over Northern Italy.
- Eliminato: s
- Eliminato: on the lee
- Eliminato: over Northern Italy,
- Eliminato: , in the following hours,
- Eliminato: also
- Eliminato: apparent
- Eliminato: Sea
- Eliminato: The cyclonic circulation over the Ligurian Sea is forced by the low-pressure over the Northern Italy.
- Eliminato: are unstable, i.e. humid and warm, and
- Eliminato: the
- Eliminato: this storm
- Eliminato: the
- Eliminato: on the lee
- Eliminato:
- Eliminato: , as well as by the more unstable air masses over the Tyrrhenian Sea that characterise the Livorno case
- Eliminato: also
- Eliminato: distribution
- Eliminato: associated with
- Eliminato: the propagation of the storm from NW to SE
- Eliminato: 170
- Eliminato: along
- Eliminato: 2
- Eliminato: twice
- Eliminato:
- Eliminato: S
- Eliminato: thermal infrared
- Eliminato: that extends
- Eliminato: and moves from north-west to south-east
- Eliminato: of

1778 clouds cause rainfall over northern Italy. The CAPPI of Figure 10a is the last assimilated by the 00-  
1779 03 UTC VSF on 10 September shown in Section 4.2.1.  
1780 Figure 10b shows the CAPPI of the national radar mosaic at 3 km above the sea level and at 06  
1781 UTC. The cloud system is moving towards Central Italy with reflectivity up to 45 dBz. Other cloud  
1782 systems are apparent over northern Italy. Figures 10a-10b well represent the movement of the  
1783 storm towards SE and Figure 10b shows the last CAPPI assimilated by the 06-09 UTC VSF shown in  
1784 Section 4.2.2.

1785

### 1786 3.Data and Methods

#### 1787 3.1 RAMS@ISAC and simulations set-up

1788 The RAMS@ISAC is used as NWP driver in this work. The model is based on the RAMS 6.0 model  
1789 (Cotton et al., 2003) with the addition of four main features, as well as a number of minor  
1790 improvements. First, it implements additional single moment microphysical schemes, whose  
1791 performance is shown in Federico (2016): among them, the WSM6 (Hong and Lim, 2006) is used in  
1792 this paper. Second, it predicts the occurrence of lightning following the diagnostic method of Dahl  
1793 et al. (2011), the implementation being discussed in Federico et al. (2014). Third, the model  
1794 assimilates lightning through nudging (Fierro et al., 2012, 2015; Federico et al., 2017a). Fourth, the  
1795 model implements a 3D-Var data assimilation system (Federico, 2013, hereafter also RAMS-  
1796 3DVar), whose extension to the radar reflectivity factor is presented in this paper (Section 3.3).

1797 The list of the main physical parameterisation schemes used in the simulations of RAMS@ISAC is  
1798 shown in Table 1.

1799 Considering the domains and the configuration of the grids (Figure 11 and Table 2), two different  
1800 set-ups are used for Serano and Livorno. For the first case, we use the domains D1 and D2, while  
1801 for Livorno we use also the domain D3. The first domain covers a large part of Europe and extends  
1802 over the North Africa. For this domain, the horizontal resolution of the grid is 10 km (R10). The  
1803 second domain extends over the whole Italy and part of Europe and the grid has 4 km horizontal  
1804 resolution (R4). The third domain covers the Tuscany Region, has 4/3 km horizontal resolution  
1805 (R1), and it is used for Livorno to represent with higher spatial detail the precipitation field over

1806 Tuscany. The fine structures of the precipitation field are smeared out over Tuscany using only  
1807 domains D1 and D2. The operational implementation of the RAMS@ISAC model uses the domains  
1808 D1 and D2 and no refinements for specific areas of Italy are used because Italy is a complex

Eliminato: are producing

Eliminato: The cloud system remained stationary over Tuscany for the period 00-06 UTC, with new cells developing over the sea and moving towards the land for six hours, causing the flood in Livorno.

Eliminato: VSF of

Eliminato: s

Eliminato: for the numerical experiments of

Eliminato: ology

Eliminato: 2

Eliminato: and

Eliminato: and performance of the scheme is

Eliminato: can

Eliminato: shown

Eliminato: the

Eliminato: discussed in this paper

Eliminato: third

Eliminato: more

1827 orography country and grid refinements for a specific event can be done only a-posteriori, i.e.  
1828 after the occurrence of the event.

1829 The resolution and the extension of the grids in the vertical direction is the same for the three  
1830 domains. The vertical grid covers the troposphere and the lower stratosphere. Vertical levels have  
1831 different spacings and are more packed close to the ground. Among the 36 levels used in this  
1832 paper 10 are below 1 km, 15 below 2 km and 18 below 3 km. The first vertical level is at 24 m  
1833 above the surface in the terrain following coordinates used by RAMS@ISAC, the level 21 is at 5200  
1834 m. Above 6 km the model levels are about 1000 m apart, with a maximum of 1200 m for the  
1835 vertical layer at the model top.

1836 The vertical grid is the same as the operational setting of RAMS@ISAC and is a compromise  
1837 between vertical resolution and computing time. In the future, the number of vertical levels will  
1838 be increased to better resolve the phenomena in this direction (Planetary Boundary Layer  
1839 processes, vertical motions, interaction between air masses and orography etc.), nevertheless the  
1840 current setting was used successfully in the forecast of several heavy precipitation events over  
1841 Italy. The nesting between the first and second domains is one-way, while the nesting between

1842 the second and the third domains is two-way.  
1843 VSF is implemented as shown in Figure 12. First a run with R10 configuration is performed using  
1844 the 0.25° horizontal resolution GFS analysis/forecast cycle issued at 12 UTC as initial and boundary  
1845 conditions. R10 run, which starts at 12 UTC on 16 September for Serano and at 12 UTC on 09  
1846 September for Livorno, lasts 36 h and doesn't assimilate neither radar reflectivity factor nor  
1847 lightning. The R10 run is not updated after the acquisition of new data by the analysis system and  
1848 this is a limitation of the results shown in this paper.

1849 Starting from 12 UTC, ten VSF are performed using R4 for Serano, and both R4 and R1 for Livorno.  
1850 The VSF lasts 9h and uses R10 simulation as initial and boundary conditions (one-way nesting). The  
1851 9h forecast is divided into two parts: the first six hours are the assimilation stage when  
1852 RAMS@ISAC simulation is adjusted by data assimilation, whereas the last three hours are the  
1853 forecast stage, without data assimilation. During the assimilation stage, flashes are assimilated by  
1854 nudging (Section 3.2), while radar reflectivity factor is assimilated every one-hour by RAMS-3DVar  
1855 (Caumont et al. (2010), Section 3.3).

1856 It is noted that data assimilation is performed over the domain D2 (R4) only, and the innovations  
1857 are transferred to the domain D3 (R1), for the Livorno case, by the two way-nesting. The domain  
1858 D3 is used for the Livorno case to refine the resolution of the precipitation field over Tuscany and

Eliminato: .

Eliminato: s

Eliminato: s

Eliminato: are

Eliminato:

Eliminato: and

Formattato: Car. predefinito paragrafo, Inglese (Regno Unito)

Formattato: Car. predefinito paragrafo, Inglese (Regno Unito)

Formattato: Car. predefinito paragrafo, Inglese (Regno Unito)

Formattato: Car. predefinito paragrafo, Inglese (Regno Unito)

Eliminato: ¶

Formattato: Car. predefinito paragrafo, Inglese americano

Eliminato: s

Eliminato: The

Eliminato: using the

Eliminato:

Eliminato: This

Eliminato: (

Eliminato: )

Eliminato: or

Eliminato: (

Eliminato: )

Eliminato: when the assimilated source of observations are continuously used to constrain the VSF to the observations

Eliminato: dedicated to

Eliminato: when the VSF freely evolve without external constrains

Eliminato: with the

Eliminato: technique

Eliminato: the

Eliminato: ) method (

Eliminato: in

1886 to show the spatial and temporal precision of the precipitation forecast over Tuscany using data  
 1887 assimilation. However, its usage is exceptional because, as stated above, Italy is a complex  
 1888 orography country and grid refinements for specific areas are used only after the occurrence of  
 1889 the event. For this reason the domain D3 is usually not used in RAMS@ISAC and no statistics about  
 1890 the background error are available for this grid.

1891 Because lightning and radar reflectivity factor are cloud scale observations, their assimilation at  
 1892 higher horizontal resolution by 3D-Var is foreseeable in future works.

1893 The verification of the VSF for precipitation is done by visual comparison of the model output with  
 1894 the raingauge network of the Department of Civil Protection, which has more than 3000  
 1895 raingauges all over Italy.

1896 In addition we consider the FBIAS (Frequency Bias; range  $[0, +\infty)$ ), where 1 is the perfect score,  
 1897 i.e. when no misses and false alarms occur), POD (Probability of Detection; range  $[0, 1]$ , where 1 is  
 1898 the perfect score and 0 the worst value) and ETS (Equitable Threat Score; range  $[-1/3, 1]$ , where 1  
 1899 is the perfect score and 0 is a useless forecast). Scores are computed from 2x2 dichotomous  
 1900 contingency tables (Wilks, 2006) for different rainfall thresholds.

### 1901 3.2 Lightning data assimilation

1903 Lightning data are provided by LINET (Lightning detection NETWORK; Betz et al., 2009;  
 1904 www.nowcast.de) which has more than 500 sensors worldwide with the greatest density over  
 1905 Europe (more than 200 sensors). The network has a good coverage over Central Europe and  
 1906 Western Mediterranean (from 10 W to 35 E and from 30 N to 60 N). The area of good coverage  
 1907 includes the region considered in this paper.

1908 LINET exploits the VLF/LF electromagnetic bands and provides measurements of both intra-cloud  
 1909 (IC) and cloud to ground (CG) discharges. IC strokes are detected as long as lightning occurs within  
 1910 120 km from the nearest sensor thanks to an optimised hardware and advanced techniques of  
 1911 data processing (TOA-3D, Betz et al., 2004). According to Betz et al. (2009), LINET has a location  
 1912 accuracy of 125 m for an average distance of 200 km among the sensors verified by strikes into  
 1913 towers of known positions.

1914 The good performance of the LINET network and its ability to detect IC strokes is shown in  
 1915 Lagouvardos et al. (2009) for a storm in southern Germany, while the good performance over  
 1916 Italy, including both CG and IC strokes, is discussed in Petracca et al. (2014).

1917 Lightning data assimilation scheme is that of Fierro et al. (2012; 2015) and uses the total lightning,  
 1918 i.e. intra-cloud plus cloud to ground flashes.

**Formattato:** Interlinea: 1.5 righe

**Eliminato:** ,

**Eliminato:** and HR (Hit Rate or correct proportion; range  $[0, 1]$ , where 1 is the perfect score and 0 the worst value)

**Eliminato:** (0.2 mm/3h, 1mm/3h and from 2mm/3h to the maximum thresholds, i.e. 40 mm/3h for Serano and 60 mm/3h for Livorno, every 2 mm/3h)

**Eliminato:** In particular, defining the hits ( $a$ , a hit occurs when both the precipitation forecast and the corresponding raingauge observation are above or equal to a rainfall threshold), false alarms ( $b$ , a false alarm occurs when the precipitation forecast is above or equal to a rainfall threshold, while the corresponding raingauge observation is below the threshold); misses ( $c$ , a missing occurs when the forecast precipitation is below a rainfall threshold, while the corresponding raingauge observation is above or equal to the threshold); ( $d$ , a correct no forecast occurs when both the precipitation forecast and the corresponding observation are below a rainfall threshold), we have:<sup>¶</sup>

$$FBIAS = \frac{a + b}{a + c}$$

$$POD = \frac{a}{a + c}$$

$$ETS = \frac{a - a_r}{a + b + c - a_r}; \quad a_r = \frac{(a + b)(a + c)}{a + b + c + d} \quad (1)^{\ddagger}$$

$$HR = \frac{a + d}{a + b + c + d}$$

<sup>¶</sup> where  $a_r$  is the probability to have a correct forecast by chance (Wilks, 2006). The hits, false alarms, misses and correct no forecast are computed comparing the precipitation forecast at four RAMS@ISAC grid points surrounding a raingauge and taking among them the closest value to the raingauge measurement (nearest-neighbour). In this way, we tolerate a spatial error of  $D \cdot (2)^{1/2}$  for the rainfall forecast, where  $D$  is the model grid spacing (4 km or 4/3 km depending by the case considered). Because the scores are computed for the second and third RAMS@ISAC domains, we tolerate spatial errors of 5.7 km and 1.9 km, respectively.<sup>¶</sup>

**Eliminato:** , introduced in previous papers (Federico et al., 2017a; 2017b), is shown here for completeness.



1953 The method starts by computing the water vapour mixing ratio  $q_v$ :

$$q_v = Aq_s + Bq_g \tanh(CX)(1 - \tanh(Dq_g^\alpha)) \quad (1)$$

1954  
1955 Where coefficients are set to  $A=0.86$ ,  $B=0.15$ ,  $C=0.30$ ,  $D=0.25$ ,  $\alpha=2.2$ ,  $q_s$  is the saturation mixing  
1956 ratio at the model atmospheric temperature, and  $q_g$  is the graupel mixing ratio ( $\text{g kg}^{-1}$ ).  $X$  is the  
1957 number of total flashes (IC+CG) falling in a grid box of domain D2 (R4) in the past five minutes. The  
1958 mixing ratio  $q_v$  of Eq. (1) is computed only for grid points where flashes are recorded. More  
1959 specifically, for each grid point we consider the number of flashes falling in a grid box centred at  
1960 the grid point in the last five minutes. The mixing ratio of Eqn. (1) is compared with that predicted  
1961 by the model. If the mixing ratio of Eqn. (1) is larger than the simulated one, the latter is nudged  
1962 towards the value of Eqn. (1), otherwise the modelled mixing ratio is left unchanged. This method  
1963 can only add water vapour to the forecast.

1964 The check and eventual substitution of the water vapour is performed every five minutes and it is  
1965 made within the mixed phase layer zone (0 °C, -25°C), wherein electrification processes caused by  
1966 the collision of ice and graupel are the most active (Takahashi 1978, Emersic and Sounders, 2010;  
1967 Fierro et al., 2015).

1968 The scheme of Fierro et al. (2012; 2014; 2015) was adapted to RAMS@ISAC in Federico et al.  
1969 (2017a). In particular, the coefficient C of Eqn. (1) was rescaled from that of Fierro et al. (2012)  
1970 considering the different spatial and temporal resolution of the gridded lightning data; then the  
1971 coefficient C was tuned (increased) by trials and errors considering two case studies of HyMeX-  
1972 SOP1 (15 and 27 October 2012). The C constant was adapted subjectively considering two  
1973 opposite requests: increasing the hits and minimising false alarms. POD and ETS scores were  
1974 considered as metrics for this purpose. Then, Eqn. (1) was applied to twenty case studies of  
1975 HyMeX-SOP1 giving a statistically significant (90, or 95% depending on the rainfall threshold)  
1976 improvement of the RAMS@ISAC precipitation VSF (3h).

1977 Nevertheless, an exhaustive statistic on the performance of rainfall VSF to nudging formulation in  
1978 RAMS@ISAC is missing and further studies are needed in this direction. Also, the optimal choice of  
1979 the coefficients A, B, C, D and  $\alpha$  is case dependent.

1980 Fierro et al (2012) applied the method using the ENTLN network, which has a detection efficiency  
1981 (DE) greater than 50% for IC over Oklahoma, where the ENTLN data were used. The emphasis on  
1982 IC flashes in the set-up of Fierro et al. (2012) is given because observational and model studies  
1983 have provided evidence that IC flashes correlate better than CG flashes with various measures of  
1984 intensifying convection (updraft strength, volume, graupel mass flux etc.; MacGorman et al. 1989;

Eliminato:  $q_v = Aq_s + Bq_g \tanh(CX)(1 - \tanh(Dq_g^\alpha))$

Formattato: Tipo di carattere: Cambria Math, Corsivo

Eliminato: 2

Eliminato: 3

Eliminato: 2

Eliminato: , i.e.  $X$  is greater than zero

Eliminato: 2

Eliminato: 2

Eliminato: changed

Eliminato: with

Eliminato: given by

Eliminato: 2

Formattato: Tipo di carattere: 12 pt, Inglese (Regno Unito)

Formattato: Tipo di carattere: 12 pt, Inglese (Regno Unito)

Formattato: Tipo di carattere: 12 pt, Inglese (Regno Unito)

Formattato: Tipo di carattere: 12 pt, Inglese (Regno Unito)

Formattato: Inglese (Regno Unito)

Formattato: Inglese (Regno Unito)

Formattato: Inglese (Regno Unito)

Formattato: Inglese (Regno Unito)

Formattato: Inglese (Regno Unito)

Formattato: Inglese (Regno Unito)

Formattato: Inglese (Regno Unito)

Formattato: Inglese (Regno Unito)

Formattato: Inglese (Regno Unito)

Formattato: Tipo di carattere: Symbol

Formattato: Inglese (Regno Unito)

1996 Carey and Rutledge 1998; MacGorman et al. 2005; Wiens et al. 2005; Kuhlman et al. 2006; Fierro  
1997 et al. 2006; Deierling and Petersen 2008; MacGorman et al. 2011). For this reason methods that  
1998 use both IC and CG flashes performs better than those using CG only, being CG flashes correlated  
1999 with the descent of reflectivity cores and the onset of the demise of the storm's updraft core  
2000 (MacGorman and Nielsen, 1991).  
2001 The analysis of the case studies shows that IC strokes are about 30% of the total number of strokes  
2002 reported. Also, the fraction of IC strokes to the total strokes depends on the position. For example,  
2003 for the Serano case, the fraction of IC strokes detected by LINET over the area hit by the largest  
2004 precipitation is more than 50% while over the Adriatic Sea it decreases to 10%.  
2005 It is also noted that DE for IC strokes cannot be reliably compared between LINET and ENTLN,  
2006 because the area is different and the technical details about IC detection remain unclear (type of  
2007 signals, VLF/LF or VHF, discrimination IC-CG).  
2008 For all the above reasons the application of the Fierro method to RAMS@ISAC is not  
2009 straightforward and it is appropriate to study the dependence of the rainfall VSF to the nudging  
2010 formulation. This subject is studied in the supplemental material of this paper (Section S.2) and  
2011 the results show that the choice of the coefficient of Eqn. (1) used in this paper is reasonable.  
2012 It is finally noted that despite the limitations noted above, lightning data assimilation, as used in  
2013 this paper, has a significant and positive impact on RAMS@ISAC rainfall VSF (Federico et al.,  
2014 2017a; 2017b).  
2015  
2016  
2017 *3.3 Radar data assimilation*  
2018 The method assimilates CAPPI of radar reflectivity factor operationally provided by the Italian  
2019 Department of Civil Protection (DPC). Radar data are provided over a regular Cartesian grid with 1  
2020 km horizontal resolution and for three vertical levels (2, 3, 5 km above the sea level). The CAPPIs  
2021 at 2, 3, and 5 km can be considered as under-sampled vertical profiles. CAPPIs are composed  
2022 starting from the 22 radars of the Italian Radar Network (Figure 13) 19 operating at the C-band  
2023 (i.e., 5.6 GHz) and 3 at X-band (i.e., 9.37 GHz). Data quality control and CAPPI composition is  
2024 performed by DPC. Data quality processing chain aims at identifying most of the uncertainty  
2025 sources as clutter, partial beam blocking and beam broadening. The radar observations are  
2026 processed according to nine steps detailed in Vulpiani et al. (2014), Petracca et al. (2018) and  
2027 references therein.

**Formattato:** Inglese americano

**Formattato:** Inglese americano

**Formattato:** SpazioDopo: 6 pt, Bordo: Superiore: (Nessun bordo), Inferiore: (Nessun bordo), A sinistra: (Nessun bordo), A destra: (Nessun bordo), Tra : (Nessun bordo), Barra : (Nessun bordo)

**Formattato:** Car. predefinito paragrafo, Inglese americano

**Formattato:** Inglese americano

**Formattato:** Car. predefinito paragrafo, Inglese americano

**Formattato:** Inglese americano

**Formattato:** Inglese (Regno Unito)

**Eliminato:** The check and eventual substitution of the water vapor is performed every five minutes and it is made only in the charging zone (0 °C, -25°C).

**Eliminato:** Lightning data are provided by the LINET network, which has more than 500 sensors over worldwide with the greatest density over Europe.¶

**Eliminato:** radar

**Eliminato:** that are

**Eliminato:** and radar observations can be considered as vertical profiles

**Eliminato:** se

**Eliminato:** the three different altitudes of

**Eliminato:** and no additional quality control is applied in this paper

2042 Radial velocity is not assimilated into RAMS@ISAC because it is not operationally processed, the  
2043 scan strategy being optimized for QPE purposes. Furthermore, the implementation of a radial  
2044 velocity data assimilation scheme is under development in RAMS-3DVAR and it is not currently  
2045 available for testing. For these reasons, we didn't consider the assimilation of this parameter.

Formattato: Colore carattere: Testo 1

Formattato: Colore carattere: Testo 1

2046 Before entering data assimilation, the Cartesian grid is reduced to 5 km by 5 km by choosing one  
2047 point every five of the Cartesian grid provided by DPC in order to reduce the numerical cost of the  
2048 data assimilation and to reduce the effect of correlated observation errors (Rohn et al., 2001). The  
2049 radar grid (Figure 4, for example) is then a Cartesian grid with 5 km grid-spacing and three vertical  
2050 levels.

Eliminato:

Eliminato: the

Eliminato: dimensionality of the problem

Eliminato: and to account, at least in part, for the correlation error of the observations

2051 It is important to note the pure sampling of the data could result in implementation of errors (for  
2052 example reflectivity given by insects or birds) or extremes. Creating superobservations would  
2053 reduce this problem, the main drawback being the missing of very localised phenomena. While  
2054 the aim of this paper is to present the update of the data assimilation system of RAMS@ISAC and  
2055 its application to two challenging cases, the problem of using superobservations will be considered  
2056 in future studies because it impacts the results.

2057 The methodology to assimilate radar reflectivity factor is that of Caumont et al. (2010), named  
2058 1D+3DVar, which is a two-step process: first, using a Bayesian approach inspired to GPROF  
2059 (Goddard Profiling Algorithm; Olson et al., 1996; Kummerow et al., 2001), 1D pseudo-profiles of  
2060 model variables are computed, then those pseudo-profiles are assimilated by 3DVar. Both steps  
2061 are discussed below.

Eliminato: shortly

2062 The first step computes a pseudo-profile of relative humidity weighting the model profiles of  
2063 relative humidity around the radar profile (Bayesian approach). The pseudo-profile is computed  
2064 by:

Eliminato: In particular

$$2065 \quad z_o^p = \frac{\sum_i RH_i W_i}{\sum_j W_j} \quad (2)$$

Eliminato: 3

2066 Where  $RH_i$  is the RAMS@ISAC vertical profile of relative humidity at a grid point inside a square of  
2067  $50 \times 50 \text{ km}^2$  centred at the radar vertical profile,  $W_i$  is the weight of each profile and  $z_o^p$  is the  
2068 relative humidity pseudo-profile. The summation is taken over all the grid points inside a square of  
2069  $50 \times 50 \text{ km}^2$  around the observed profile and the denominator is a normalisation factor. The  
2070 weights are determined by the agreement between the simulated and observed reflectivity factor:

Formattato: Tipo di carattere: Non Corsivo

Eliminato: considering

$$W_i = \exp\left\{-\frac{1}{2}[\mathbf{z}_o - h_z(x_i)]^T \mathbf{R}_z^{-1} [\mathbf{z}_o - h_z(x_i)]\right\} \quad (3)$$

Where  $h_z$  is the forward observation operator, transforming the background column  $\mathbf{x}_i$  into the observed reflectivity factor. The forward radar observation operator is taken from the RIP (Read/Interpolate/Plot) software (https://dtcenter.org/wrf-nmm/users/OnLineTutorial/NMM/RIP/index.php, last access 03 March 2019) and is given in the supplemental material of this paper (Section S4). It assumes a Marshall-Palmer hydrometeors size-distribution, Rayleigh scattering, and depends on the mixing ratios of rain, graupel and snow.

The matrix  $\mathbf{R}_z$  in Eqn. (3) is diagonal, and its value is  $n\sigma^2$ , where  $\sigma$  is 1 dBz and  $n$  is the number of available observations in the vertical profile (from 1 to 3). In this way, we give more weight to vertical profiles containing more data.

The error of radar data is assumed small (1dBz) for two reasons: a) reflectivity data are carefully checked by the Civil Protection Department; b) the performance of control simulation, not assimilating any data, is rather poor for the case studies. This setting, however, could not be optimal for cases when the control forecast performs better.

It is important to point out that the 50 km length-scale of the above step doesn't represent the horizontal correlation length-scale of the background error, which determines the horizontal spread of the innovations in the 3D-Var data assimilation (the latter length-scale is between 14 and 25 km depending on the level). The 50 km length-scale is used to set a square for computing the pseudo-profile of relative humidity (Eqn. (2)). This profile is given by a weighted average whose weights are determined by the agreement between the simulated and observed reflectivity factor. The larger the agreement the larger the weight. This distance is appropriate because the spatial error of meteorological models in simulating meteorological features, for example fronts, can be of this order. The control simulation of the two events considered in this paper confirms this choice.

The method is not able to force convection when the model has no rain, snow or graupel in a square around (50\*50 km<sup>2</sup>) a radar profile with reflectivity factor greater than zero. In this case, the pseudo-profile of relative humidity is assumed saturated above the lifting condensation level and with no data below (Caumont et al., 2010).

It is also noted that the method is able to reduce spurious convection when the reflectivity factor is simulated but not observed, because the pseudo-profile of relative humidity gives more weight to the drier relative humidity profiles simulated by RAMS@ISAC inside the 50\*50 km<sup>2</sup> square

Eliminato: 4

Eliminato: is specific for the WSM6 microphysics scheme and is available in WRF release 3.8

Eliminato: ¶

Eliminato: observation error

Eliminato: 4

Eliminato: assumed diagonal, i.e. observation errors are uncorrelated,

Formattato: Inglese americano

Formattato: Inglese americano

Eliminato: It is important to note that

Eliminato: t

Eliminato: and

Eliminato: specific

Eliminato:

Eliminato: to force convection into the model

Eliminato: to dry the model

Eliminato: by giving

Eliminato: in Eqn. (3).

2128 centred at the radar profile. Of course, the ability to reduce spurious convection depends on the  
 2129 availability of dry model profiles around the specific radar profile (see the example below). Finally,  
 2130 if the observed profile is dry and the profile simulated by RAMS@ISAC is dry too, the pseudo-  
 2131 profile is not computed.

2132 In summary, pseudo-profiles are computed for each profile of the radar grid whenever reflectivity  
 2133 is observed or simulated.

2134 The pseudo-profiles computed with the procedure introduced above, are then used as  
 2135 observations in the RAMS-3DVar data assimilation (Federico, 2013), minimising the cost-function:

$$J(\mathbf{x}) = \frac{1}{2} (\mathbf{x} - \mathbf{x}_b)^T \mathbf{B}^{-1} (\mathbf{x} - \mathbf{x}_b) + \frac{1}{2} (\mathbf{z}_o^p - h(\mathbf{x}))^T \mathbf{R}^{-1} (\mathbf{z}_o^p - h(\mathbf{x})) \quad (4)$$

2136 Where  $\mathbf{x}$  is the state vector giving the analysis when  $J$  is minimized,  $\mathbf{x}_b$  is the background,  $\mathbf{B}$  and  $\mathbf{R}$   
 2137 are the background and observations error covariance matrices,  $\mathbf{z}_o^p$  is the pseudo vertical profile  
 2138 computed by Eqn. (2) and  $h$  is the forward observation operator transforming the state vector  
 2139 (RAMS@ISAC water vapour mixing ratio) into observations. The cost function in RAMS-3DVar is  
 2140 implemented in incremental form (Courtier et al., 1994) and its minimization is performed by the  
 2141 conjugate-gradient method (Press et al., 1992). No multi-scale approach is used.

2142 The background error matrix is divided into three components along the three spatial directions  
 2143 ( $x$ ,  $y$ ,  $z$ ). The  $\mathbf{B}_x$  and  $\mathbf{B}_y$  matrices account for the spatial correlation of the background error. The  
 2144 correlations are Gaussian with length-scales between 14 and 25 km, depending on the vertical  
 2145 level. These distances are computed using the NMC method (Barker et al., 2012) applied to the  
 2146 HyMeX-SOP1 (Hydrological cycle in the Mediterranean Experiment – First Special Observing Period  
 2147 occurred in the period 6 September-6 November 2012; Ducrog et al., 2014) period. It is again  
 2148 stressed that the spread of the innovations along the horizontal spatial directions in the 3D-Var  
 2149 analysis is determined by the length scales of  $\mathbf{B}_x$  and  $\mathbf{B}_y$  matrices and varies between 14 and 25 km,  
 2150 depending on the level.

2151 The  $\mathbf{B}_z$  matrix contains the error for the water vapour mixing ratio, which is the control variable  
 2152 used in RAMS-3DVar. This error is about 2 g/kg at the surface and decreases with height. In  
 2153 particular, it is larger than 0.5 g/kg below 4 km, and less than 0.2 g/kg above 5 km. The vertical  
 2154 decorrelation of the background error depends on the level and can be roughly estimated in 500-  
 2155 2000 m. The observation error matrix  $\mathbf{R}$  in Eqn. (4) is diagonal and observations' errors are  
 2156 uncorrelated. This choice is partially justified by under sampling the radar reflectivity factor  
 2157 observation by choosing one point every five grid points in both horizontal directions of the radar  
 2158

Formattato: Car. predefinito paragrafo, Italiano

Formattato: Inglese (Regno Unito)

Formattato: Allineato al centro

Eliminato: ¶

$$J(\mathbf{x}) = \frac{1}{2} (\mathbf{x} - \mathbf{x}_b)^T \mathbf{B}^{-1} (\mathbf{x} - \mathbf{x}_b) + \frac{1}{2} (\mathbf{y}_o - h(\mathbf{x}))^T \mathbf{B}$$

Eliminato: 5

Formattato: Nessuno, Controllo ortografia e grammatica

Formattato: Abbassato 12 pt

Formattato: Inglese (Regno Unito)

Formattato: Tipo di carattere: Corsivo

Eliminato: y

Formattato: Apice

Eliminato: observation

Eliminato: vector

Eliminato: ; see Federico 2013 for the details

Eliminato: .

Spostato (inserimento) [8]

Eliminato: 2

Eliminato: ¶

Formattato: Tipo di carattere: Grassetto

2170 Cartesian grid. However, correlation observations errors have significant impact on the final  
 2171 analysis, as shown for example in Stewart et al. (2013), and different choices of the matrix  $R$  will  
 2172 be considered in future studies.

2173 The value of the elements on the diagonal of  $R$  depends on the vertical level and are 1/4 of the  
 2174 diagonal element of the  $B_z$  matrix at the corresponding height. By this choice, we give more credit  
 2175 to the observations than to the background and analyses strongly adjust the background towards  
 2176 observations. The background error matrix is computed using the NMC method (Parrish and  
 2177 Derber, 1992; Barker et al. 2004) applied to the HyMeX-SOP1 (Hydrological cycle in the  
 2178 Mediterranean Experiment – First Special Observing Period occurred from 6 September to 6  
 2179 November 2012; Ducroq et al., 2014). This choice is motivated by the fact that HyMeX-SOP1  
 2180 contains several heavy precipitation events over Italy and the background error matrix is  
 2181 representative of the convective environment of the cases considered in this paper. In particular,  
 2182 10 out of 20 declared IOP (Intense Observing Period) of HyMeX-SOP1 occurred in Italy (Ferretti et  
 2183 al., 2014). On the contrary, the period of September 2017, especially before the events selected in  
 2184 this study was characterized by fair and stable weather conditions over Italy and the background  
 2185 error matrix for September 2017 is less representative of the convective environment that  
 2186 characterise the events of this paper.

2187 Because it is the first time that we show the assimilation of radar reflectivity factor in  
 2188 RAMS@ISAC, it is useful to discuss an example of analysis. We select the analysis of Livorno case  
 2189 study at 06 UTC. The observed CAPPI at 3km above sea level is shown in Figure 10b. The  
 2190 corresponding CAPPI simulated by the background is shown in Figure 14a. In general, the  
 2191 comparison between simulated and observed reflectivity factor shows the difficulty of the model  
 2192 to represent convection properly. In particular, the model is able to represent the convection over  
 2193 Northern Italy but it has poor performance over Sardinia, south of Sicily and over Central Italy. The  
 2194 difference between the analysis and background relative humidity after and before the analysis is  
 2195 shown in Figure 14b (absolute values less than 1% are suppressed in the figure for clarity). Both  
 2196 positive (convection enhancing) and negative (convection suppressing) adjustments are found.  
 2197 Over Central Italy, Sardinia and South of Sicily relative humidity is increased because the model  
 2198 doesn't simulate the observed reflectivity (Figure 10b). Over northern Italy the model is partially  
 2199 dried for two different reasons: over northwest of Italy because RAMS@ISAC simulates  
 2200 unobserved reflectivity, over north and northeast of Italy because the model simulates larger  
 2201 values of reflectivity factor compared to the observations. The RAMS-3DVar is able to dry the

Formattato: Tipo di carattere: Grassetto

Formattato: Tipo di carattere: Grassetto

Formattato: Tipo di carattere: Grassetto

Formattato: Tipo di carattere: Grassetto, Pedice

Eliminato: ¶

Eliminato: in the period

Eliminato: -

Eliminato: ,

Eliminato: which has been chosen because it

Eliminato: (Ferretti et al., 2014)

Formattato: Non Evidenziato

Eliminato: . ¶

2209 relative humidity field north of Corsica island, where the RAMS@ISAC predicts unobserved  
2210 reflectivity, while RAMS-3DVar didn't suppress the unobserved convection west of Sardinia  
2211 because the pseudo profiles computed over this area weren't appreciably drier than the  
2212 background.

2213 Cross correlations among different variables of the data assimilation system are neglected in this  
2214 study and the application of the RAMS-3DVar affects the water vapour mixing ratio only. Cross  
2215 correlations among different variables can improve the performance of data assimilation system,  
2216 and an example of their impact in the RAMS-3DVar is shown in Federico (2013). Nevertheless, the  
2217 impact of cross correlations among different variables in the precipitation VSF will be explored in  
2218 future works.

2219 Because also lightning data assimilation adjusts the water vapour mixing ratio, it follows that the  
2220 data assimilation presented in this study adjusts only this parameter.

2221 Lightning and radar data assimilation may produce sharp gradients in vertical direction caused by  
2222 the addition of water vapour to specific layers. In the case of lightning, the water vapour is added  
2223 by nudging to reduce sharp gradients. However, radar data assimilation, which accounts for the  
2224 largest mass of water added to RAMS@ISAC (see Section S.1 of the supplemental material),  
2225 directly adjusts the water vapour into the model. Our experience with RAMS@ISAC, however,  
2226 shows that results are reliable and the sudden addition of water vapour doesn't cause shocks to  
2227 the model simulation, despite the notable gradients of specific humidity.

2228 It is finally noted that the data assimilation increase/decrease the water vapour into the model  
2229 depending on the cases. The eventual increase/decrease of the forecasted rainfall depends on the  
2230 physical and dynamical processes occurring into the meteorological model, without any specific  
2231 tuning.

#### 2232 4. Results

2233 In this section, we discuss the most intense phase of the Serano case, 03-06 UTC on 16 September,  
2234 and two VSF forecasts, 00-03 UTC and 06-09 UTC on 10 September, for the Livorno case. The two  
2235 VSF for Livorno correspond to the most intense phase of the storm in Livorno and to a very intense  
2236 phase over Lazio region, Central Italy. The aim of the section is to show the notable improvement  
2237 given by lightning and radar reflectivity factor data assimilation to the VSF.

2238 We consider four types of VSF (Table 3): a) CTRL, without radar reflectivity factor and lightning  
2239 data assimilation; b) LIGHT, assimilating lightning but not radar reflectivity factor; c) RAD,

**Eliminato:** In the RAMS-3DVar, the background error matrix is divided in three components along the three spatial directions (x, y, z). The  $B_x$  and  $B_y$  matrices take into account for the spatial correlation of the background error. They are assumed Gaussian with length-scales between 20 and 30 km, depending on the vertical level. Again, these distances are computed using the NMC methods (Barker et al., 2012).

**Formattato:** Tipo di carattere: Colore carattere: Nero, Bordo: : (Nessun bordo)

**Spostato in su [8]:** The  $B_z$  matrix contains the error for the water vapor mixing ratio, which is the control variable used in RAMS-3DVar. This error is about 2 g/kg at the surface and decreases with height. In particular, it is larger than 0.5 g/kg below 4 km, and less than 0.2 g/kg above 5 km.

**Eliminato:** It is noted that c

**Eliminato:** s

**Formattato:** Nessuno, Tipo di carattere: Colore carattere: Nero, Bordo: : (Nessun bordo)

**Eliminato:** vapor

**Formattato:** Nessuno, Tipo di carattere: (Predefinito) Calibri, Inglese (Regno Unito)

**Formattato:** Nessuno, Tipo di carattere: (Predefinito) Calibri, Inglese (Regno Unito)

**Eliminato:** . ¶

**Eliminato:** the

**Eliminato:** perturbs

**Eliminato:** vapor

**Eliminato:** changes

**Formattato:** Inglese americano

**Formattato:** Inglese americano

**Formattato:** Inglese americano

**Formattato:** Inglese americano

**Formattato:** Car. predefinito paragrafo, Colore carattere: Automatico, Inglese (Regno Unito)

**Formattato:** Normale, Giustificato, Interlinea: 1.5 righe

**Formattato:** Colore carattere: Automatico, Inglese (Regno Unito)

**Formattato:** Livello 1

**Eliminato:** ¶

4.1 Serano ¶

In this section we analyse two VSF forecasts of the Serano case. The first period (03-06 UTC) is the most intense, while the second period (18-21 UTC) corresponds to a rejuvenating phase of the storm. ¶

**Formattato:** Non Evidenziato

**Formattato:** Non Evidenziato

2267 assimilating radar reflectivity factor but not lightning; d) RADLI, assimilating both lightning and  
2268 radar reflectivity factor.

2269 In order to avoid excessive length two specific topics are considered in the supplemental material  
2270 of this paper; specifically, we study: a) the relative contribution to the total water mass given by  
2271 lightning and radar reflectivity factor data assimilation (Section S.1); b) the sensitivity of the  
2272 precipitation VSF to the nudging formulation (Section S2). Also, the supplemental material gives  
2273 different plots of Figures 15-17 (Section S3) and the forward radar operator used in RAMS-3DVar  
2274 (Section S4).

2275

#### 2276 4.1 Serano: 03-06 UTC on 16 September 2017

2277 In this period, an intense and localised storm hit central Italy, while light precipitation occurred  
2278 over northern Italy (Figure 15a). Considering the storm over central Italy, 10 raingauges observed  
2279 more than 30 mm/3h, 6 more than 40 mm/3h, 3 more than 50 mm/3h and 1 more than 60  
2280 mm/3h, the maximum observed value being 63 mm/3h.

2281 The CTRL forecast, Figure 15b, misses the storm over central Italy and considerably  
2282 underestimates the precipitation area over Northern Italy, giving unsatisfactory results.

2283 The assimilation of the radar reflectivity factor improves the forecast, as shown in Figure 15c. In  
2284 particular, RAD forecast shows localized precipitation (30-35 mm/3h) close to the area where the  
2285 most abundant precipitation was observed. However, the maximum precipitation is  
2286 underestimated. Also, the RAD forecast better represents the precipitation over Northern Italy  
2287 compared to CTRL.

2288 The rainfall forecast of LIGHT, Figure 15d, shows some improvements compared to CTRL because  
2289 the precipitation over central Italy has a maximum of 25-30 mm/3h, close to the area where the  
2290 maximum precipitation was observed. LIGHT, however, has a worse performance compared to  
2291 RAD because it underestimates the area of light precipitation over northern Italy. Also, similarly to  
2292 RAD, LIGHT underestimates the maximum precipitation in central Italy.

2293 RADLI forecast, Figure 15e, has the best performance. The precipitation over central Italy is well  
2294 represented because the maximum rainfall (40-45 mm/3h) is in reasonable agreement with  
2295 observations, and also because the area of intense precipitation (> 25 mm/3h) is elongated in the  
2296 SW-NE direction in agreement with raingauge observations, giving a much better idea of the real  
2297 storm intensity compared to RAD and LIGHT, as well as CTRL. The precipitation over northern Italy  
2298 is well represented by RADLI.

Eliminato: .1

Eliminato:

Eliminato: November

Eliminato: the

Eliminato: 4

Eliminato: 4

Eliminato: underestimates

Eliminato: by

Eliminato: 4

Eliminato: Another interesting improvement of the

Eliminato: forecast compared to CTRL is the precipitation over northern Italy,

Eliminato: whose

Eliminato: area

Eliminato: is much more in agreement with observations compared to CTRL

Eliminato: precipitation

Eliminato: given by

Eliminato: 4

Eliminato: misses the light precipitation

Eliminato: 4

Eliminato: shows

Eliminato: better

Eliminato: with

Eliminato: measurements

Eliminato: light



2325 Table 4 shows the ETS and POD scores for selected rainfall thresholds for different neighbourhood  
 2326 radii. Different radii are considered to account for the well-known double penalty error (Mass et  
 2327 al., 2002; Mittermaier et al., 2013) caused by displacement errors of the detailed precipitation  
 2328 forecast in convection allowing grids. CTRL was unable to predict rainfall larger than 6 mm/3h. The  
 2329 comparison between RAD and LIGHT shows that assimilating radar reflectivity factor performs  
 2330 better than assimilating lightning. This behaviour, however, is not general and sometimes the  
 2331 assimilation of lightning has a better performance than assimilating radar reflectivity factor (see  
 2332 section 4.2.1).  
 2333 RADLI forecast has the best performance among all model configurations. In particular, it is the  
 2334 only forecast having positive scores for thresholds larger than 30 mm/3h.  
 2335 In conclusion, for this VSF, the assimilation of lightning and radar reflectivity factor acted  
 2336 synergistically to improve the precipitation VSF and the simulation assimilating both data performs  
 2337 considerably better than simulations assimilating either lightning or radar reflectivity factor.

2338 ▼  
 2339 **4.2 Livorno**

2340 The Livorno case study lasted for several hours starting at 18 UTC on 9 September 2017 and  
 2341 ending more than a day later. The most intense phase in Livorno and its surroundings was  
 2342 observed during the night between 9 and 10 September. In the following, we will show two  
 2343 representative VSF (3h), including the most intense phase in Livorno.

2344 ▼  
 2345 **4.2.1 Livorno: 00-03 UTC on 10 September 2017**

2346 This period represents the most intense phase of the storm in Livorno. In particular, the raingauge  
 2347 close to the label A (Figure 16a) reported 151 mm/3h (Collesalveti), while the one close to the  
 2348 label B measured 82 mm/3h. Among the 518 raingauges reporting valid data, 75 observed more  
 2349 than 10 mm/3h, 31 more than 20 mm/3h, 17 more than 30 mm/3h, 9 more than 40 mm/3h, and 6  
 2350 more than 50 mm/3h.

2351 The CTRL precipitation forecast is shown in Figure 16b. The forecast is poor because it misses the  
 2352 precipitation swath from the coast towards NE. A precipitation swath is forecasted about 50 km to  
 2353 the North of the real occurrence, but it is less wide compared to the observations.

2354 The RAD forecast, Figure 16c, shows that the assimilation of radar reflectivity factor gives a clear  
 2355 improvement to the forecast. The largest precipitation in the coastal part of the swath (we  
 2356 searched for the maximum in the area with longitudes between 10.20E and 10.70E and latitudes

**Eliminato:** ¶

**Eliminato:** Figure 14f shows the POD, computed for the domain of Figure 14a, for the time period considered. CTRL and LIGHT show a poor forecast compared to RAD and RADLI, underlining the importance of the assimilation of reflectivity factor observations for this phase of the storm. The POD of RADLI is 0.33 for the 30 mm/3h threshold (3 stations out of 10 where correctly predicted). This represents a good performance considering that the intense precipitation is localized and we used the nearest neighbour methodology to compute the score, which, for the specific grid resolution, limits to 5.7 km the displacement error. ¶ Figure 14f also shows the significant improvement of RAD and RADLI for the light rainfall forecast because the POD for the 0.2 mm/3h threshold increases from 0.5 of CTRL (0.55 for LIGHT) to about 0.85 for both RAD and RADLI. ¶ The ETS score shows again the positive impact of the data assimilation, especially radar reflectivity factor, on the rainfall forecast for this phase of the storm, the best performance given by RADLI. ¶ The proportion of correct forecast, Figure 14h, is larger than 84% for all configurations. HR, however, is lower for RAD and RADLI compared to other configurations because of the larger number of false alarms given by the assimilation of radar reflectivity factor. ¶ It is finally remarked that lightning and reflectivity factor data assimilation acted synergistically because the simulation assimilating both data performs much better than the simulations assimilating only one kind of observation, either radar reflectivity factor or lightning. ¶

¶ **4.1.2 Serano: 18-21 UTC 16 September 2017** ¶

In this phase, rainfall occurred mainly over central Italy with moderate-heavy amounts. In particular, 51 raingauges measured more than 10 mm/3h, 13 more than 20 mm/3h, 3 more than 30 mm/3h and 2 between 40 mm/3h and 50 mm/3h (Figure 15a). Rainfall was also observed over north-western Italy with 12 raingauges observing more than 10 mm/3h, 7 more than 20 mm/3h, 4 more than 30 mm/3h, and 3 between 40 mm/3h and 50 mm/3h. ¶ The CTRL forecast, Figure 15b, shows little precipitation over central Italy, giving an unsatisfactory forecast, while the forecast over north-western Italy is well represented even if displaced few tens of kilometres to the North of the real occurrence. ¶ ... [1]

**Eliminato:** three

**Eliminato:** ¶

¶ **4.2.1 Livorno: 18-21 UTC 9 September 2017** ¶

During this period, the precipitation started to hit intensely Livorno and its surroundings (point A in the Figure 16a). ... [2]

**Eliminato:** 2

**Eliminato:** 7

**Eliminato:** (also 60)

**Eliminato:** 7

**Eliminato:** Indeed, a

**Eliminato:** of RAD

**Eliminato:** 7

**Eliminato:** value

2566 between 43.10N and 43.60N) is 94 mm/3h. Another local maximum is in the southern part of the  
 2567 domain (label B of Figure 16a). The maximum location is well represented, but the forecast value  
 2568 (55 mm/3h) underestimates the observed maximum (82 mm/3h).

2569 An improvement, compared to both CTRL and RAD, is given by the assimilation of lightning (Figure  
 2570 16d). Also for this simulation there is a precipitation swath from coastal Tuscany to the Apennines,  
 2571 but the shape of the swath better resembles that observed. The maximum value close to Livorno,  
 2572 i.e. in the coastal part of the swath, is 158 mm/3h.

2573 LIGHT simulation shows the local maximum in the southern part of the domain (about 50 mm/3h),  
 2574 but the amount is underestimated.

2575 Figure 16e shows the RADLI rainfall forecast. The precipitation swath from coastal Tuscany  
 2576 towards NE is more apparent compared to LIGHT and RAD. The maximum rainfall accumulated  
 2577 close to Livorno is 186 mm/3h. Also, the second precipitation maximum in the southern part of  
 2578 the domain reaches 70 mm/3h in good agreement with observations (82 mm/3h). RADLI is the  
 2579 only run giving a satisfactory precipitation VSF over the south-eastern Emilia Romagna (north-  
 2580 eastern part of the domain), to the lee of the Apennines. It is also noted that the main  
 2581 precipitation swath forecasted by RADLI is too broad in the direction crossing the swath compared  
 2582 to the observations. This is confirmed by the FBIAS of RADLI (not shown), which is more than 3 for  
 2583 thresholds larger than 42 mm/3h.

2584 The analysis of the scores (Table 5) confirms the results outlined above. CTRL has the lowest  
 2585 performance and the improvement given by the data assimilation to the VSF is apparent for POD  
 2586 and ETS for all thresholds and neighbourhood radii considered. For this specific VSF, lightning data  
 2587 assimilation gives a better improvement to rainfall forecast compared to RAD. RADLI has the best  
 2588 performance, especially for 25 km and 50 km neighbourhood radii, nevertheless it over forecast  
 2589 the precipitation field. Because ETS penalises false alarms, the value of this score for RADLI is  
 2590 sometimes lower than that of LIGHT.

2591

2592 4.2.3 Livorno: 06-09 UTC on 10 September 2017

2593 In this period, the most intense precipitation occurred over the coastal part of Lazio (Figure 17a).  
 2594 More in detail, among the 2695 raingauges reporting valid data over the domain of Figure 17a,  
 2595 307 reported more than 10 mm/3h, 132 more than 20 mm/3h, 86 more than 30 mm/3h, 66 more  
 2596 than 40 mm/3h, 49 more than 50 mm/3h and 35 more than 60 mm/3h. Among the 35 raingauges

- Eliminato: , clearly showing the occurrence of a heavy precipitation event
- Eliminato: s shown
- Eliminato: 7
- Eliminato: compared to RAD
- Eliminato: , clearly showing the occurrence of a severe storm
- Eliminato: The
- Eliminato: also
- Eliminato: 7
- Eliminato: by RADLI
- Eliminato: Also,
- Eliminato: producing
- Eliminato: field
- Eliminato: on the lee
- Eliminato: ¶
- Eliminato: ¶
- Eliminato: Considering the POD, Figure 17f, we note the considerable improvement given to the score by data assimilation (lightning and/or radar reflectivity factor). POD is larger than 0.5 for RADLI and LIGHT up to the 52 mm/3h thresholds, clearly showing that those two configurations are able to catch the position and timing of the very intense precipitation, especially considering that the maximum displacement error for the precipitation field is 1.9 km. ¶ RAD has a lower capability to correctly forecast the precipitation inland compared to FLASH and RADLI, however: a) it qualitatively reveals the heavy precipitation occurring in the Livorno area; b) the POD score is considerably improved compared to CTRL. ¶ The ETS score, Figure 17g, underlines the good performance of RAD, LIGHT and RADLI compared to CTRL. RAD has a useful forecast (ETS > 0) up to 42 mm/3h, while LIGHT and RADLI show useful forecast up to 60 mm/3h. The lower ETS of RADLI compared to LIGHT for thresholds larger than 42 mm/3h is caused by the greater number of false alarms occurring in RADLI. The large variations of the scores for thresholds above 40 mm/3h is caused by the low number of raingauges observing those rainfall amounts. ¶ CTRL has the lowest HR, Figure 17h, up to 16 mm/3h because of the lower number of hits compared to other configurations. For thresholds larger than 32 mm/3h RADLI has the lowest HR due to the comparatively higher number of false alarms. ¶ In summary, for the most intense precipitation period over Livorno, the data assimilation of lightning and radar reflectivity factor plays a key role for the correct representation of the storm intensity, timing and position, giving an improvement of paramount practical importance. ¶
- Formattato: Bordo: : (Nessun bordo)
- Eliminato: phase of the
- Eliminato: over Central Italy,
- Eliminato: 8
- Eliminato: 8

2651 measuring more than 60 mm/3h, 33 were over Lazio, showing the heavy rainfall occurred over the  
2652 Region.

2653 Some precipitation persisted over Tuscany but the rainfall is much lower compared to previous 6h  
2654 (the rainfall over Tuscany between 03 and 06 UTC was very intense, not shown). Other notable  
2655 precipitation areas are over the NE of Italy (moderate to low amounts), over central Alps  
2656 (moderate values) and over the whole Sardinia (small amounts).

2657 Figure 17b shows the rainfall simulated by CTRL. The forecast is unsatisfactory, mainly for the  
2658 following two reasons: a) heavy precipitation is simulated over Tuscany (> 75 mm/3h), also close  
2659 to the Livorno area; b) few millimetres of precipitation are forecasted over central Italy. The  
2660 rainfall over NE Italy is well represented in space, but overestimated.

2661 Considering the evolution of CTRL forecast for the two VSF of Livorno, we conclude that it was  
2662 able to predict abundant rain over Livorno, but the rainfall forecast was delayed compared to the  
2663 real occurrence. A similar behaviour was found in Ricciardelli et al. (2018) using the WRF model,  
2664 showing that the results of this paper for Livorno are likely not tied to the specific model used.

2665 The rainfall simulated by RAD (Figure 17c) clearly improves the forecast compared to CTRL. First,  
2666 the precipitation over Lazio is very well predicted and the rainfall values are up to 65 mm/3h, so  
2667 RAD forecast well represents the main precipitation spot over Italy for this VSF. Second, the  
2668 precipitation over Tuscany is less than for CTRL, showing the ability of radar reflectivity factor data  
2669 assimilation to dry the model when it predicts reflectivity that is not observed. This is confirmed  
2670 by the inspection of the analysis of Figure 14b, the last analysis used before this VSF, which gives a  
2671 decrease of the relative humidity over most of Tuscany and over the sea in front of Livorno. Third,  
2672 the precipitation over central Alps is represented, even if located about 30 km to the East. It is  
2673 noted, however, that the area of intense rainfall (>60 mm/3h) is overestimated by RAD, showing a  
2674 wet forecast. This is confirmed by the wet frequency bias of the RAD simulation, which is greater  
2675 than 3 between 14 and 44 mm/3h. The wet bias of the RAD forecast is apparent in the  
2676 representation of the rainfall VSF shown in the supplemental material of this paper (Figure S5).

2677 LIGHT forecast, Figure 17d, shows a worse performance compared to RAD for this time period. The  
2678 precipitation forecast is mainly over Tuscany, where it is overestimated, with a small precipitation  
2679 spot over Lazio.

2680 The precipitation forecast of RADLI, Figure 17e, represents very well the precipitation over Lazio,  
2681 and the rainfall amount is better predicted compared to RAD. The precipitation over Sardinia is

Eliminato: the

Eliminato: C

Eliminato: 8

Eliminato: very small

Eliminato: is

Eliminato: C

Eliminato: because the forecast is higher than 50 mm/3h in correspondence of some raingauges, while observed values are 20-25 mm/3h. The small precipitation over Sardinia is not forecast by CTRL

Eliminato: rainfall

Eliminato: different

Eliminato: phases of the storm

Eliminato: CTRL

Eliminato: this

Eliminato: event

Eliminato: 8

Eliminato: higher than 40 mm/3h (

Eliminato: )

Eliminato: the

Eliminato: period of time

Eliminato: lowered compared to

Eliminato: rain

Eliminato: C

Eliminato: There are also aspects of the rainfall forecast that are less satisfactory: the small precipitation over Sardinia is not represented by RAD; the precipitation over NE Italy is well represented in space but overestimated.

Eliminato: 8

Eliminato: There are, however, three improvements compared to CTRL and RAD: a) the small precipitation over Sardinia is well represented in LIGHT; b) the precipitation over Central Alps is well predicted; c) the rainfall forecast over NE Italy is overestimated by LIGHT but to a less extent compared to RAD.

Eliminato: 8

2718 well represented by RADLI as well as the precipitation over Central Alps, giving the best results  
2719 among all VSF.

2720 The analysis of the scores confirms the above results (Table 6). CTRL has a poor performance as  
2721 shown by the POD and ETS values, close to zero, for all thresholds above 30 mm/3h and for all  
2722 neighbourhood radii. The simulations assimilating radar reflectivity factor performs better than  
2723 LIGHT, the difference being larger for higher rainfall thresholds and for smaller neighbourhood  
2724 radii.

2725 It is also notable the good performance of RADLI forecast for the nearest neighbourhood radii  
2726 (ETS=0.43, POD=0.92) for the 50 mm/3h threshold.

## 2728 5. Discussion and Conclusions

2729 In this paper, we showed the impact of lightning and radar reflectivity factor data assimilation on  
2730 the very short term precipitation forecast (3h) for two case studies occurred in Italy. We used  
2731 RAMS@ISAC model, whose 3DVar extension to the assimilation of radar reflectivity factor is  
2732 shown in this paper for the first time.

2733 The first case study occurred on 16 September 2017 and it is a moderate case with localised  
2734 rainfall over central Italy. It was chosen because the control forecast, i.e. without radar reflectivity  
2735 factor or lightning data assimilation, missed the event. The second event, occurred on 9-10  
2736 September 2017, was characterised by exceptional rainfall over several parts of Italy. This event  
2737 was partially represented by the control forecast. In particular, the forecast of the event was  
2738 incorrect because: a) the control forecast was delayed compared to the observations; b) the  
2739 control forecast missed the rainfall over central Italy (Lazio Region).

2740 It is important to recall that the impact of lightning data assimilation on the precipitation forecast  
2741 of RAMS@ISAC was already studied for the HyMeX-SOP1 period (Federico et al., 2017a, 2017b),  
2742 and a robust statistic is already available. The results of this study confirm the important role of  
2743 lightning data assimilation on the rainfall forecast for other two case studies. However,  
2744 considering the assimilation of radar reflectivity factor, and its combination with lightning data  
2745 assimilation in RAMS@ISAC, the results of this paper are new.

2746 Because we analysed only two case studies, no definitive conclusions can be derived on the  
2747 performance of RAMS@ISAC for radar reflectivity factor data assimilation. There are, however,  
2748 few points worth of mention.

Eliminato: forecasts

Eliminato: ¶

Eliminato: The POD score (Figure 18f) confirms the above analysis. All the experiments with data assimilation outperform the CTRL forecast, and, for this time period, RAD performs better than LIGHT. RADLI shows the best POD among all configurations because it represents better the amount of rainfall over Lazio. ¶  
Similar considerations apply to ETS (Figure 18g); it is worth of note the high value of ETS for thresholds larger than 50 mm/3h, which represent heavy rainfall. Again, a forecast that was missed by CTRL is correctly represented by the assimilation of both radar reflectivity factor and lightning. ¶  
The HR score (Figure 18h) shows that CTRL has the lowest score for thresholds below 14 mm/3h because it has a lower number of hits. For higher thresholds (> 32 mm/3h), the impact of the false alarms become important and RADLI has the lowest HR. ¶

Eliminato: have shown

Eliminato: the

Eliminato: of precipitation

Eliminato: s

Eliminato: the

Eliminato: C

2773 The VSF performance of RAMS@ISAC is systematically improved by the assimilation of radar  
 2774 reflectivity factor. This improvement is of paramount importance for some specific VSF (for  
 2775 example for the 00-03 UTC of Livorno), when the control forecast missed the event while it was  
 2776 correctly predicted by radar reflectivity factor data assimilation. Sometimes the improvement of  
 2777 reflectivity factor data assimilation has a lower impact on the precipitation forecast, as for the  
 2778 period 18-21 UTC on 9 September 2017 (Livorno, not shown, see the discussion paper Federico et  
 2779 al. (2018) for a description of this VSF), This suggests that there is space for improvement for all  
 2780 components of the VSF: observations, data assimilation, meteorological model.

2781 Lightning and radar observations are different and both add value to the VSF. In particular, flashes  
 2782 are recorded when deep convection develops, while radar reflectivity factor is observed also for  
 2783 light stratiform rain. Flashes of ground based network, as LINET, are available over the open sea,  
 2784 even if with a reduced detection efficiency, while radar reflectivity factor is confined to the range  
 2785 of coastal radars in the network. Lightning has a seasonal dependence over Italy, with the  
 2786 maximum in summer and fall, while radar reflectivity factor is available in all seasons.

2787 For the above reasons, the impact of the two kinds of data on the rainfall VSF is expected  
 2788 different. Some examples have been shown: the light precipitation over Northern Italy for Serano  
 2789 is well forecasted assimilating radar reflectivity factor, while it is not simulated assimilating flashes  
 2790 because they are too few in this area to force convection; lightning data assimilation is able to  
 2791 better represent the deep convection occurring during the intense phase of the Livorno case (00-  
 2792 03 UTC), especially because it is able to force convection where it occurs, reducing false alarms.

2793 The ability of lightning data assimilation to reduce false alarms compared to RAD and RADLI it is  
 2794 shown by the fact that the ETS score for LIGHT is sometimes the best among all simulations (see  
 2795 also the section S2 of the supplemental material of this paper). These results show also that the  
 2796 influence of different observations depends on the meteorological situation.

2797 The model configuration assimilating both radar reflectivity factor and lightning (RADLI) is able to  
 2798 retain important features of both data assimilation. For example, the simulation of the Livorno  
 2799 case in the phase 06-09 UTC was able to simulate the heavy precipitation over Lazio thanks to the  
 2800 radar reflectivity factor data assimilation and the precipitation over Sardinia, as well as the  
 2801 moderate precipitation over central Alps, thanks to lightning data assimilation.

2802 The property of RADLI to retain the precipitation features of both RAD and LIGHT it is shown by  
 2803 the POD score, which is the best, for most cases and thresholds, for RADLI.

Eliminato: for

Eliminato: or for the second stage (18-21 UTC) of the Serano case; however, also for these cases the assimilation of reflectivity improves the precipitation forecast

Eliminato: for

Eliminato: the

Eliminato: ve

Eliminato:

Eliminato: case

Eliminato: into the model

Eliminato: The last characteristic has been found in some others VSF of the case studies considered, and

Eliminato: C

Eliminato: the

Eliminato: Another example of synergistic interaction between the two types of data assimilation was found for the most intense phase of the Serano case (03-06 UTC on 16 September 2017). In this period, the light precipitation over the Alps was forecast by RADLI because of the assimilation of radar reflectivity factor, while the localised precipitation maximum over Central Italy was better forecast thanks to the synergistic action of lightning and reflectivity factor data assimilation.<sup>†</sup>

Eliminato: forecast

Eliminato: data

2829 Another interesting feature is the considerable improvement of the POD of RADLI compared to  
 2830 CTRL for the lowest thresholds.

2831 It is also underlined that the data assimilated, both lightning and radar reflectivity factor, are  
 2832 available in real time and could be used for an operational implementation of the VSF.

2833 All the above features are promising and deserve future studies to better understand the role of  
 2834 radar reflectivity factor and its interaction with lightning data assimilation to improve the  
 2835 precipitation forecast.

2836 There are, however, less satisfactory aspects of assimilating both radar reflectivity factor and  
 2837 lightning data. In particular, the wet bias of RAD and RADLI forecast is the main drawback of the  
 2838 results of this paper. To reduce the moisture added by radar and lightning data assimilation  
 2839 further research is needed and different approaches are possible (Fierro et al., 2016). In particular:  
 2840 a) assimilating for a shorter time (0-6h in this paper); b) reducing the length-scales of the 3D-Var in  
 2841 the horizontal directions to limit the spreading of the innovations, or assuming an innovation  
 2842 equal to zero for grid points without lightning and with zero reflectivity factor; c) reducing the  
 2843 amount of water vapour added to the model (for example reducing the values of A and B  
 2844 constants for lightning data assimilation or relaxing the request of saturation when radar  
 2845 reflectivity is observed in areas where the model has zero reflectivity); d) adding moisture to a  
 2846 shallower vertical layer.

2847 It is also noted that a combination of heating and moistening could provide the same buoyancy  
 2848 with less water vapour addition (Marchand and Fulberg, 2014) and this approach could be used in  
 2849 future studies.

2850 In addition to the acquisition of more case studies, there are two directions of future development  
 2851 of this work. Lightning data assimilation can be formulated by 3DVar, using a strategy similar to  
 2852 the radar reflectivity factor in which pseudo-profiles of relative humidity are first generated where  
 2853 flashes are recorded, and then those profiles are assimilated by 3DVar. This methodology was  
 2854 already reported in Fierro et al. (2016). The assimilation of both radar reflectivity factor and  
 2855 lightning using RAMS-3DVar will be explored in future studies.

2856 Another important point to study is how long the innovations introduced by data assimilation lasts  
 2857 in the forecast. While in this study we consider the VSF at 3h, future studies must explore longer  
 2858 time ranges. This kind of study was performed for lightning data assimilation (Fierro et al., (2015);  
 2859 Federico et al., 2017b; Lynn et al. (2015) among others) and for radar data assimilation (Hu et al.  
 2860 (2006); Jones et al. (2014), among others), using a rationale similar to that used in this paper.

**Eliminato:** , showing the better ability of RADLI to predict the area where precipitation will occur at the short term

**Eliminato:** ¶

**Eliminato:** produced operationally and

**Eliminato:** model

**Eliminato:** ;

**Eliminato:** t

**Eliminato:** The RADLI forecast has more false alarms compared to RAD and LIGHT and this penalises the usefulness of RADLI forecast. This is shown by the lower ETS and HR score of RADLI, especially compared to LIGHT, for some thresholds and VSF, despite the larger values of the POD of RADLI.

**Eliminato:** The RADLI forecast can miss intense precipitation: this is shown, for example, by the VSF of 18-21 UTC on 9 September 2017 (Livorno), when RADLI underestimated the most intense phase of the storm in Livorno. ¶

**Eliminato:** model

**Eliminato:** explored

**Eliminato:** A similar study was

**Eliminato:** model set-up very

2883 In general, the performance of the forecast and the impact of lightning and radar data assimilation  
2884 decrease with forecasting time because of the propagation of boundary conditions inside the  
2885 domain and because of model errors growth. Improving the data assimilation system also  
2886 contributes to a longer resilience of model performance. The studies cited above showed that  
2887 lightning and radar data assimilation can have an impact up to 24h depending on several factors  
2888 (meteorological model, data assimilation, quality of the data, meteorological conditions, initial and  
2889 boundary conditions).

2890 A study considering both radar reflectivity factor and lightning should be performed to understand  
2891 the resilience of the innovations introduced by data assimilation.

2892

#### 2893 ACKNOWLEDGMENTS

2894 This work is a contribution to the HyMeX program. Part of the computational time used for this  
2895 paper was granted by the ECMWF (European Centre for Medium Weather range Forecast)  
2896 throughout the special project SPITFEDE. LINET data were provided by Nowcast GmbH  
2897 (<https://www.nowcast.de/>) within a scientific agreement between H.D. Betz and the Satellite  
2898 Meteorological Group of CNR-ISAC in Rome.

2899 This work was partially funded by the agreement between CNR-ISAC and the Italian Department of  
2900 Civil Protection.

2901

2902

#### 2903 References

2904 Alexander, G. D., Weinman, J. A., Karyampoudi, V. M., Olson, W. S., and Lee, A. C. L.: The effect of  
2905 assimilating rain rates derived from satellites and lightning on forecasts of the 1993 superstorm,  
2906 Mon. Weather Rev., 127, 1433–1457, 1999.

2907 Barker, D.M., Huang, W., Guo, Y.-R., and Xiao, Q.N.: A Three-Dimensional Variational Data  
2908 Assimilation System for MM5: Implementation And Initial Results, Monthly Weather Review, 132,  
2909 897-914, 2004.

2910 Barker, D. M., Huang, X.-Y., Liu, Z., Aulignè, T., Zhang, X., Rugg, S., Ajjaji, R., Bourgeois, A., Bray, J.,  
2911 Chen, Y., Demirtas, M., Guo, Y.-R., Henderson, T., Huang, W., Lin, H.C., Michalakes, J., Rizvi, S., and  
2912 Zhang, X.: The Weather Research and Forecasting (WRF) Model's Community  
2913 Variational/Ensemble Data Assimilation System: WRFDA. Bull. Amer. Meteor. Soc., 93, 831–843,  
2914 2012.

2915 Betz, H.-D., Schmidt, K., Laroche, P., Blanchet, P., Oettinger, P., Defer, E., Dziejewit, Z., and Konarski,  
2916 J.: LINET-an international lightning detection network in Europe, Atmos. Res., 91, 564– 573, 2009.

**Eliminato:** Results showed that the lightning data assimilation gave a small and positive contribution to the precipitation forecast up to 24 h. However, the impact of data assimilation decreased rapidly, and the improvement of the rainfall forecast was significant after 6h, small after 12h and negligible after 24 h.

**Formattato:** Inglese (Regno Unito)

**Spostato (inserimento) [2]**

**Eliminato:** F

**Eliminato:** ¶

**Formattato:** Inglese (Regno Unito)

**Spostato in su [2]:** Barker, D.M., Huang, W., Guo, Y.-R., and Xiao, Q.N.: A Three-Dimensional Variational Data Assimilation System For MM5: Implementation And Initial Results, Monthly Weather Review, 132, 897-914, 2004.

2929 Buzzi, A. and Tibaldi, S.: Cyclogenesis in the lee of the Alps: A case study. Q.J.R. Meteorol. Soc.,  
 2930 104: 271-287. <https://doi.org/10.1002/qj.49710444004>, 1978.

2931 Caumont, O., Ducrocq, V., Wattrelot, E., Jaubert, G., and Pradier-Vabre, S.: 1D+3DVar assimilation  
 2932 of radar reflectivity data: a proof of concept, Tellus A: Dynamic Meteorology and  
 2933 Oceanography, 62:2, 173-187, <https://www.tandfonline.com/doi/abs/10.1111/j.1600-0870.2009.00430.x>, 2010.

2935 Carey, L. D., and S. A. Rutledge: Electrical and multiparameter radar observations of a severe  
 2936 hailstorm. J. Geophys. Res., 103, 13 979–14 000, doi:10.1029/97JD02626, 1998.

2937 Chang, D. E., Weinman, J. A., Morales, C. A., and Olson, W. S.: The effect of spaceborn microwave  
 2938 and ground-based continuous lightning measurements on forecasts of the 1998 Groundhog Day  
 2939 storm, Mon. Weather Rev., 129, 1809–1833, 2001.

2940 Chen, C. and Cotton, W.R.: A One-Dimensional Simulation of the Stratocumulus-Capped Mixed  
 2941 Layer, Boundary Layer Meteorology, 25, 289-321, 1983.

2942 Cotton, W.R., Pielke Sr., R.A., Walko, R.L., Liston, G.E., Tremback, C.J., Jiang, H., McAnelly, R.L.,  
 2943 Harrington, J.Y.m Nicholls, M.E., Carrio, G.G., and McFadden, J.P.: RAMS 2001: Current status and  
 2944 future directions, Meteorology and Atmospheric Physics, 82, 5-29,2003.

2945 Courtier, P., Thépaut, J. N., and Hollingsworth, A.: A strategy for operational implementation of  
 2946 4D-Var, using an incremental approach, Q. J. Roy. Meteorol. Soc., 120, 1367–1387, 1994.

2947 Dahl, J. M. L., Höller, H., and Schumann, U.: Modeling the Flash Rate of Thunderstorms. Part II:  
 2948 Implementation. Monthly Weather Review, 139, 3112-3124, 2011.

2949 Deierling, W., and W. A. Petersen: Total lightning activity as an indicator of updraft characteristics.  
 2950 J. Geophys. Res., 113, D16210, doi:10.1029/2007JD009598, 2008.

2951 Ducrocq, V., Braud, I., Davolio, S., Ferretti, R., Flamant, C., Jansa, A., Kalthoff, N., Richard, E.,  
 2952 Taupier-Letage, I., Ayrat, P.-A., Belamari, S., Berne, A., Borga, M., Boudevillain, B., Bock, O.,  
 2953 Boichard, J.-L., Bouin, M.-N., Bousquet, O., Bouvier, C., Chiggiato, J., Cimini, D., Corsmeier, U.,  
 2954 Coppola, L., Cocquerez, P., Defer, E., Delanoë, J., Di Girolamo, P., Doerenbecher, A., Drobinski, P.,  
 2955 Dufournet, Y., Fourrié, N., Gourley, J.J., Labatut, L., Lambert, D., Le Coz, J., Marzano, F.S., Molinié,  
 2956 G., Montani, A., Nord, G., Nuret, M., Ramage, K., Rison, W., Roussot, O., Said, F., Schwarzenboeck,  
 2957 A., Testor, P., Van Baelen, J., Vincendon, B., Aran, M., and Tamayo, J.: HYMEX-SOP1 The Field  
 2958 Campaign Dedicated to Heavy Precipitation and Flash Flooding in the Northwestern  
 2959 Mediterranean. Bull. Amer. Meteor. Soc., 95, 1083–1100, <https://doi.org/10.1175/BAMS-D-12-00244.1>, 2014.

2961 Emersic, C., and C. P. R. Saunders: Further laboratory investigations into the relative diffusional  
 2962 growth rate theory of thunderstorm electrification. Atmos. Res., 98, 327–340,  
 2963 doi:<https://doi.org/10.1016/j.atmosres.2010.07.011>, 2010.

Formattato: Inglese (Regno Unito)

Formattato: Car. predefinito paragrafo, Inglese (Regno Unito)

Formattato: Inglese (Regno Unito)

Formattato: Car. predefinito paragrafo, Italiano

Formattato: Inglese (Regno Unito)

Formattato: Inglese (Regno Unito)

Formattato: Inglese americano

Formattato: Inglese (Regno Unito)

Formattato: Car. predefinito paragrafo, Tipo di carattere: Colore carattere: Nero, Inglese (Regno Unito)

Formattato: Inglese (Regno Unito)

Formattato: Colore carattere: Testo 1

Formattato: Colore carattere: Testo 1



2964 Fabry, F., and Sun, J: For how long should what data be assimilated for the mesoscale forecasting  
 2965 of convection and why? Part I: On the propagation of initial condition errors and their implications  
 2966 for data assimilation. *Monthly Weather Review*, 138(1), 242–255, [https://doi.org/](https://doi.org/2009mwr2883.1)  
 2967 /2009mwr2883.1, 2010.

2968 [Federico, S.: Implementation of a 3D-Var system for atmospheric profiling data assimilation into  
 2969 the RAMS model: Initial results, \*Atmospheric Measurement Techniques\*, 6\(12\), 3563-3576, 2013.](#)

2970 [Federico, S.: Implementation of the WSM5 and WSM6 Single Moment Microphysics Scheme into  
 2971 the RAMS Model: Verification for the HyMeX-SOP1, \*Advances in Meteorology, Volume 2016\*,  
 2972 2016.](#)

2973 Federico, S., Petracca, M., Panegrossi, G., and Dietrich, S.: Improvement of RAMS precipitation  
 2974 forecast at the short-range through lightning data assimilation, *Nat. Hazards Earth Syst. Sci.*, 17,  
 2975 61–76, <https://doi.org/10.5194/nhess-17-61-2017>, 2017a.

2976 [Federico, S., Avolio, E., Petracca, M., Panegrossi, G., Sanò, P., Casella, D., and Dietrich S.: Simulating  
 2977 lightning into the RAMS model: Implementation and preliminary results, \*Natural Hazards and  
 2978 Earth System Sciences, Volume 14, Number 11, p.2933-2950, 2014.\*](#)

2979 Federico, S., Petracca, M., Panegrossi, G., Transerici, C., and Dietrich, S.: Impact of the assimilation  
 2980 of lightning data on the precipitation forecast at different forecast ranges. *Adv. Sci. Res.*, 14, 187–  
 2981 194, 2017b.

2982 Federico, S., Torcasio, R. C., Avolio, E., Caumont, O., Montopoli, M., Baldini, L., Vulpiani, G., and  
 2983 Dietrich, S.: The impact of lightning and radar data assimilation on the performance of very short  
 2984 term rainfall forecast for two case studies in Italy, *Nat. Hazards Earth Syst. Sci. Discuss.*,  
 2985 <https://doi.org/10.5194/nhess-2018-319>, in review, 2018.

2986 [Ferretti, R., Pichelli, E., Gentile, S., Maiello, I., Cimini, D., Davolio, S., Miglietta, M. M., Panegrossi,  
 2987 G., Baldini, L., Pasi, F., Marzano, F. S., Zinzi, A., Mariani, S., Casaioli, M., Bartolini, G., Loglisci, N.,  
 2988 Montani, A., Marsigli, C., Manzato, A., Pucillo, A., Ferrario, M. E., Colaiuda, V., and Rotunno, R.:  
 2989 Overview of the first HyMeX Special Observation Period over Italy: observations and model  
 2990 results, \*Hydrol. Earth Syst. Sci.\*, 18, 1953–1977, <https://doi.org/10.5194/hess-18-1953-2014>, 2014.](#)

2991 [Fierro, A. O., A. J. Clark, E. R. Mansell, D. R. MacGorman, S. Dembek, and C. Ziegler: Impact of  
 2992 storm-scale lightning data assimilation on WRF-ARW precipitation forecasts during the 2013 warm  
 2993 season over the contiguous United States. \*Mon. Wea. Rev.\*, 143, 757–777,  
 2994 \[doi:https://doi.org/10.1175/MWR-D-14-00183.1\]\(https://doi.org/10.1175/MWR-D-14-00183.1\), 2015.](#)

2995 [Fierro, A.O., Gao, I., Ziegler, C. L., Calhoun, K. M., Mansell, E. R., and MacGorman, D.  
 2996 R.: Assimilation of Flash Extent Data in the Variational Framework at Convection-Allowing Scales:  
 2997 Proof-of-Concept and Evaluation for the Short-Term Forecast of the 24 May 2011 Tornado  
 2998 Outbreak. \*Mon. Wea. Rev.\*, 144, 4373–4393, 2016, <https://doi.org/10.1175/MWR-D-16-0053.1>  
 2999 2016.](#)

**Eliminato:** Jones, C. D., and Macpherson, B.: A latent heat nudging scheme for the assimilation of precipitation into an operational mesoscale model, *Meteorol. Appl.*, 4, 269–277, 1997.¶

**Formattato:** Inglese (Regno Unito)

**Spostato (inserimento) [3]**

**Eliminato:** ¶

**Formattato:** Inglese (Regno Unito)

**Spostato (inserimento) [4]**

**Eliminato:** ¶

**Formattato:** Inglese americano

**Eliminato:** Federico, S.: Implementation of the WSM5 and WSM6 Single Moment Microphysics Scheme into the RAMS Model: Verification for the HyMeX-SOP1, *Advances in Meteorology, Volume 2016*, 2016.¶

**Spostato in su [4]:** Federico, S., Avolio, E., Petracca, M., Panegrossi, G., Sanò, P., Casella, D., and Dietrich S.: Simulating lightning into the RAMS model: Implementation and preliminary results, *Natural Hazards and Earth System Sciences, Volume 14, Number 11, p.2933-2950, 2014.*¶

Federico, S., Torcasio, R. C., Avolio, E., Caumont, O., Montopoli, M., Baldini, L., Vulpiani, G., and Dietrich, S.: The impact of lightning and radar data assimilation on the performance of very short term rainfall forecast for two case studies in Italy, *Nat. Hazards Earth Syst. Sci. Discuss.*, <https://doi.org/10.5194/nhess-2018-319>, in review, 2018.¶

**Formattato:** Car. predefinito paragrafo, Inglese (Regno Unito)

**Formattato:** Car. predefinito paragrafo, Inglese (Regno Unito)

**Formattato:** Car. predefinito paragrafo, Inglese (Regno Unito)

**Formattato:** Car. predefinito paragrafo, Inglese (Regno Unito)

**Formattato:** Car. predefinito paragrafo, Inglese (Regno Unito)

**Formattato:** Inglese americano

**Formattato:** Inglese americano

**Spostato in su [3]:** Federico, S.: Implementation of a 3D-Var system for atmospheric profiling data assimilation into the RAMS model: Initial results, *Atmospheric Measurement Techniques*, 6(12), 3563-3576, 2013.

**Formattato:** Italiano

**Formattato:** Colore carattere: Testo 1, Inglese americano

**Spostato in giù [5]:** Fierro, A. O., Mansell, E., Ziegler, C., and MacGorman, D.: Application of a lightning data assimilation technique in the WRFARW model at cloud-

**Eliminato:** Fierro, A. O., Mansell, E., Ziegler, C., and MacGorman, D.: Application of a lightning data ... [3]

**Formattato:** Colore carattere: Testo 1, Inglese americano

**Formattato:** Car. predefinito paragrafo, Italiano

**Eliminato:** .

3042 [Fierro, A. O., J. Gao, C. Ziegler, E. R. Mansell, D. R. MacGorman, and S. Dembek: Evaluation of a](#)  
3043 [cloud scale lightning data assimilation technique and a 3DVAR method for the analysis and short-](#)  
3044 [term forecast of the 29 June 2012 derecho event. Mon. Wea. Rev., 142, 183–202, doi:10.1175/](#)  
3045 [MWR-D-13-00142.1](#), 2014

3046 Fierro, A. O., M. S. Gilmore, E. R. Mansell, L. J. Wicker, and J. M. Straka: Electrification and lightning  
3047 in an idealized boundary-crossing supercell simulation of 2 June 1995. Mon. Wea. Rev., 134, 3149–  
3048 3172, doi:10.1175/MWR3231.1, 2006.

3049 [Fierro, A. O., Mansell, E., Ziegler, C., and MacGorman, D.: Application of a lightning data](#)  
3050 [assimilation technique in the WRFARW model at cloud-resolving scales for the tornado outbreak](#)  
3051 [of 24 May 2011, Mon. Weather Rev., 140, 2609–2627, 2012.](#)

3052 [Giannaros, T. M., Kotroni, V., and Lagouvardos, K.: WRFLNGDA: A lightning data assimilation](#)  
3053 [technique implemented in the WRF model for improving precipitation forecasts, Environ. Model.](#)  
3054 [Softw., 76, 54–68, doi:10.1016/j.envsoft.2015.11.017, 2016.](#)

3055 Hong, S.Y., Lim, J.J.O.: The WRF single-moment 6-class microphysics scheme (WSM6). J. Korean  
3056 Meteorol. Soc. 42, 129–151, 2006.

3057 [Hu, M., M. Xue, and K. Brewster: 3DVAR and cloud analysis with WSR-88D level-II data for the](#)  
3058 [prediction of the Fort Worth, Texas, tornadic thunderstorms. Part I: Cloud analysis and its impact.](#)  
3059 [Mon. Wea. Rev., 134, 675–698, doi:10.1175/MWR3092.1, 2006.](#)

3060 [Ikuta, Y. and Honda, Y.: Development of 1D+4DVAR data assimilation of radar reflectivity in JNOVA.](#)  
3061 [Tech. Report, 01.09–01.10. \[http://www.wcrp-climate.org/WGNE/BlueBook/2011/individual-\]\(http://www.wcrp-climate.org/WGNE/BlueBook/2011/individual-articles/01\_Ikuta\_Yasutaka\_WGNE2011\_1D4DVAR.pdf\)](#)  
3062 [articles/01\\_Ikuta\\_Yasutaka\\_WGNE2011\\_1D4DVAR.pdf](#), 2011.

3063 [Jones, C. D., and Macpherson, B.: A latent heat nudging scheme for the assimilation of](#)  
3064 [precipitation into an operational mesoscale model, Meteorol. Appl., 4, 269–277, 1997.](#)

3065 [Jones, T. A., J. A. Otkin, D. J. Stensrud, and K. Knopfmeier: Forecast evaluation of an observing](#)  
3066 [system simulation experiment assimilating both radar and satellite data. Mon. Wea. Rev., 142,](#)  
3067 [107–124, doi:10.1175/MWR-D-13-00151.1, 2014.](#)

3068 [Kain, J. S. and Fritsch, J. M.: Convective parameterization for mesoscale models: the Kain-Fritsch](#)  
3069 [scheme. The representation of cumulus convection in numerical models, Meteor. Monogr. No. 46,](#)  
3070 [Am. Meteor. Soc., Boston, 165–170, 1993.](#)

3071 [Kuhlman, K. M., C. L. Zielger, E. R. Mansell, D. R. MacGorman, and J. M. Straka: Numerically](#)  
3072 [simulated electrification and lightning of the 29 June 2000 STEPS supercell storm. Mon. Wea. Rev.,](#)  
3073 [134, 2734–2757, doi:10.1175/MWR3217.1, 2006.](#)

Formattato: Colore carattere: Testo 1

Spostato (inserimento) [5]

Eliminato: ¶

Formattato: Inglese (Regno Unito)

Formattato: Nessuno, Inglese (Regno Unito)

Formattato: Inglese (Regno Unito)

Eliminato: [http://www.wcrp-climate.org/WGNE/BlueBook/2011/individual-articles/01\\_Ikuta\\_Yasutaka\\_WGNE2011\\_1D4DVAR.pdf](http://www.wcrp-climate.org/WGNE/BlueBook/2011/individual-articles/01_Ikuta_Yasutaka_WGNE2011_1D4DVAR.pdf)

Formattato: Car. predefinito paragrafo, Inglese (Regno Unito)

Formattato: Car. predefinito paragrafo, Inglese (Regno Unito)

Formattato: Nessuna sottolineatura, Inglese (Regno Unito)

Formattato: Inglese (Regno Unito)

Spostato (inserimento) [6]

Eliminato: ¶

Formattato: Inglese (Regno Unito)

Formattato: Inglese (Regno Unito)

Spostato in su [6]: Jones, C. D., and Macpherson, B.: A latent heat nudging scheme for the assimilation of precipitation into an operational mesoscale model, Meteorol. Appl., 4, 269–277, 1997.

Formattato: Allineato a sinistra

Formattato: Inglese (Regno Unito)

3083 Kummerow, C., Hong, Y., Olson, W.S., Yang, S., Adler, R.F., McCollum, J., Ferraro, R., Petty, G., Shin.  
3084 D.-B., and Wilheit, T.T.: The evolution of the Goddard profiling algorithm (GPROF) for rainfall  
3085 estimation from passive microwave sensors. *J. Appl. Meteor.*, 40, 1801–1820, 2001.

3086 [Lagouvardos, K., Kotroni, V., Betz, H.-D., and Schmidt, K.: A comparison of lightning data provided  
3087 by ZEUS and LINET networks over Western Europe, \*Nat. Hazards Earth Syst. Sci.\*, 9, 1713–1717,  
3088 <https://doi.org/10.5194/nhess-9-1713-2009>, 2009.](#)

3089 [Lynn, B. H., Kelman, G., and Ellrod, G.: An evaluation of the efficacy of using observed lightning to  
3090 improve convective lightning forecasts. \*Wea. Forecasting\*, 30, 405–423 doi:10.1175/WAF-D-13-  
3091 00028.1, 2015.](#)

3092 [Lynn, B.H.: The Usefulness and Economic Value of Total Lightning Forecasts Made with a Dynamic  
3093 Lightning Scheme Coupled with Lightning Data Assimilation. \*Wea. Forecasting\*, 32, 645–  
3094 663, <https://doi.org/10.1175/WAF-D-16-0031.1>, 2017.](#)

3095 [MacGorman, I. R. Apostolopoulos, N. R. Lund, N. W. S. Demetriades, M. J. Murphy, and P. R.  
3096 Krehbiel: The timing of cloud-to-ground lightning relative to total lightning activity. \*Mon. Wea.\*  
3097 \*Rev.\*, 139, 3871–3886, doi:10.1175/MWR-D-11-00047.1, 2011.](#)

3098 [MacGorman, D. W. Burgess, V. Mazur, W. D. Rust, W. L. Taylor, and B. C. Johnson: Lightning rates  
3099 relative to tornadic storm evolution on 22 May 1981. \*J. Atmos. Sci.\*, 46, 221–251, doi:10.1175/  
3100 1520-0469\(1989\)046,0221:LRRTTS.2.0.CO;2, 1989.](#)

3101 [MacGorman, W. D. Rust, P. Krehbiel, W. Rison, E. Bruning, and K. Wiens: The electrical structure of  
3102 two supercell storms during STEPS. \*Mon. Wea. Rev.\*, 133, 2583–2607, doi:10.1175/MWR2994.1,  
3103 2005.](#)

3104 [MacGorman, D.R. and K.E. Nielsen: Cloud-to-Ground Lightning in a Tornadic Storm on 8 May 1986.  
3105 \*Mon. Wea. Rev.\*, 119, 1557–1574, \[https://doi.org/10.1175/1520-  
3106 0493\\(1991\\)119<1557:CTGLIA>2.0.CO;2\]\(https://doi.org/10.1175/1520-0493\(1991\)119<1557:CTGLIA>2.0.CO;2\), 1991.](#)

3107 [Maiello, I., Ferretti, R., Gentile, S., Montopoli, M., Picciotti, E., Marzano, F. S., and Faccani, C.:  
3108 Impact of radar data assimilation for the simulation of a heavy rainfall case in central Italy using  
3109 WRF–3DVAR, \*Atmos. Meas. Tech.\*, 7, 2919–2935, <https://doi.org/10.5194/amt-7-2919-2014>, 2014.](#)

3110 Mansell, E. R., Ziegler, C. L., and MacGorman, D. R.: A lightning data assimilation technique for  
3111 mesoscale forecast models, *Mon. Weather Rev.*, 135, 1732–1748, 2007.

3112 [Marchand, M., and H. Fuelberg: Assimilation of lightning data using a nudging method involving  
3113 low-level warming. \*Mon. Wea. Rev.\*, 142, 4850–4871, doi:10.1175/MWR-D-14-00076.1, 2014.](#)

3114 [Mass, C. F., Ovens, D., Westrick, K., and Colle, B. A.: Does increasing horizontal resolution produce  
3115 more skilful forecasts?, \*B. Am. Meteorol. Soc.\*, 83, 407–430, 2002.](#)

3117 [Mellor, G., and Yamada, T.: Development of a Turbulence Closure Model for Geophysical Fluid  
3118 Problems, \*Review of Geophysics and Space Physics\*, 20, 851–875, 1982.](#)

**Formattato:** SpazioDopo: 9 pt, Interlinea: singola, Bordo: Superiore: (Nessun bordo), Inferiore: (Nessun bordo), A sinistra: (Nessun bordo), A destra: (Nessun bordo), Tra : (Nessun bordo), Barra : (Nessun bordo)

**Formattato:** Colore carattere: Testo 1

**Formattato:** Colore carattere: Testo 1

**Formattato:** Colore carattere: Testo 1

**Formattato:** Colore carattere: Testo 1

**Formattato:** Car. predefinito paragrafo, Colore carattere: Testo 1, Inglese americano

**Formattato:** Tipo di carattere: Non Corsivo, Colore carattere: Testo 1, Inglese americano

**Formattato:** Car. predefinito paragrafo, Colore carattere: Testo 1, Inglese americano

**Formattato:** Colore carattere: Testo 1, Inglese americano

**Formattato:** SpazioDopo: 9 pt, Interlinea: singola, Bordo: Superiore: (Nessun bordo), Inferiore: (Nessun bordo), A sinistra: (Nessun bordo), A destra: (Nessun bordo), Tra : (Nessun bordo), Barra : (Nessun bordo)

**Formattato:** Colore carattere: Testo 1

**Formattato:** Colore carattere: Testo 1

**Formattato:** Colore carattere: Testo 1

**Eliminato:** ¶

**Formattato:** Colore carattere: Testo 1, Inglese americano

**Formattato:** Inglese (Regno Unito)

**Formattato:** Nessuno, Inglese (Regno Unito)

**Formattato:** Giustificato

**Formattato:** Colore carattere: Testo 1

**Formattato:** Colore carattere: Testo 1

**Eliminato:** ¶

3121 [Mittermaier, M., N. Roberts, and S. A. Thompson, 2013: A long-term assessment of precipitation](#)  
3122 [forecast skill using the Fractions Skill Score. Meteor. Appl., 20, 176–186,](#)  
3123 [doi:https://doi.org/10.1002/met.296.](https://doi.org/10.1002/met.296)

3124 Molinari, J., and Corsetti, T.: Incorporation of cloud-scale and mesoscale down-drafts into a  
3125 cumulus parametrization: results of one and three-dimensional integrations, Monthly Weather  
3126 Review, 113, 485-501, 1985.

3127 Olson, W. S., Kummerow, C. D. , Heymsfield, G. M., and Giglio, L.: A method for combined passive-  
3128 active microwave retrievals of cloud and precipitation profiles. J. Appl. Meteor., 35, 1763-1789,  
3129 1996.

3130 [Papadopoulos, A., Chronis, T.G., Anagnostou, E.N. Improving convective precipitation forecasting](#)  
3131 [through assimilation of regional lightning measurements in a mesoscale model. Mon. Weather](#)  
3132 [Rev. 133, 1961-1977, 2005.](#)

3133 Parrish, D.F., and Derber, J.C.: The National Meteorological Center’s Spectral Statistical  
3134 Interpolation analysis system, Monthly Weather Review, 120, 1747-1763, 1992.

3135 [Pessi, A.T. and S. Businger,: Relationships among Lightning, Precipitation, and Hydrometeor](#)  
3136 [Characteristics over the North Pacific Ocean. J. Appl. Meteor. Climatol., 48, 833–](#)  
3137 [848, https://doi.org/10.1175/2008JAMC1817.1, 2009.](https://doi.org/10.1175/2008JAMC1817.1)

3138 [Petracca M., Casella D., Dietrich S., Milani L., Panegrossi G., Sanò P., Möhrlein M., Riso S. and Betz](#)  
3139 [H.D: “Lightning strokes frequency homogenization for climatological analysis: application to LINET](#)  
3140 [data records over Europe”, 2nd TEA – IS Summer School, June 23 – 27, 2014, Collioure, France,](#)  
3141 [2014.](#)

3142 [Petracca, M., L. P. D’Adderio, F. Porcù, G. Vulpiani, S. Sebastianelli, and S. Puca: Validation of GPM](#)  
3143 [Dual-Frequency Precipitation Radar \(DPR\) rainfall products over Italy. J. Hydrometeor., 19, 907–](#)  
3144 [925, 2018. https://doi.org/10.1175/JHM-D-17-0144.1, 2018.](https://doi.org/10.1175/JHM-D-17-0144.1)

3145 [Press, W. H., Teukolsky, S. A., Vetterling, W. T., and Flannery, B. P.: Numerical recipes in Fortran](#)  
3146 [77, second ed., Cambridge Uni- versity Press, Cambridge, 992 pp., 1992.](#)

3147 Qie, X., Zhu, R., Yuan, T., Wu, X., Li, W., and Liu, D.: Application of total-lightning data assimilation  
3148 in a mesoscale convective system based on the WRF model, Atmos. Res., 145–146, 255–266, 2014.

3149 [Ricciardelli, E.; Di Paola, F.; Gentile, S.; Cersosimo, A.; Cimini, D.; Gallucci, D.; Gerdali, E.; Larosa, S.;](#)  
3150 [Nilo, S.T.; Ripepi, E.; Romano, F.; Viggiano, M. Analysis of Livorno Heavy Rainfall Event: Examples](#)  
3151 [of Satellite-Based Observation Techniques in Support of Numerical Weather Prediction. Remote](#)  
3152 [Sens. 2018, 10, 1549, 2018.](#)

3153

3154 [Ridal, M., and Dahlbom, M.: Assimilation of multinational radar reflectivity data in a mesoscale](#)  
3155 [model: a proof of concept, Journal of Applied Meteorology and Climatology, 56\(6\), 1739–1751,](#)  
3156 [https://doi.org/10.1175/jamc-d-16-0247.1, 2017.](https://doi.org/10.1175/jamc-d-16-0247.1)

**Formattato:** Nessuno, Tipo di carattere: (Predefinito)  
**Calibri,** Inglese (Regno Unito), **Bordo:** : (Nessun bordo)

**Formattato:** Inglese americano

**Formattato:** Inglese americano

**Formattato:** Inglese americano

**Formattato:** Inglese americano

**Codice campo modificato**

**Formattato:** Inglese americano

**Formattato:** Inglese americano

**Formattato:** Tipo di carattere: Non Corsivo, Inglese americano

**Formattato:** Inglese americano

**Formattato:** Tipo di carattere: Non Grassetto, Inglese americano

**Formattato:** Inglese americano

**Codice campo modificato**

**Formattato:** Inglese americano

**Formattato:** Inglese americano

**Formattato:** Inglese americano

**Formattato:** Nessuno, Inglese (Regno Unito)

**Formattato:** Nessuno, Inglese (Regno Unito)

**Formattato:** Nessuno, Tipo di carattere: (Predefinito)  
**Calibri,** 12 pt, Inglese (Regno Unito)

**Formattato:** Nessuno, Tipo di carattere: (Predefinito)  
**Calibri,** 12 pt, Inglese (Regno Unito)

**Formattato:** Nessuno, Tipo di carattere: Inglese (Regno Unito)

**Formattato:** Inglese (Regno Unito)

**Formattato:** Colore carattere: Nero

**Formattato:** SpazioDopo: 0 pt, Interlinea: singola,  
**Bordo:** Superiore: (Nessun bordo), Inferiore: (Nessun  
bordo), A sinistra: (Nessun bordo), A destra: (Nessun  
bordo), Tra : (Nessun bordo), Barra : (Nessun bordo)

**Formattato:** Inglese (Regno Unito)

**Eliminato:** .

**Formattato:** Inglese (Regno Unito)

**Codice campo modificato**

**Formattato:** Collegamento ipertestuale, Inglese (Regno Unito)

**Eliminato:** , 2017

**Eliminato:** .

**Formattato:** Inglese (Regno Unito)

**Formattato:** Inglese (Regno Unito)

3160 [Rohn, M., Kelly, G., Saunders, R. W.: Impact of a New Cloud Motion Wind Product from Meteosat](#)  
3161 [on NWP Analyses and Forecasts, Monthly Weather Review, 129, 2392-2403, 2001.](#)

3162 [Skamarock, W. C., Klemm, J. B., Dudhia, J., Gill, D. O., Barker, D. M., Duda, M. G., Huang, X.-Y.,](#)  
3163 [Wang, W., and Powers, J. G.: A description of the Advanced Research WRF Version 3. NCAR](#)  
3164 [Technical Note, TN 475+STR, 113 pp., available at:](#)  
3165 [http://www2.mmm.ucar.edu/wrf/users/docs/arw\\_v3.pdf](http://www2.mmm.ucar.edu/wrf/users/docs/arw_v3.pdf) (last access: November 2018), 2008.

Eliminato: ¶

Formattato: Inglese (Regno Unito)

3166 Smagorinsky, J.: General circulation experiments with the primitive equations. Part I, The basic  
3167 experiment, Monthly Weather Review, 91, 99-164, 1963.

3168 [Stensrud, D. J., and Fritsch, J. M.: Mesoscale convective systems in weakly forced large-scale](#)  
3169 [environments. Part II: Generation of a mesoscale initial condition, Mon. Weather Rev., 122, 2068-](#)  
3170 [2083, 1994.](#)

Formattato: Inglese (Regno Unito)

3171 [Stensrud, D.J., M. Xue, L.J. Wicker, K.E. Kelleher, M.P. Foster, J.T. Schaefer, R.S. Schneider, S.G.](#)  
3172 [Benjamin, S.S. Weygandt, J.T. Ferree, and J.P. Tuell: Convective-Scale Warn-on-Forecast System.](#)  
3173 [Bull. Amer. Meteor. Soc., 90, 1487-1500, https://doi.org/10.1175/2009BAMS2795.1, 2009.](#)

3174 [Stewart, L. M., Dance, S. L., Nichols, N. K.: Data assimilation with correlated observation errors:](#)  
3175 [experiments with a 1-D shallow water model, Tellus A: Dynamic Meteorology and](#)  
3176 [Oceanography, 65:1, 2013, DOI: 10.3402/tellusa.v65i0.19546, 2013.](#)

Formattato: Inglese americano

Formattato: Inglese americano

Formattato: Inglese americano

Formattato: Inglese americano

Formattato: Inglese americano

Codice campo modificato

Formattato: Inglese americano

Formattato: Inglese (Regno Unito)

3177 [Sun, J., and Crook, N. A.: Dynamical and Microphysical Retrieval from Doppler RADAR](#)  
3178 [Observations Using a Cloud Model and Its Adjoint, Part I: Model Development and Simulated Data](#)  
3179 [Experiments, J. Atmos. Sci., 54, 1642-1661, 1997.](#)

3180 Sun, J., and Crook, N. A.: Dynamical and Microphysical Retrieval from Doppler RADAR  
3181 Observations Using a Cloud Model and Its Adjoint, Part II: Retrieval Experiments of an Observed  
3182 Florida Convective Storm, J. Atmos. Sci., 55, 835-852, 1998.

3183 Sun, J. and Wang, H.: Radar data assimilation with WRF 4DVar. Part II: comparison with 3D-Var for  
3184 a squall line over the US Great Plains, Mon. Weather Rev., 11, 2245-2264,  
3185 <https://doi.org/10.1175/MWR-D-12-00169.1>, 2012.

Formattato: Inglese (Regno Unito)

3186 [Takahashi, T.: Riming electrification as a charge generation mechanism in thunderstorms. J.](#)  
3187 [Atmos. Sci., 35, 1536-1548, doi:https://doi.org/10.1175/1520-0469\(1978\)0352.0.CO;2, 1978.](#)

Formattato: Colore carattere: Testo 1

Formattato: Colore carattere: Testo 1

3188 [Vulpiani, G., A. Rinollo, S. Puca, and M. Montopoli, 2014: A quality-based approach for radar rain](#)  
3189 [field reconstruction and the H-SAF precipitation products validation. Proc. Eighth European Radar](#)  
3190 [Conf., Garmish-Partenkirchen, Germany, ERAD, Abstract 220, 6 pp.,](#)  
3191 [http://www.pa.op.dlr.de/erad2014/programme/ExtendedAbstracts/220\\_Vulpiani.pdf](http://www.pa.op.dlr.de/erad2014/programme/ExtendedAbstracts/220_Vulpiani.pdf) (last access  
3192 [January 2019\), 2014.](#)

Formattato: Inglese (Regno Unito)

Formattato: Inglese (Regno Unito)

Formattato: Inglese (Regno Unito)

Formattato: Inglese (Regno Unito)

3194 Walko, R.L., Band, L.E., Baron, J., Kittel, T.G., Lammers, R., Lee, T.J., Ojima, D., Pielke Sr., R.A.,  
3195 Taylor, C., Tague, C., Tremback, C.J., and Vidale, P.L.: Coupled Atmosphere-Biosphere-Hydrology  
3196 Models for environmental prediction, *Journal of Applied Meteorology*, 39, 931-944, 2000.

3197 [Wang, H., Sun, J., Zhang, X., Huang, X., and Auligne, T.: Radar data assimilation with WRF 4D-Var.](#)  
3198 [Part I: system development and preliminary testing, \*Mon. Weather Rev.\*, 141, 2224–2244, 2013.](#)

Formattato: Inglese (Regno Unito)

3199 Wattrelot, É., Caumont, O. and Mahfouf, J. F.: Operational implementation of the 1D+3D-Var  
3200 assimilation method of radar reflectivity data in the AROME model. *Monthly Weather Review*,  
3201 142(5), 1852–1873. <https://doi.org/10.1175/MWR-D-13-00230.1>, 2014.

Formattato: Inglese (Regno Unito)

3202 Weisman, M. L., Skamarock, W. C., and Klemp, J. B.: The resolution dependence of explicitly  
3203 modeled convective systems, *Mon. Weather Rev.*, 125, 527–548, 1997.

3204 Weygandt, S. S., Benjamin, S. G., Hu, M., Smirnova, T. G., and Brown, J. M.: Use of lightning data to  
3205 enhance radar assimilation within the RUC and Rapid Refresh models. *Third Conf. on*  
3206 *Meteorological Applications of Lightning Data*, 20–24 January 2008, New Orleans, LA, Amer.  
3207 Meteor. Soc., 8.4, available at:  
3208 <https://ams.confex.com/ams/88Annual/webprogram/Paper134112.html> (last access: 03 October  
3209 2018), 2008.

3210 [Wiens, K. C., S. A. Rutledge, and S. A. Tessendorf, A: The 29 June 2000 supercell observed during](#)  
3211 [STEPS. Part II: Lightning and charge structure. \*J. Atmos. Sci.\*, 62, 4151–4177,](#)  
3212 [doi:10.1175/JAS3615.1, 2005.](#)

Formattato: SpazioDopo: 9 pt, Interlinea: singola, Bordo: Superiore: (Nessun bordo), Inferiore: (Nessun bordo), A sinistra: (Nessun bordo), A destra: (Nessun bordo), Tra : (Nessun bordo), Barra : (Nessun bordo)

3213 [Xiao, Q., Kuo, Y.-H., Sun, J., Chaulee, W., and Barker, D. M.: An Approach of RADAR Reflectivity](#)  
3214 [Data Assimilation and Its Assessment with the Inland QPF of Typhoon Rusa \(2002\) at Landfall, \*J.\*](#)  
3215 [Appl. Meteor. Climatol.](#), 46, 14–22, 2007.

Spostato (inserimento) [7]

3216 Xiao, Q., Kuo, Y.-H., Sun, J., and Lee, W. C.: Assimilation of Doppler RADAR Observations with a  
3217 Regional 3DVAR System: Impact of Doppler Velocities on Forecasts of a Heavy Rainfall Case, *J.*  
3218 *Appl. Meteor.*, 44, 768–788, 2005.

Eliminato: ¶

Formattato: Inglese (Regno Unito)

3219 Xu, Q., Wei, L., Gu, W., Gong, J., and Zhao, Q.: A 3.5-dimensional variational method for Doppler  
3220 radar data assimilation and its application to phased array radar observations, *Adv. Meteorol.*, vol.  
3221 2010, Article ID 797265, <https://doi.org/10.1155/2010/797265>, 2010.

Spostato in su [7]: Xiao, Q., Kuo, Y.-H., Sun, J., Chaulee, W., and Barker, D. M.: An Approach of RADAR Reflectivity Data Assimilation and Its Assessment with the Inland QPF of Typhoon Rusa (2002) at Landfall, *J. Appl. Meteor. Climatol.*, 46, 14–22, 2007.¶

Eliminato: ¶

Formattato: Inglese (Regno Unito)

3222 Xue, M., Wang, D., Gao, J., Brewster, K., and Droegemeier, K. K: The Advanced Regional Prediction  
3223 System (ARPS), storm scale numerical weather prediction and data assimilation, *Meteor. Atmos.*  
3224 *Phys.*, 82, 139–170, 2003.

3225 Zhao, Q., Cook, J., Xu, Q., and Harasti, P. R.: Using radar wind observations to improve mesoscale  
3226 numerical weather prediction, *Weather Forecast*, 21, 502–522, 2006.

3227

3235 **TABLES**

3236 Table 1: List of physical parameterisations used for RAMS@ISAC in this paper.

Physical parameterization	Selected scheme
Parametrized cumulus convection	Modified Kuo scheme to account for updraft and downdraft (Molinari and Corsetti, 1985). The scheme is applied to R10 only.
Explicit precipitation parameterization	Bulk microphysics with six hydrometeors (cloud, rain, graupel, snow, ice, water <u>vapour</u> ). Described in Hong and Lim (2006).
Exchange between the surface, the biosphere and atmosphere.	LEAF3 (Walko et al., 2000). LEAF includes prognostic equations for soil temperature and moisture for multiple layers, vegetation temperature and surface water, and temperature and water <u>vapour</u> mixing ratio of canopy air.
Sub-grid mixing	The turbulent mixing in the horizontal directions is parameterised following Smagorinsky (1963), vertical diffusion is parameterised according to the Mellor and Yamada (1982) scheme, which employs a prognostic turbulent kinetic energy.
Radiation scheme	Chen-Cotton (Chen and Cotton, 1983). The scheme accounts for condensate in the atmosphere.

Eliminato: vapor

Eliminato: vapor

3237  
3238 Table 2: Basic parameters of the RAMS@ISAC grids (R10, R4 and R1, corresponding, respectively, to the domains D1,  
3239 D2 and D3). NNXP is the number of grid points in the WE direction, NNYP is the number of grid-points in the NS  
3240 direction, NNZP is the number of vertical levels, DX is the size of the grid spacing in the WE direction, DY is the grid  
3241 spacing in the SN direction. Lx, Ly, and Lz are the domain extensions in the NS, WE, and vertical directions. CENTLON  
3242 and CENTLAT are the coordinates of the grid centres.

	R10, D1	R4, D2	R1, D3
NNXP	301	401	203
NNYP	301	401	203
NNZP	36	36	36
Lx	3000 km	1600 km	~270 km
Ly	3000 km	1600 km	~270 km
Lz	~22400 m	~22400 m	~22400 m
DX	10 km	4 km	4/3 km
DY	10 km	4 km	4/3 km
CENTLAT (°)	43.0 N	43.0 N	43.7 N

Eliminato: 

- 
- 
- 
- 
- 
- 
- 
- 
- 
- 
- 
- 

3267  
3268  
3269  
3270  
3271  
3272  
3273  
3274  
3275  
3276  
3277  
3278  
3279  
3280  
3281  
3282  
3283  
3284

CENTLON (°)	12.5 E	12.5 E	11.0 E
-------------	--------	--------	--------

Formattato: Bordo: : (Nessun bordo)

3285

Table 3: Types of simulations performed.

Experiment	Description	Data assimilated	Model variable impacted
CTRL	Control run	None	None
RAD	RADAR data assimilation	Reflectivity factor CAPPI (RAMS-3DVar)	Water vapour mixing ratio
LIGHT	Lightning data assimilation (A=0.85; B=0.16 in Eqn (1))	Lightning density (nudging)	Water vapour mixing ratio
RADLI	RADAR + lightning data assimilation (A=0.86; B=0.15 in Eqn (1))	Reflectivity factor CAPPI (RAMS-3DVar) + Lightning density (nudging)	Water vapour mixing ratio

Formattato: Bordo: : (Nessun bordo)

Formattato: Bordo: : (Nessun bordo)

Formattato: Bordo: : (Nessun bordo)

Formattato: Bordo: : (Nessun bordo)

Formattato: Bordo: : (Nessun bordo)

Formattato: Bordo: : (Nessun bordo)

Formattato: Bordo: : (Nessun bordo)

Formattato: Bordo: : (Nessun bordo)

Formattato: Bordo: : (Nessun bordo)

Formattato: Bordo: : (Nessun bordo)

Formattato: Bordo: : (Nessun bordo)

Formattato: Bordo: : (Nessun bordo)

Formattato: Bordo: : (Nessun bordo)

Formattato: Bordo: : (Nessun bordo)

Formattato: Bordo: : (Nessun bordo)

Formattato: Bordo: : (Nessun bordo)

Formattato: Bordo: : (Nessun bordo)

Formattato: Bordo: : (Nessun bordo)

Formattato: Bordo: : (Nessun bordo)

3286



3287 Table 4: ETS and POD scores for three different neighbourhood radii. Scores are computed over  
 3288 the domain D2.

Thresh	ETS nearest	POD nearest	ETS 25 km	POD 25 km	ETS 50 km	POD 50 km
old	neighbourhood	neighbourhood	(CTRL, RAD,	(CTRL, RAD,	(CTRL, RAD,	(CTRL, RAD,
(mm/3	(CTRL, RAD,	(CTRL, RAD,	LIGHT, RADLI)	LIGHT, RADLI)	LIGHT, RADLI)	LIGHT, RADLI)
h)	LIGHT, RADLI)	LIGHT, RADLI)				
1	(0.42,0.36,0.44, 0.33)	(0.57,0.87,0.60, 0.81)	(0.68,0.73,0.68, 0.73)	(0.77,0.93,0.75, 0.89)	(0.79,0.89,0.82, 0.87)	(0.84,0.92,0.84, 0.90)
6	(0.06,0.10,0.14, 0.13)	(0.0,0.5,0.20,0. 72)	(0.11,0.44,0.72, 0.41)	(0.11,0.86,0.72, 0.83)	(0.19,0.86,0.86, 0.92)	(0.19,0.86,0.86, 0.92)
10	(0.,0.05,0.,0.15)	(0.,0.26,0.,0.79)	(0.,0.66,0.58,0. 74)	(0.0,0.84,0.58,0 .89)	(0.,0.95,0.74,0. 90)	(0.,0.95,0.74,0. 90)
20	(0.,0.,0.,0.41)	(0.,0.,0.,0.8)	(0.0,0.41,0.33,0 .87)	(0.,0.47,0.3,0.9)	(0.,0.73,0.80,1 0)	(0.,0.73,0.80,1 0)
30	(0.,0.,0.,0.31)	(0.,0.,0.,0.5)	(0.,0.,0.,0.90)	(0.,0.,0.,0.9)	(0.,0.,0.,1.0)	(0.,0.,0.,1.0)
40	(0.,0.,0.,0.)	(0.,0.,0.,0.)	(0.,0.,0.,0.33)	(0.,0.,0.,0.33)	(0.,0.,0.,0.50)	(0.,0.,0.,0.50)

3289  
 3290  
 3291 Table 5: ETS and POD scores for three different neighbourhood radii. Scores are computed over  
 3292 the domain D3.

Thresh	ETS nearest	POD nearest	ETS 25 km	POD 25 km	ETS 50 km	POD 50 km
old	neighbourhood	neighbourhood	(CTRL, RAD,	(CTRL, RAD,	(CTRL, RAD,	(CTRL, RAD,
(mm/3	(CTRL, RAD,	(CTRL, RAD,	LIGHT, RADLI)	LIGHT, RADLI)	LIGHT, RADLI)	LIGHT, RADLI)
h)	LIGHT, RADLI)	LIGHT, RADLI)				
1	(0.43,0.64,0.70, 0.56)	(0.67,0.86,0.98, 0.99)	(0.68,0.80,0.82, 0.71)	(0.83,0.92,0.98, 0.99)	(0.68,0.80,0.82, 0.71)	(0.83,0.92,0.98, 0.99)
6	(0.1,0.31,0.60,0 .49)	(0.24,0.58,0.89, 0.95)	(0.49,0.70,0.91, 0.96)	(0.55,0.76,0.96, 0.97)	(0.49,0.70,0.91, 0.96)	(0.55,0.76,0.96, 0.97)
10	(0.11,0.33,0.56, 0.54)	(0.19,0.56,0.75, 0.80)	(0.48,0.76,0.91, 0.97)	(0.52,0.79,0.92, 0.97)	(0.48,0.76,0.91, 0.97)	(0.52,0.79,0.92, 0.97)
20	(0.02,0.30,0.52, 0.59)	(0.03,0.39,0.74, 0.81)	(0.18,0.73,0.97, 0.93)	(0.19,0.74,0.97, 0.97)	(0.18,0.73,0.96, 0.93)	(0.19,0.74,0.97, 0.97)
30	(0.,0.27,0.51,0. 47)	(0.,0.29,0.76,0. 76)	(0.,0.64,0.94,1. )	(0.,0.65,1.,1.)	(0.,0.64,0.94,1. )	(0.,0.65,1.,1.)
40	(0.,0.44,0.27,0. 27)	(0.,0.44,0.56,0. 67)	(0.,0.89,1.,1.)	(0.,0.89,1.,1.)	(0.,0.89,1.,1.)	(0.,0.89,1.,1.)
50	(0.,0.33,0.66,0. 50)	(0.,0.33,0.67,0. 67)	(0.,0.67,1.,1.)	(0.,0.67,1.,1.)	(0.,0.66,1.,1.)	(0.,0.67,1.,1.)

- Formattato ... [4]
- Formattato ... [8]
- Formattato ... [9]
- Formattato ... [10]
- Formattato ... [11]
- Formattato ... [5]
- Formattato ... [6]
- Formattato ... [7]
- Formattato ... [12]
- Formattato ... [13]
- Formattato ... [14]
- Formattato ... [15]
- Formattato ... [16]
- Formattato ... [17]
- Formattato ... [18]
- Formattato ... [19]
- Formattato ... [20]
- Formattato ... [21]
- Formattato ... [22]
- Formattato ... [23]
- Formattato ... [24]
- Formattato ... [25]
- Formattato ... [26]
- Formattato ... [27]
- Formattato ... [28]
- Formattato ... [29]
- Formattato ... [30]
- Formattato ... [31]
- Formattato ... [33]
- Formattato ... [32]
- Formattato ... [34]
- Formattato ... [35]
- Formattato ... [36]
- Formattato ... [37]
- Formattato ... [38]
- Formattato ... [39]
- Formattato ... [40]
- Formattato ... [41]
- Formattato ... [42]
- Formattato ... [43]
- Formattato ... [44]
- Formattato ... [45]
- Formattato ... [46]
- Formattato ... [47]
- Formattato ... [48]
- Formattato ... [53]
- Formattato ... [54]
- Formattato ... [55]
- Formattato ... [56]
- Formattato ... [50]
- Formattato ... [51]
- Formattato ... [52]
- Formattato ... [57]
- Formattato ... [58]
- Formattato ... [59]
- Formattato ... [60]
- Formattato ... [61]
- Formattato ... [62]
- Formattato ... [63]
- Formattato ... [64]
- Formattato ... [65]
- Formattato ... [66]
- Formattato ... [67]
- Formattato ... [68]

3293  
 3294  
 3295  
 3296  
 3297  
 3298  
 3299  
 3300  
 3301  
 3302  
 3303  
 3304  
 3305  
 3306

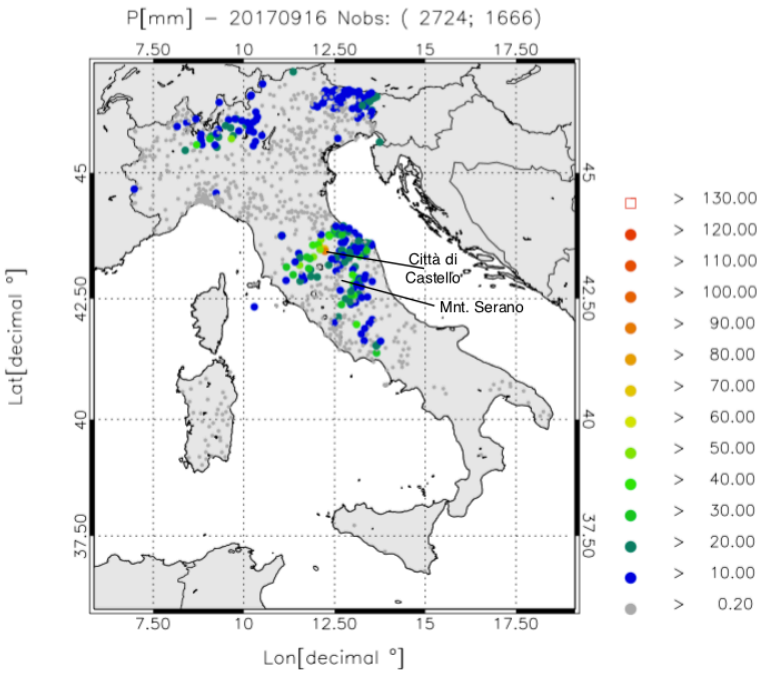
Table 6 ETS and POD scores for three different neighbourhood radii. Scores are computed over the domain D2.

Thresh old (mm/3 h)	ETS nearest neighborhood (CTRL, RAD, LIGHT, RADLI)	POD nearest neighbourhood (CTRL, RAD, LIGHT, RADLI)	ETS 25 km (CTRL, RAD, LIGHT, RADLI)	POD 25 km (CTRL, RAD, LIGHT, RADLI)	ETS 50 km (CTRL, RAD, LIGHT, RADLI)	POD 50 km (CTRL, RAD, LIGHT, RADLI)
1	(0.41,0.63,0.61,0.65)	(0.66,0.89,0.89,0.93)	(0.79,0.83,0.82,0.83)	(0.89,0.95,0.95,0.96)	(0.88,0.92,0.93,0.94)	(0.93,0.97,0.98,0.98)
6	(0.2,0.4,0.39,0.47)	(0.43,0.82,0.77,0.88)	(0.45,0.63,0.71,0.76)	(0.63,0.90,0.95,0.96)	(0.72,0.86,0.88,0.92)	(0.82,0.96,0.97,0.96)
10	(0.,0.24,0.18,0.28)	(0.14,0.78,0.55,0.80)	(0.14,0.47,0.58,0.62)	(0.24,0.86,0.82,0.93)	(0.32,0.91,0.96,0.95)	(0.35,0.95,0.97,0.97)
20	(0.03,0.18,0.13,0.22)	(0.01,0.81,0.30,0.80)	(0.09,0.46,0.57,0.61)	(0.11,0.86,0.59,0.90)	(0.15,0.84,0.91,0.96)	(0.15,0.90,0.92,0.97)
30	(0.02,0.22,0.13,0.28)	(0.,0.90,0.23,0.88)	(0.01,0.79,0.46,0.80)	(0.01,0.93,0.47,0.94)	(0.02,0.95,0.93,0.99)	(0.02,0.95,0.93,0.99)
40	(0.1,0.24,0.08,0.36)	(0.,0.83,0.12,0.89)	(0.01,0.83,0.37,0.83)	(0.02,0.97,0.38,0.97)	(0.1,0.97,0.95,0.98)	(0.02,0.98,0.95,0.98)
50	(0.01,0.27,0.,0.43)	(0.,0.67,0.,0.92)	(0.,0.90,0.,0.90)	(0.,0.94,0.,0.96)	(0.,0.96,0.,0.96)	(0.,0.96,0.,0.96)

- Formattato ... [99]
- Eliminato: ¶
- Formattato ... [100]
- Formattato ... [104]
- Formattato ... [105]
- Formattato ... [106]
- Formattato ... [107]
- Formattato ... [101]
- Formattato ... [102]
- Formattato ... [103]
- Formattato ... [108]
- Formattato ... [109]
- Formattato ... [110]
- Formattato ... [111]
- Formattato ... [112]
- Formattato ... [113]
- Formattato ... [114]
- Formattato ... [115]
- Formattato ... [116]
- Formattato ... [117]
- Formattato ... [118]
- Formattato ... [119]
- Formattato ... [120]
- Formattato ... [121]
- Formattato ... [122]
- Formattato ... [123]
- Formattato ... [124]
- Formattato ... [125]
- Formattato ... [127]
- Formattato ... [128]
- Formattato ... [129]
- Formattato ... [130]
- Formattato ... [131]
- Formattato ... [126]
- Formattato ... [133]
- Formattato ... [134]
- Formattato ... [135]
- Formattato ... [136]
- Formattato ... [137]
- Formattato ... [132]
- Formattato ... [139]
- Formattato ... [140]
- Formattato ... [141]
- Formattato ... [142]
- Formattato ... [143]
- Formattato ... [138]
- Formattato ... [145]
- Formattato ... [146]
- Formattato ... [147]
- Formattato ... [148]
- Formattato ... [149]
- Formattato ... [144]
- Formattato ... [150]
- Formattato ... [151]
- Eliminato: ¶
- Formattato ... [152]

3311 **FIGURES**

3312



3313

3314 Figure 1: Daily precipitation (P) [mm] over Italy on 16 September 2017. Only raingauges observing at least 0.2 mm/day  
3315 are shown. The first number in the figure title within brackets represents the available raingauges, while the second  
3316 number represents raingauges observing at least 0.2 mm/3h. The lowest precipitation class is represented by smaller  
3317 dots, the largest by a red square. The locations of Città di Castello and Mount Serano are indicated.

3318

3319

3320

3321

3322

3323

3324

3325

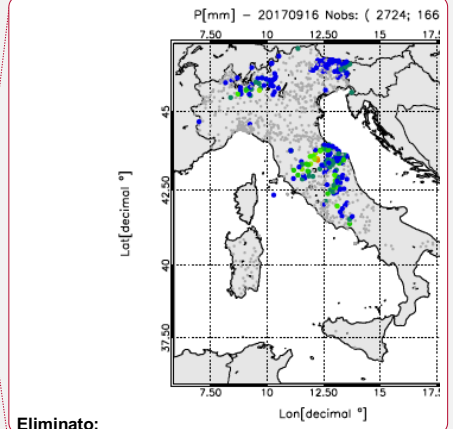
3326

3327

3328

a)

Eliminato: ¶



Eliminato:

Formattato: Giustificato

Eliminato: from the network of the Department of Civil Protection

Formattato: Giustificato

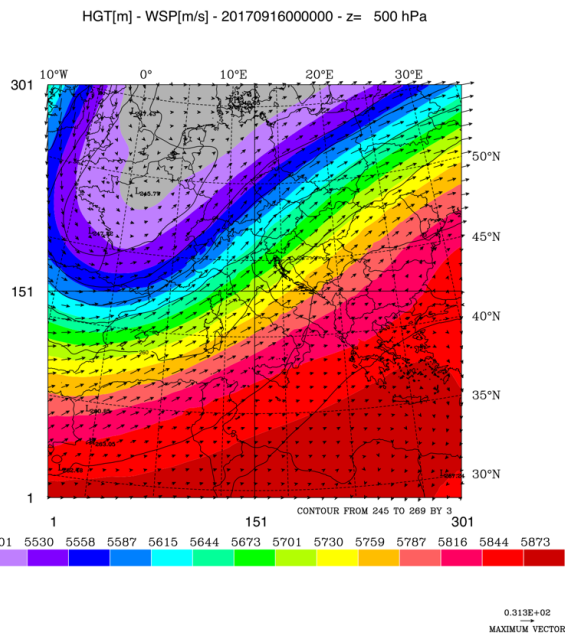
Eliminato: ¶

Eliminato: ¶

¶

¶

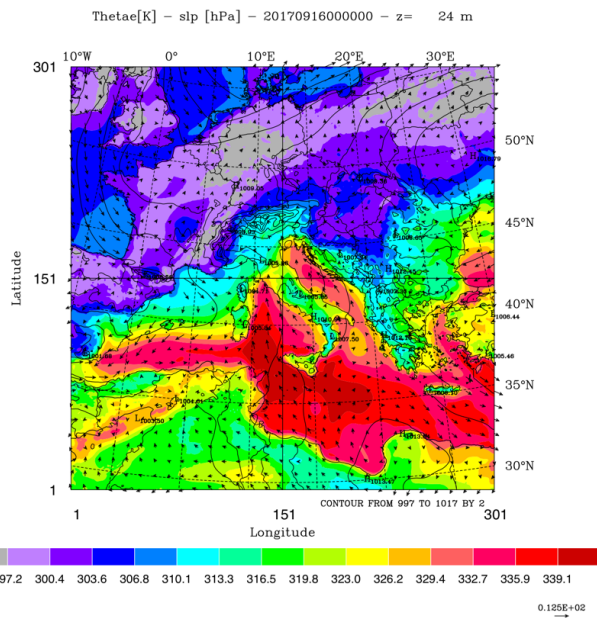
¶



3354

3355

b)



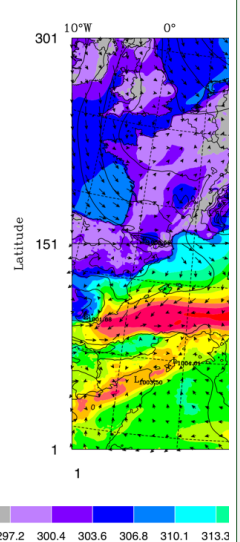
3356

Eliminato: a) ¶

Eliminato: ¶



Thetae[K] - slp [hPa]

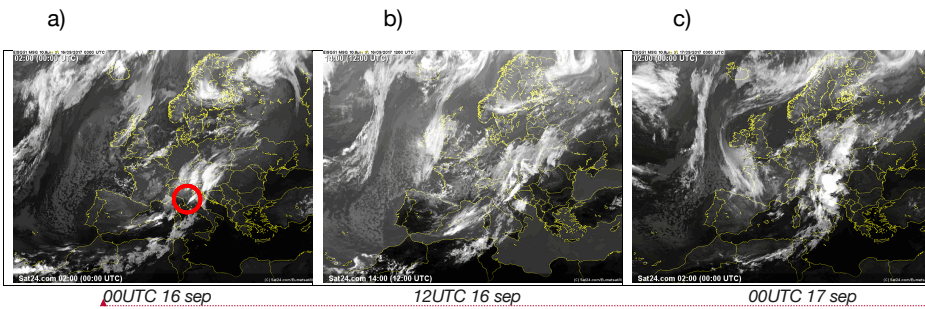


Spostato in giù [1]:

Formattato: Giustificato

Spostato (inserimento) [1]

3363 Figure 2: a) Geopotential height (filled contours), temperature (contours) and wind vectors at 500 hPa on 16  
 3364 September 2017 at 00 UTC. Maximum velocity is 31 m/s; b) equivalent potential temperature (filled contours), sea-  
 3365 level pressure (contours) and wind vectors at 24 m above the surface (first vertical level of RAMS@ISAC, maximum  
 3366 value 13 m/s). A low-pressure pattern is forming over northern Italy, with a front in the western Mediterranean.  
 3367  
 3368  
 3369



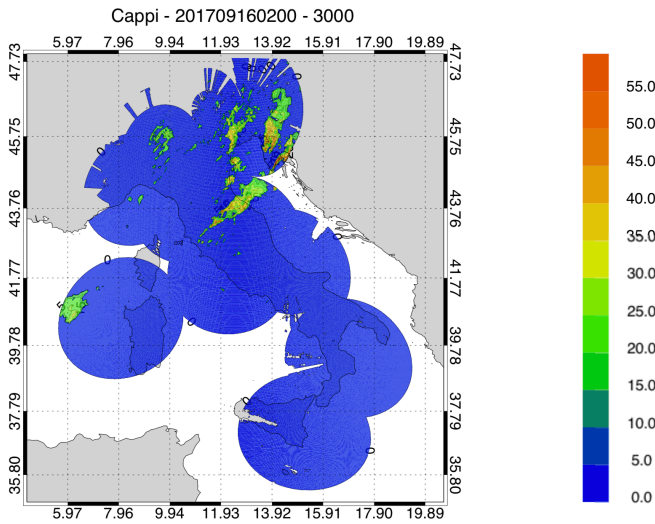
Eliminato: at 00 UTC

3370  
 3371 Figure 3: a) Satellite images (METEOSAT second generation) of the infrared channel, 10.8 micron, at 00 UTC and 12  
 3372 UTC on 16 September, and at 00 UTC on 17 September 2017. A well-defined cloud system is apparent inside the red  
 3373 circle of the image at 00 UTC on 16 September 2017.  
 3374

Formattato: Colore carattere: Sfondo 1

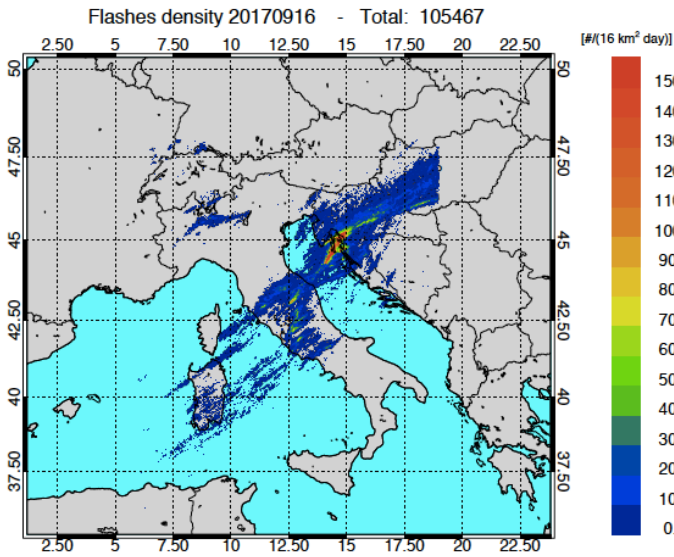
Eliminato: for

Eliminato: for



Formattato: Giustificato

3375  
 3376 Figure 4: National radar mosaic at 3 km above the sea level observed at 02 UTC on 16 September 2017.  
 3377



3381

3382 Figure 5: Lightning density (number of lightning per 16 km<sup>2</sup> for the whole day) recorded on 16 September 2017. The  
 3383 total number of flashes recorded is shown in the title.

3384

3385

3386

3387

3388

3389

3390

3391

3392

3393

3394

3395

3396

3397

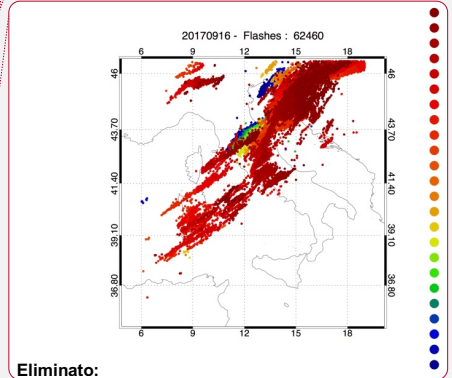
3398

3399

**Formattato:** Tipo di carattere: (Predefinito) +Corpo (Helvetica Neue), Colore carattere: Automatico, Bordo: (Nessun bordo)

**Formattato:** Tipo di carattere: (Predefinito) +Corpo (Helvetica Neue), Colore carattere: Automatico, Bordo: (Nessun bordo)

**Formattato:** Giustificato



**Eliminato:**

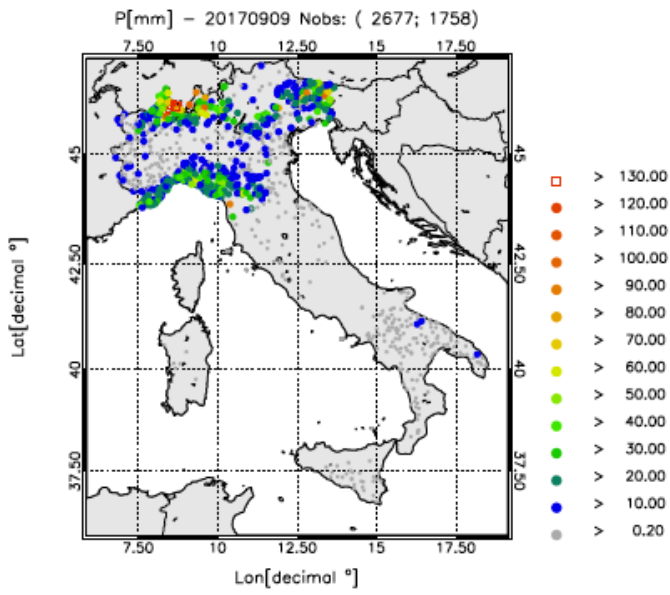
**Formattato:** Apice

**Eliminato:** Different colours represent the time (UTC) of occurrence of the lightning.<sup>1</sup>

3403

a)

Eliminato: b)

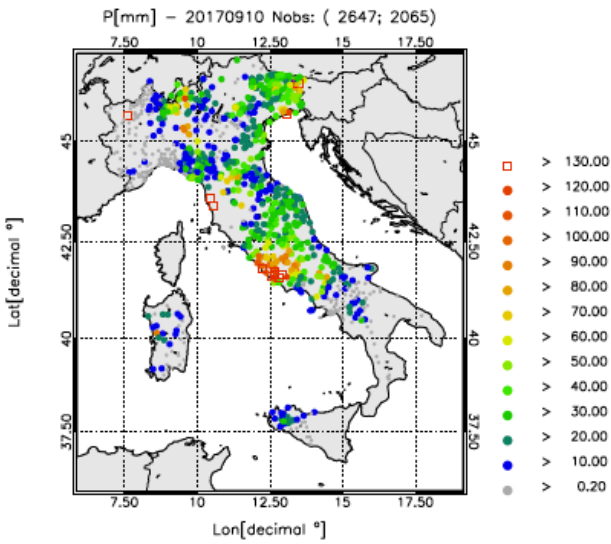


3404

3405

b)

Formattato: Tipo di carattere: Non Grassetto



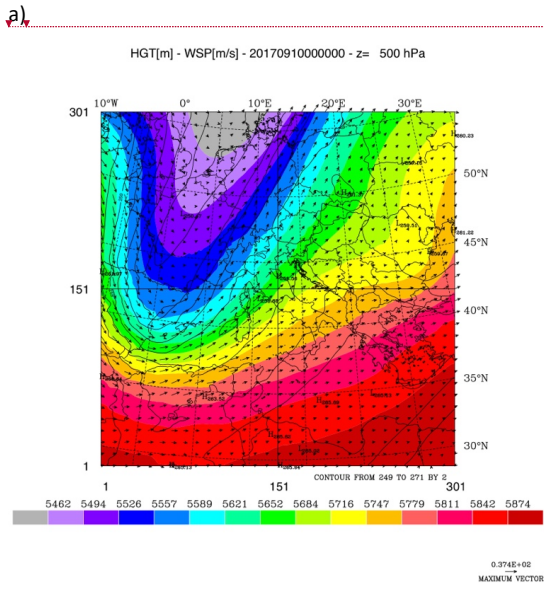
3406

3407

3408

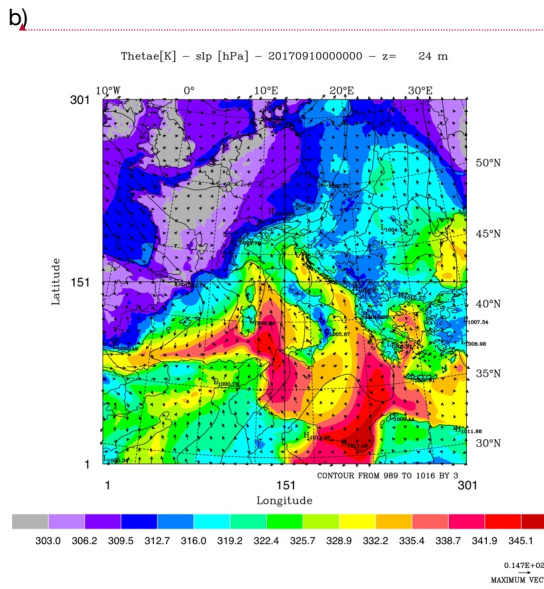
Figure 6: a) As in Figure 1 but for a) 9 September 2017 and b) 10 September 2017.

3410  
3411



Eliminato: ¶  
¶  
Eliminato: ¶  
Eliminato: ¶

3412  
3413



Formattato: Inglese (Regno Unito)  
Formattato: Rientro: Sinistro: 0 cm, Prima riga: 0 cm

3414  
3415  
3416  
3417  
3418

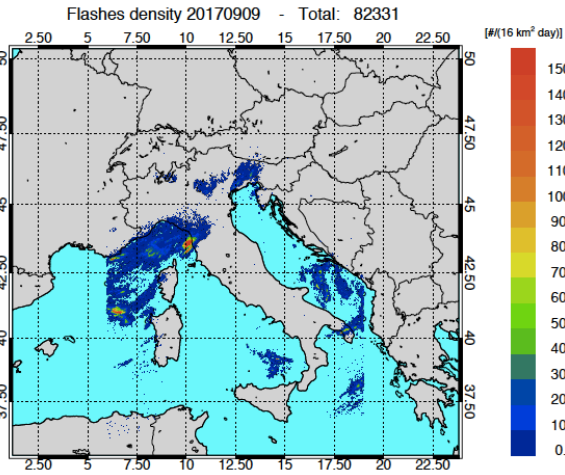
Figure 7: a) Geopotential height (filled contours), temperature (contours) and wind vectors at 500 hPa at 00 UTC on 10 September 2017. Maximum velocity is 37 m/s; b) equivalent potential temperature (filled contours), sea-level pressure (contours) and wind vectors at 24 m above the surface (first vertical level, maximum value 15 m/s).

Eliminato: ¶  
¶



3427

a)



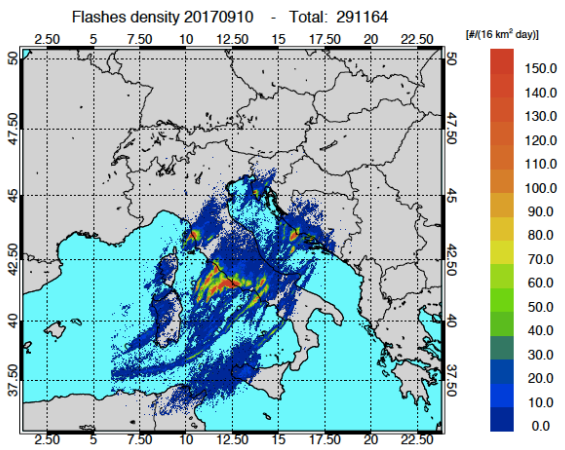
3428

3429

3430

3431

b)



3432

3433

3434

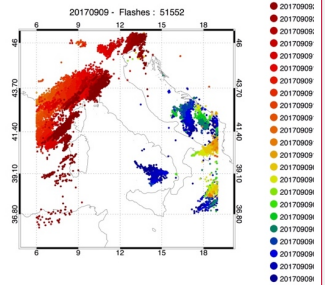
3435

3436

3437

Figure 8: a) Lightning density (lightning number per 16 km<sup>2</sup> for the whole day) recorded on 09 September 2017; b) as in a) for 9 September 2017. The number of flashes recorded on each day is shown in the title.

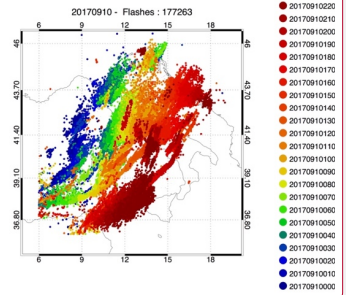
Eliminato: b)



Eliminato:

Formattato: Tipo di carattere: (Predefinito) +Corpo (Helvetica Neue), Grassetto, Colore carattere: Automatico, Bordo: (Nessun bordo)

Formattato: Tipo di carattere: (Predefinito) +Corpo (Helvetica Neue), Colore carattere: Automatico, Bordo: (Nessun bordo)



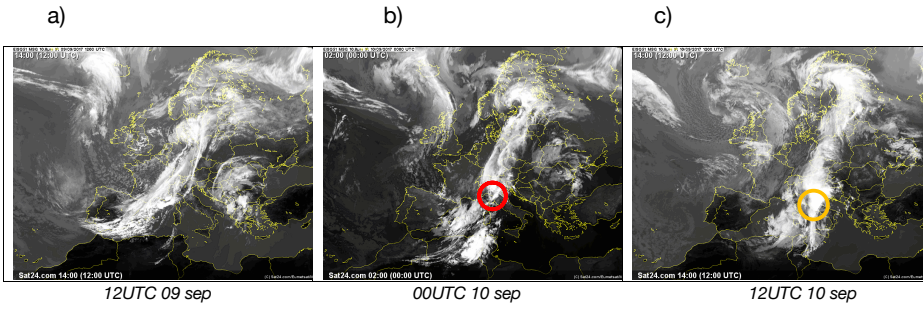
Eliminato:

Formattato: Apice

Eliminato: Lightning recorded on 10 September

Eliminato: Different colours represent the time of occurrence of the lightning.

3444  
3445



3446

3447  
3448  
3449

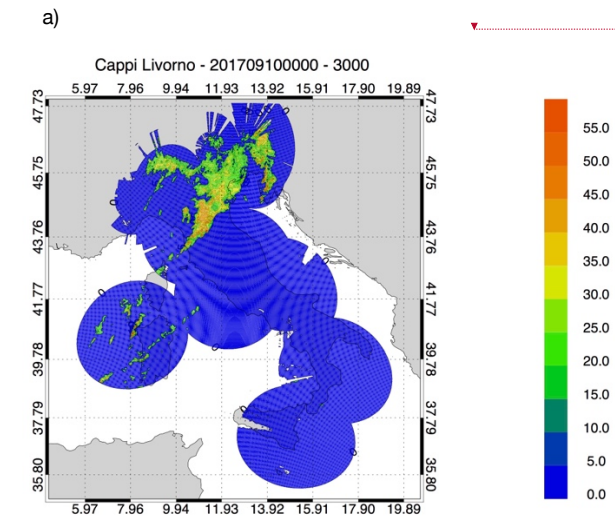
Figure 9: a) Satellite images (METEOSAT second generation) of the infrared channel, 10.8 micron, at 12 UTC on 9 September 2017, at 00 UTC, 00 UTC and 12 UTC on 10 September 2017. The red circle in Figure 9b and the orange circle in Figure 9c show the Livorno and Lazio area, respectively.

Formattato: Giustificato  
Eliminato: for

3450

3451

3452



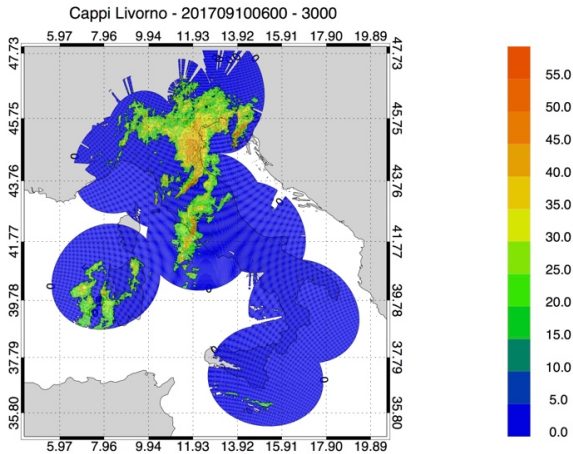
Eliminato:

Eliminato: b)

3453

3454

b)



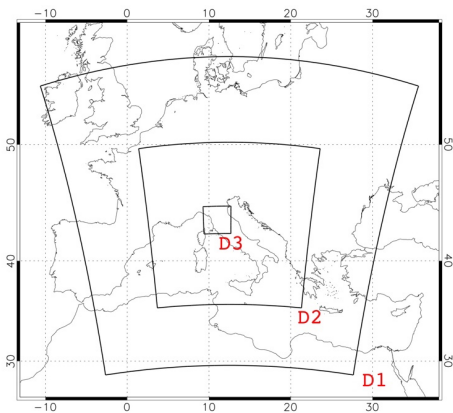
3467

3468 Figure 10: a) National radar mosaic at 3 km above the sea level observed at 00 UTC on 10 September 2017; b) as in a)  
 3469 at 06 UTC.

Formattato: Giustificato

Eliminato: for the

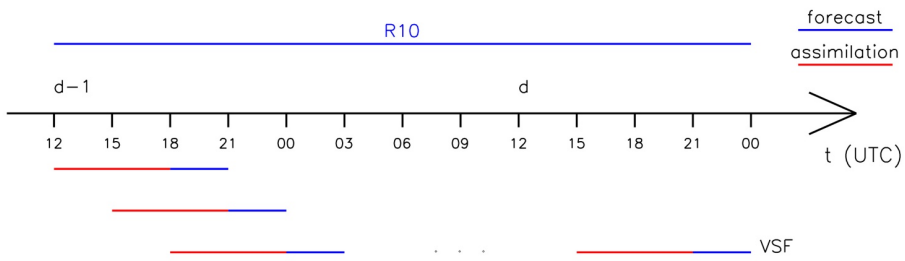
3470



3471

3472 Figure 11: The three domains used in RAMS@ISAC. The model grid over domain D1 has 301 grid points in the NS and  
 3473 WE directions and has 10 km horizontal resolution, the model grid over domain D2 has 401 grid points in the NS and  
 3474 WE directions and has 4 km horizontal resolution. The model grid over domain D3 has 203 grid points in the NS and  
 3475 WE directions and has 4/3 km horizontal resolution. All grids have the same thirty-six vertical levels spanning the 0-  
 3476 22.4 km vertical layer.

Formattato: Giustificato



3478  
3479  
3480

Figure 12: The implementation of the RAMS@ISAC very short-term forecast.

Eliminato: time



3481  
3482  
3483  
3484  
3485  
3486  
3487  
3488  
3489

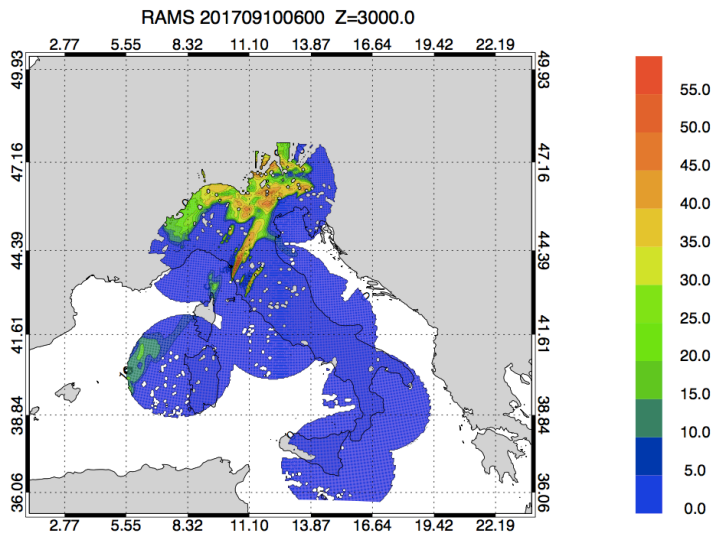
Figure 13: The radar network of the Department of Civil Protection. Green radars operate with dual-polarisation, blue radars have single polarisation.

Formattato: Rientro: Sinistro: 0 cm

Formattato: Giustificato

3491  
3492  
3493  
3494  
3495  
3496  
3497  
3498  
3499  
3500  
3501  
3502

a)

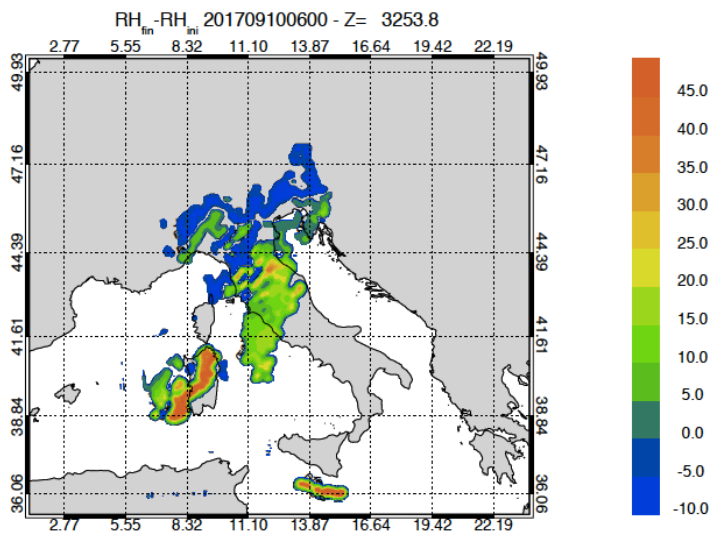


3503

3504

b)

Formattato: Nessuno, Controllo ortografia e grammatica



Formattato: Nessuno, Controllo ortografia e grammatica

3505  
 3506 Figure 14: a) RAMS@ISAC reflectivity factor simulated 3 km above sea level at 06 UTC on 10  
 3507 September 2017; b) relative humidity difference between the analysis and the background at 06  
 3508 UTC at 3.2 km level in the terrain following vertical coordinate of RAMS@ISAC.

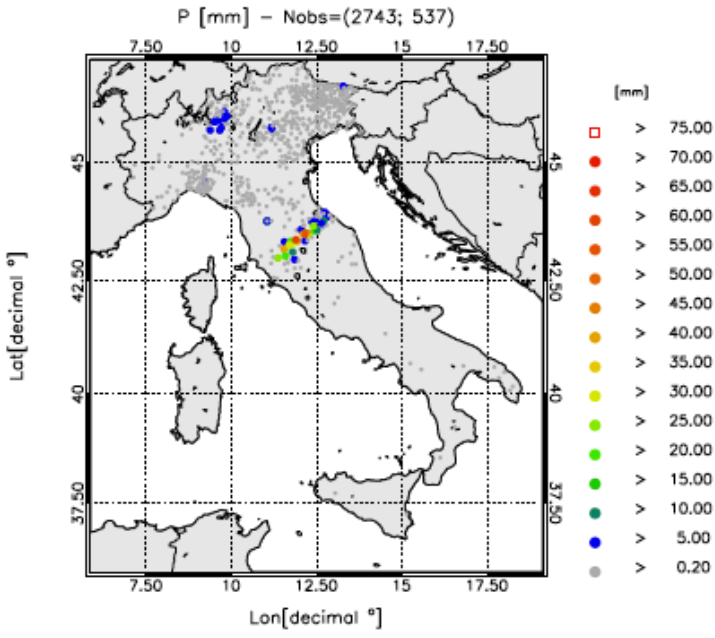
Formattato: Giustificato

Eliminato: ¶

Formattato: Tipo di carattere: 12 pt

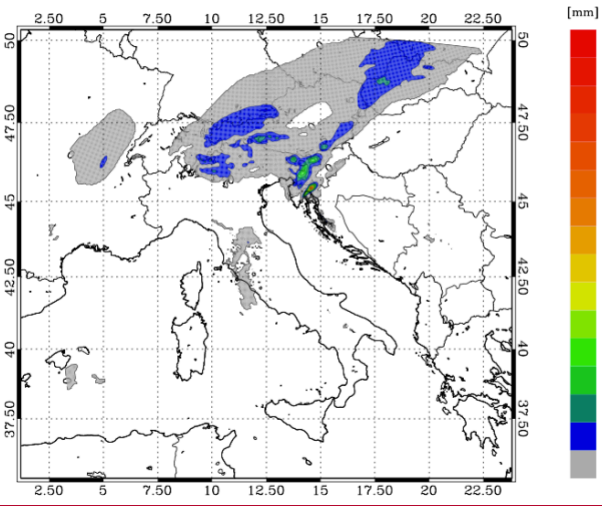
3509  
 3510 a)

Eliminato: b)



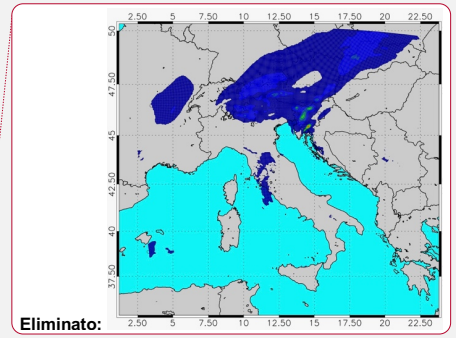
3513  
3514  
3515

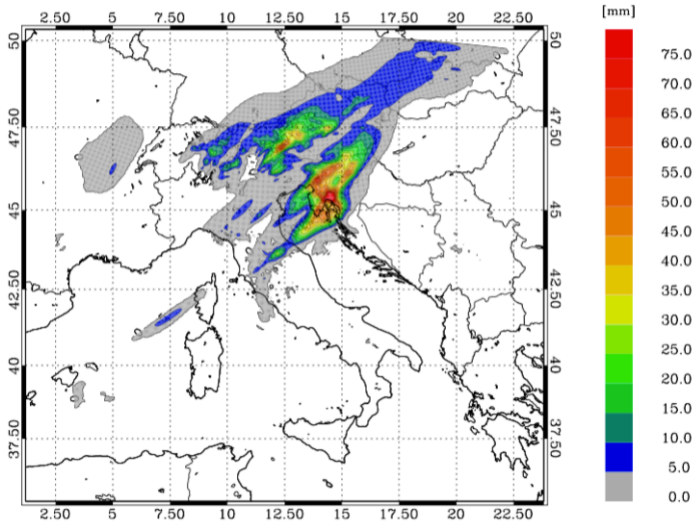
b)



3516  
3517  
3518

c)





3520

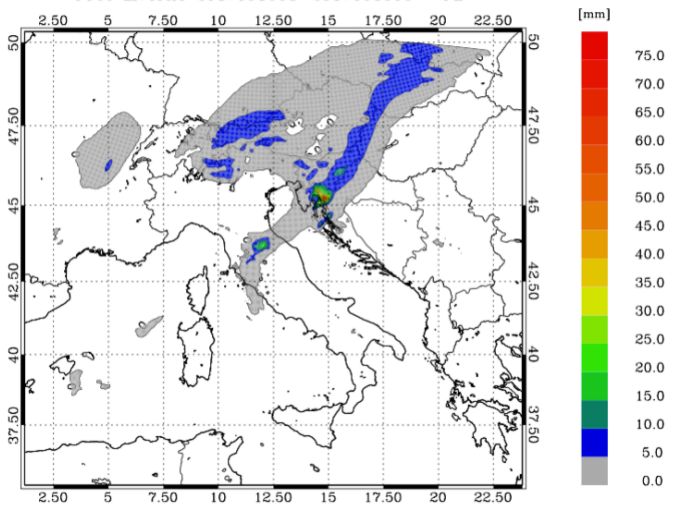
3521

3522

3523

3524

d)

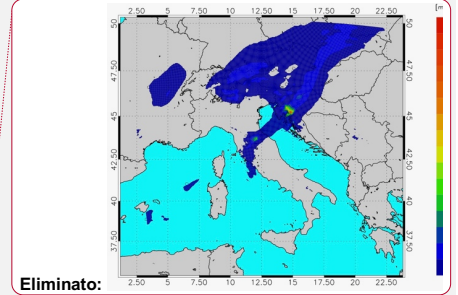
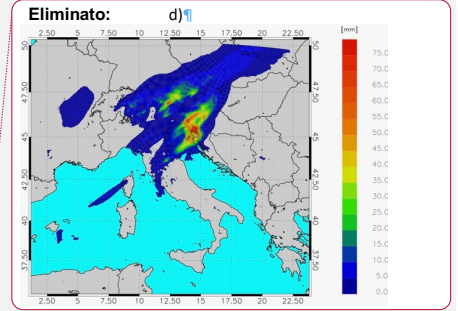


3525

3526

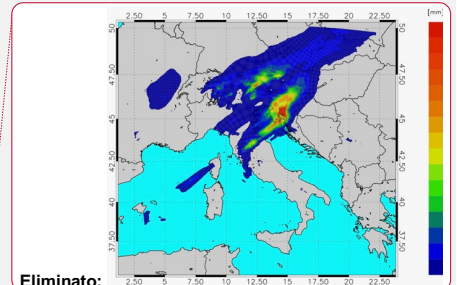
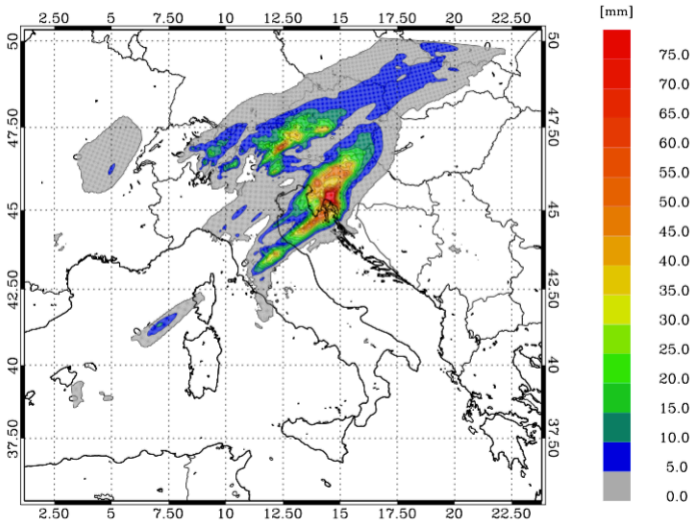
3527

e)

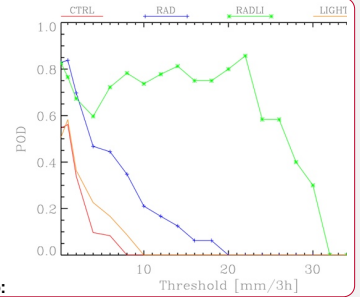


Eliminato: f)





Eliminato:

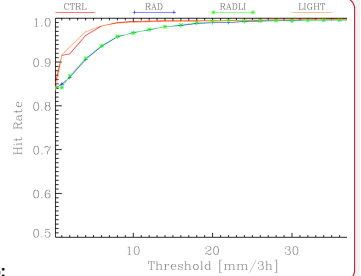


Eliminato:

Eliminato: g)

h) |

... [153]



Eliminato:

Eliminato: 4

Eliminato: as in a) for the

Eliminato: forecast

Eliminato: a

Eliminato: the

Eliminato: a

Eliminato: the

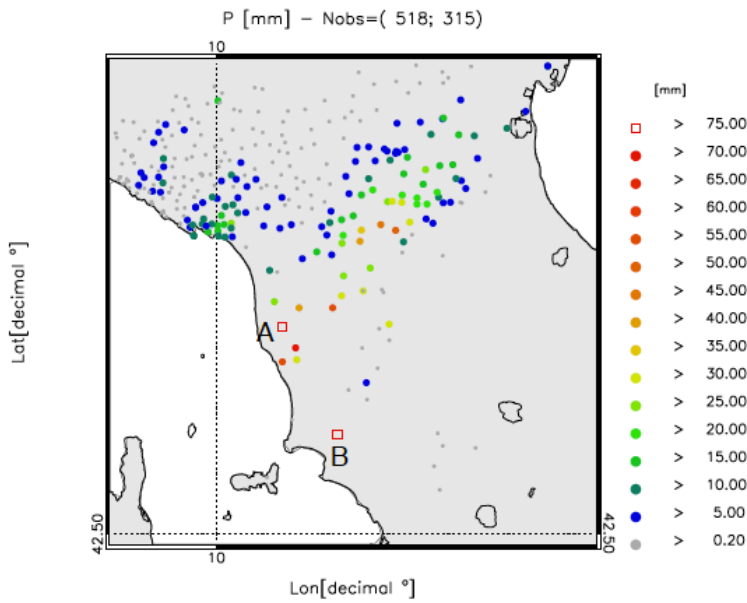
Eliminato: a

Eliminato: the

Eliminato: ; f) POD score for the period 03-06 UTC on 16 September 2017; g) as in f) for the ETS score. POD and ETS scores are computed over the domain of Figure 14a

3574

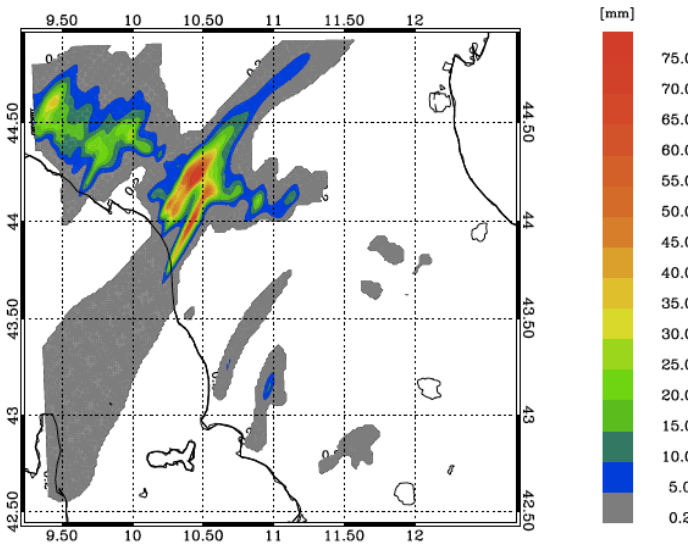
a)



3575

3576

b)



3577

3578

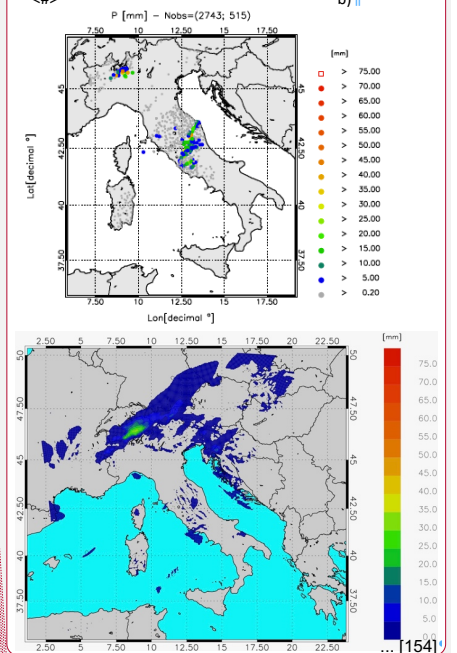
3579

c)

Eliminato:



<#>



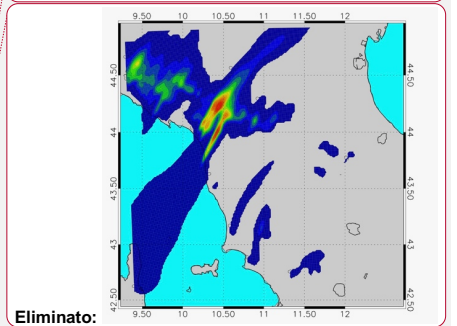
Formattato: Inglese (Regno Unito)

Eliminato: b)

Formattato: Inglese (Regno Unito)

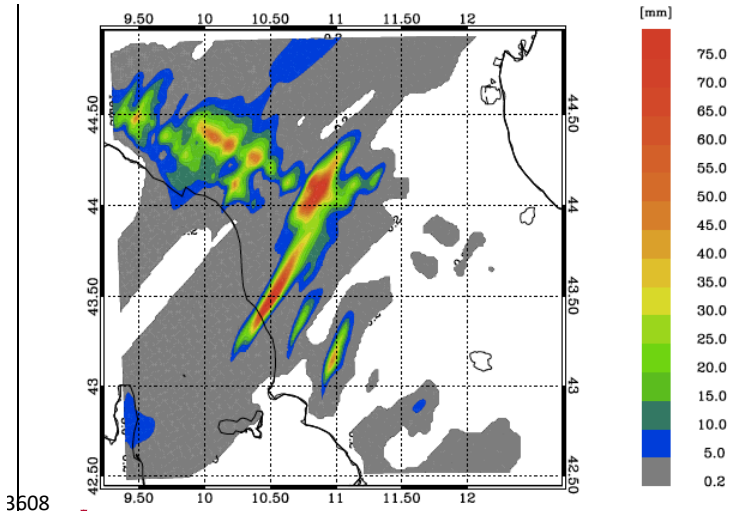
Formattato: Inglese (Regno Unito)

Formattato: Nessuno, Controllo ortografia e grammatica



Eliminato:

Eliminato: d)

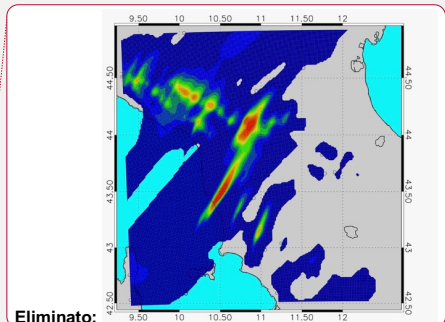


3508

3509

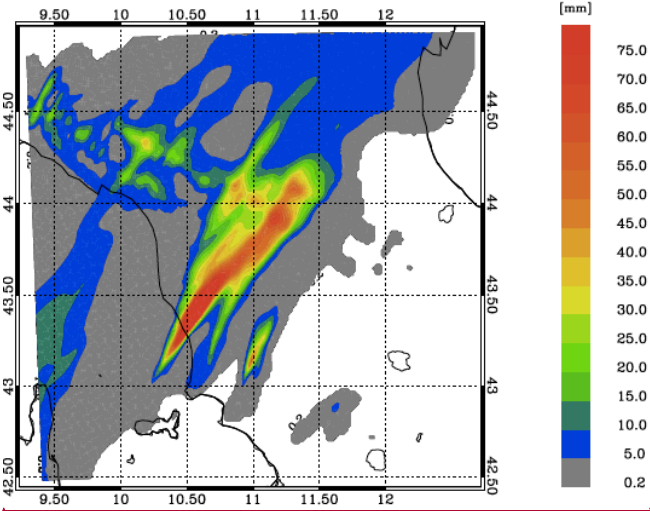
3510

c)



Eliminato:

Formattato: Nessuno, Controllo ortografia e grammatica



3511

3512

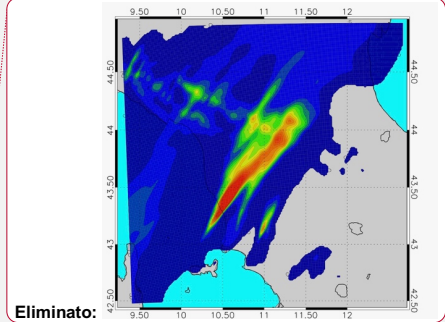
3513

3514

3515

3516

e)

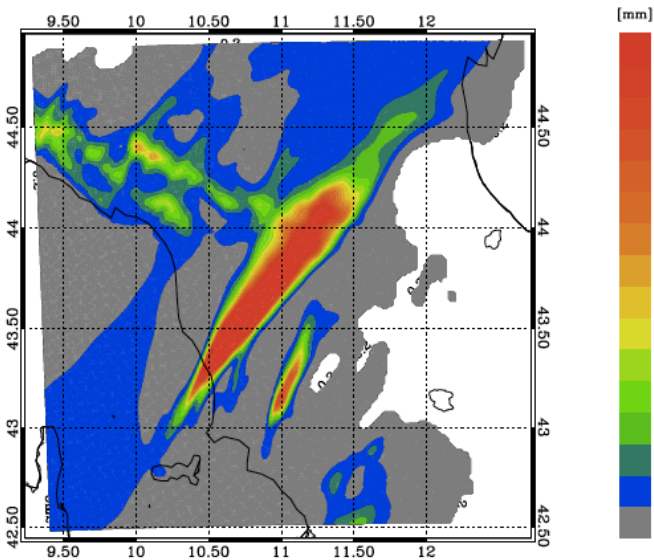


Eliminato:

Formattato: Nessuno, Controllo ortografia e grammatica

Eliminato: f)

3620



3621

3622

3623

3624

3625

3626

3627

3628

3629

3630

3631

3632

3633

3634

3635

3636

3637

3638

3639

3640

3641

3642

3643

3644

3645

3646

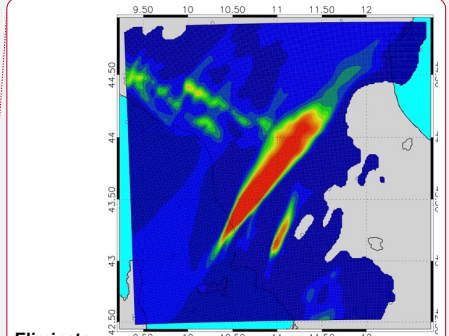
3647

3648

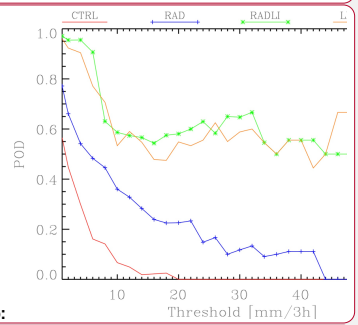
3649

3650

Figure 16; a) rainfall reported by raingauges between 00 and 03 UTC on 10 September 2017. Only stations reporting at least 0.2 mm/3h are shown. The first number in the title within brackets represents the number of raingauges available over the domain, while the second number shows those observing at least 0.2 mm/3h; b) rainfall VSF of CTRL for the same time interval as in a); c) as in b) for RAD forecast; d) as in b) for LIGHT forecast; e) as in b) for RADLI forecast. Labels A and B help to identify the positions of two rainfall maxima discussed into the text.



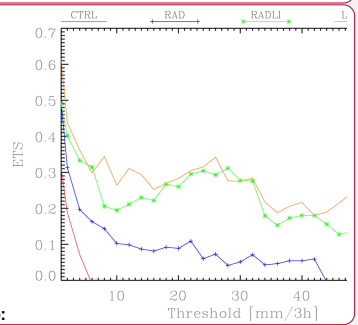
Eliminato:



Eliminato:

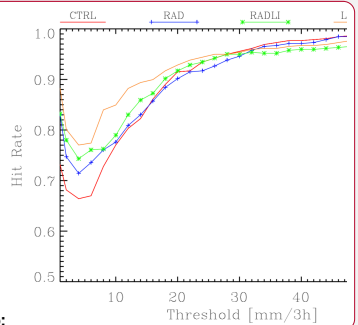
Formattato: Nessuno, Controllo ortografia e grammatica

Eliminato: g) h)



Eliminato:

Formattato: Nessuno, Controllo ortografia e grammatica



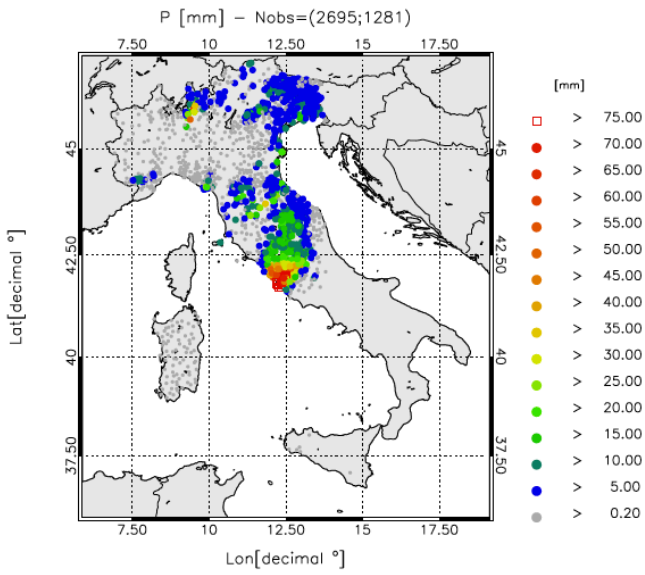
Eliminato:

Eliminato: 7: a) rainfall reported by raingauges between 00 and 03 UTC on 10 September 2017. Only stations reporting at least 0.2 mm/3h are shown. The first number in the title within brackets represents the number of raingauges available over the domain, while the second number shows those observing at least 0.2 mm/3h; b) rainfall VSF of CTRL for the same time interval as in a); c) as in b) for RAD forecast; d) as in b) for LIGHT forecast; e) as in b) for RADLI forecast. Labels A and B help to identify the positions of two rainfall maxima discussed into the text.

Eliminato: POD and ETS scores are computed over the domain of Figure 17a.

3680

a)



Eliminato: b)

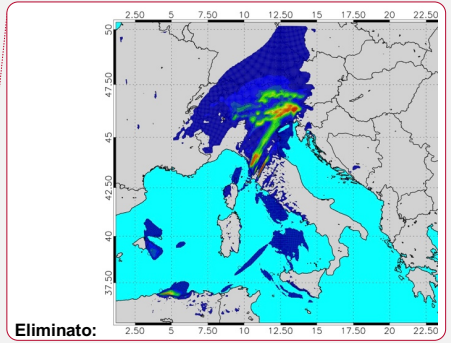
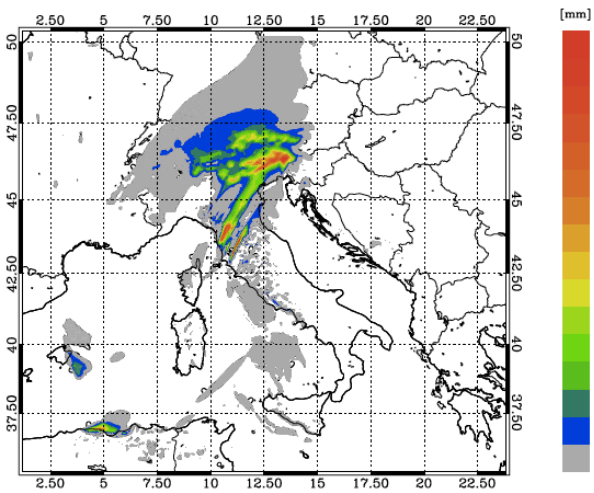
Formattato: Tipo di carattere: Corsivo

3681

3682

3683

b)



3684

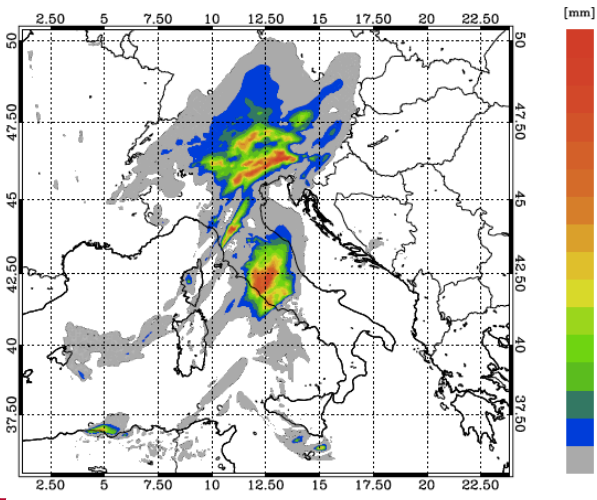
3685

3686

3687

3690

c)

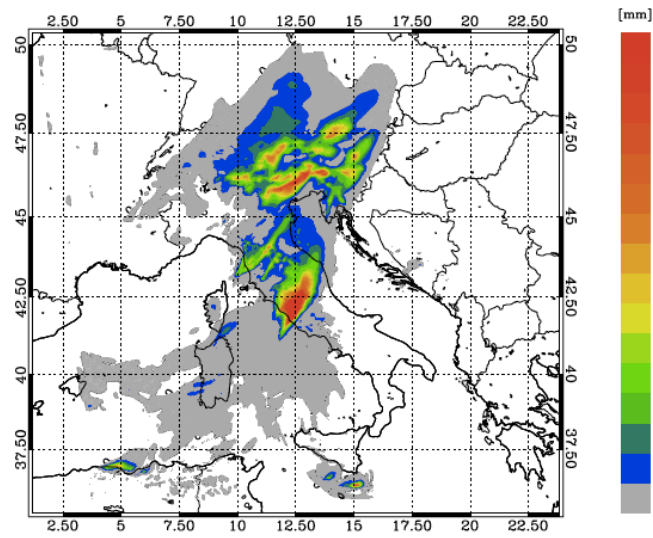


3691

3692

3693

d)



3694

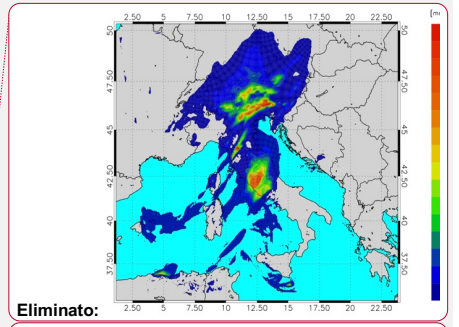
3695

3696

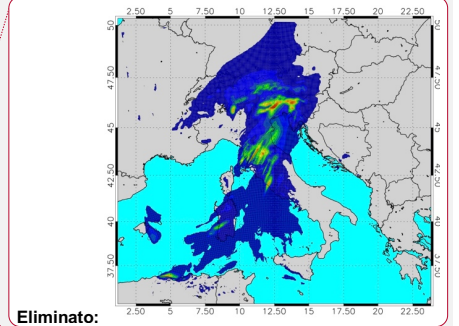
3697

e)

Eliminato: d)



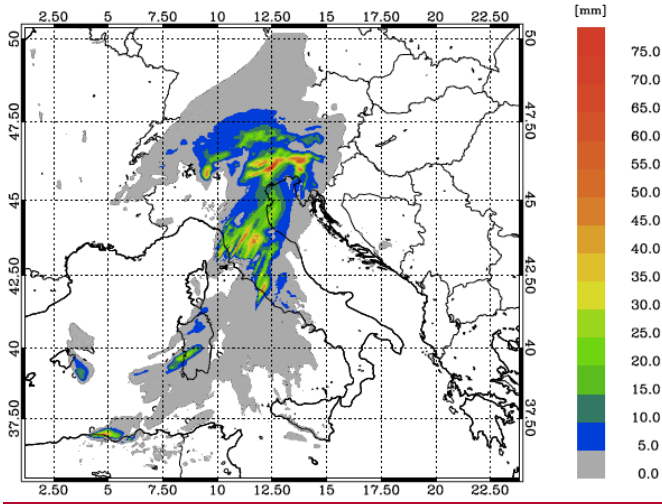
Eliminato:



Eliminato:

Eliminato:

Eliminato: f)

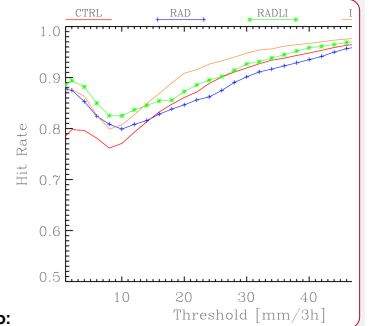


3703  
3704  
3705  
3706  
3707  
3708  
3709  
3710  
3711  
3712  
3713  
3714  
3715  
3716  
3717  
3718  
3719  
3720  
3721  
3722  
3723  
3724  
3725  
3726  
3727  
3728

Figure 17: a) rainfall reported by raingauges between 06 - 09 UTC on 10 September 2017. For this time period 2695 raingauges reported valid observations in the domain, however only stations reporting at least 0.2 mm/3h are shown. The first number in the title within brackets represents the number of raingauges available over the domain, while the second number shows those observing at least 0.2 mm/3h; b) rainfall VSF of CTRL in the same time interval as a); c) as in b) for RAD forecast; d) as in b) for LIGHT forecast; e) as in b) for RADLI forecast.

Eliminato: e) ... [156]

Formattato: Inglese (Regno Unito)



Eliminato:

Eliminato: 8

Eliminato: as in

Eliminato: a) for the CTRL forecast

Eliminato: t

Eliminato: a

Eliminato: the

Eliminato: a

Eliminato: the

Eliminato: a

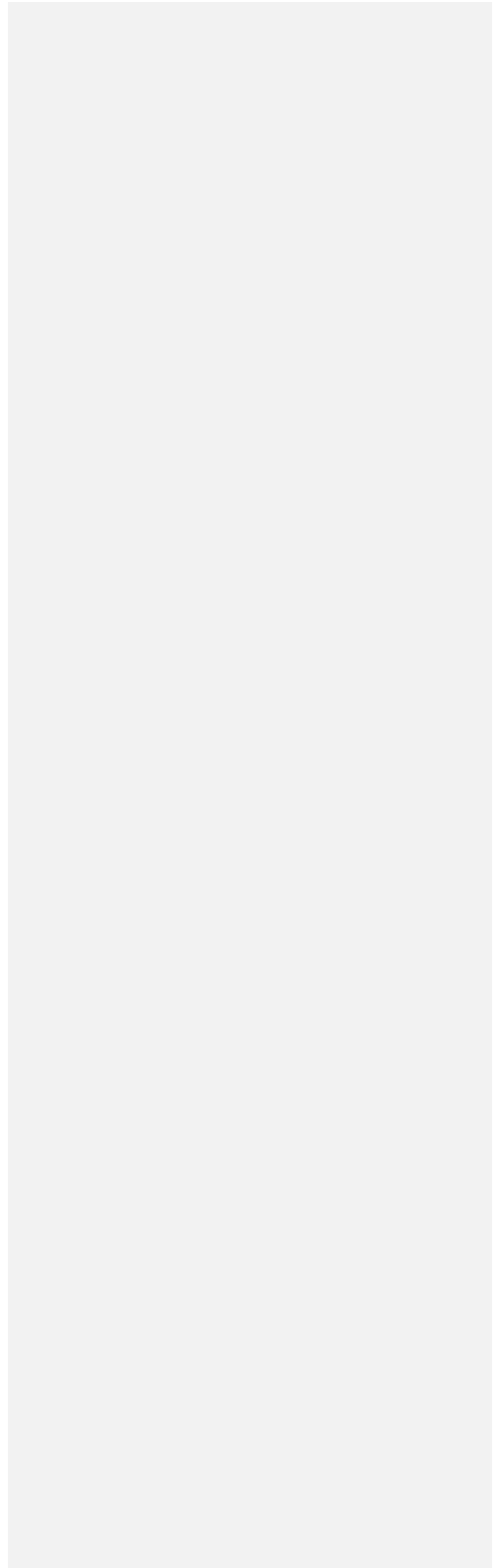
Eliminato: the

Eliminato: ; f) POD score for the period 06-09 UTC on 10 September; e) as in f) for the ETS score. POD and ETS scores are computed over the domain of Figure 18a

Eliminato: 1

Formattato: Interlinea: 1.5 righe

3753





<b>Pagina 49: [1] Eliminato</b>	<b>stefano federico</b>	<b>14/01/19 13:56:00</b>
<b>Pagina 49: [2] Eliminato</b>	<b>stefano federico</b>	<b>14/01/19 12:04:00</b>
<b>Pagina 57: [3] Eliminato</b>	<b>stefano federico</b>	<b>21/03/19 07:27:00</b>
<b>Pagina 65: [4] Formattato</b>	<b>stefano federico</b>	<b>02/02/19 19:23:00</b>
Tipo di carattere: 12 pt		
<b>Pagina 65: [4] Formattato</b>	<b>stefano federico</b>	<b>02/02/19 19:23:00</b>
Tipo di carattere: 12 pt		
<b>Pagina 65: [5] Formattato</b>	<b>stefano federico</b>	<b>02/02/19 19:23:00</b>
Bordo: : (Nessun bordo)		
<b>Pagina 65: [6] Formattato</b>	<b>stefano federico</b>	<b>02/02/19 19:23:00</b>
Bordo: : (Nessun bordo)		
<b>Pagina 65: [7] Formattato</b>	<b>stefano federico</b>	<b>02/02/19 19:23:00</b>
Bordo: : (Nessun bordo)		
<b>Pagina 65: [8] Formattato</b>	<b>stefano federico</b>	<b>02/02/19 19:23:00</b>
Bordo: : (Nessun bordo)		
<b>Pagina 65: [9] Formattato</b>	<b>stefano federico</b>	<b>02/02/19 19:23:00</b>
Bordo: : (Nessun bordo)		
<b>Pagina 65: [10] Formattato</b>	<b>stefano federico</b>	<b>02/02/19 19:23:00</b>
Bordo: : (Nessun bordo)		
<b>Pagina 65: [11] Formattato</b>	<b>stefano federico</b>	<b>02/02/19 19:23:00</b>
Bordo: : (Nessun bordo)		
<b>Pagina 65: [12] Formattato</b>	<b>stefano federico</b>	<b>02/02/19 19:23:00</b>
Bordo: : (Nessun bordo)		
<b>Pagina 65: [13] Formattato</b>	<b>stefano federico</b>	<b>02/02/19 19:23:00</b>
Bordo: : (Nessun bordo)		
<b>Pagina 65: [14] Formattato</b>	<b>stefano federico</b>	<b>02/02/19 19:23:00</b>
Bordo: : (Nessun bordo)		
<b>Pagina 65: [15] Formattato</b>	<b>stefano federico</b>	<b>02/02/19 19:23:00</b>
Bordo: : (Nessun bordo)		
<b>Pagina 65: [16] Formattato</b>	<b>stefano federico</b>	<b>02/02/19 19:23:00</b>
Bordo: : (Nessun bordo)		
<b>Pagina 65: [17] Formattato</b>	<b>stefano federico</b>	<b>02/02/19 19:23:00</b>
Bordo: : (Nessun bordo)		
<b>Pagina 65: [18] Formattato</b>	<b>stefano federico</b>	<b>02/02/19 19:23:00</b>
Bordo: : (Nessun bordo)		
<b>Pagina 65: [19] Formattato</b>	<b>stefano federico</b>	<b>02/02/19 19:23:00</b>
Bordo: : (Nessun bordo)		
<b>Pagina 65: [20] Formattato</b>	<b>stefano federico</b>	<b>02/02/19 19:23:00</b>
Bordo: : (Nessun bordo)		

<b>Pagina 65: [21] Formattato</b>	<b>stefano federico</b>	<b>02/02/19 19:23:00</b>
Bordo: : (Nessun bordo)		
<b>Pagina 65: [22] Formattato</b>	<b>stefano federico</b>	<b>02/02/19 19:23:00</b>
Bordo: : (Nessun bordo)		
<b>Pagina 65: [23] Formattato</b>	<b>stefano federico</b>	<b>02/02/19 19:23:00</b>
Bordo: : (Nessun bordo)		
<b>Pagina 65: [24] Formattato</b>	<b>stefano federico</b>	<b>02/02/19 19:23:00</b>
Bordo: : (Nessun bordo)		
<b>Pagina 65: [25] Formattato</b>	<b>stefano federico</b>	<b>02/02/19 19:23:00</b>
Bordo: : (Nessun bordo)		
<b>Pagina 65: [26] Formattato</b>	<b>stefano federico</b>	<b>02/02/19 19:23:00</b>
Bordo: : (Nessun bordo)		
<b>Pagina 65: [27] Formattato</b>	<b>stefano federico</b>	<b>02/02/19 19:23:00</b>
Bordo: : (Nessun bordo)		
<b>Pagina 65: [28] Formattato</b>	<b>stefano federico</b>	<b>02/02/19 19:23:00</b>
Bordo: : (Nessun bordo)		
<b>Pagina 65: [29] Formattato</b>	<b>stefano federico</b>	<b>02/02/19 19:23:00</b>
Bordo: : (Nessun bordo)		
<b>Pagina 65: [30] Formattato</b>	<b>stefano federico</b>	<b>02/02/19 19:23:00</b>
Bordo: : (Nessun bordo)		
<b>Pagina 65: [31] Formattato</b>	<b>stefano federico</b>	<b>02/02/19 19:23:00</b>
Bordo: : (Nessun bordo)		
<b>Pagina 65: [32] Formattato</b>	<b>stefano federico</b>	<b>02/02/19 19:23:00</b>
Bordo: : (Nessun bordo)		
<b>Pagina 65: [33] Formattato</b>	<b>stefano federico</b>	<b>02/02/19 19:23:00</b>
Bordo: : (Nessun bordo)		
<b>Pagina 65: [34] Formattato</b>	<b>stefano federico</b>	<b>02/02/19 19:23:00</b>
Bordo: : (Nessun bordo)		
<b>Pagina 65: [35] Formattato</b>	<b>stefano federico</b>	<b>02/02/19 19:23:00</b>
Bordo: : (Nessun bordo)		
<b>Pagina 65: [36] Formattato</b>	<b>stefano federico</b>	<b>02/02/19 19:23:00</b>
Bordo: : (Nessun bordo)		
<b>Pagina 65: [37] Formattato</b>	<b>stefano federico</b>	<b>02/02/19 19:23:00</b>
Bordo: : (Nessun bordo)		
<b>Pagina 65: [38] Formattato</b>	<b>stefano federico</b>	<b>02/02/19 19:23:00</b>
Bordo: : (Nessun bordo)		
<b>Pagina 65: [39] Formattato</b>	<b>stefano federico</b>	<b>02/02/19 19:23:00</b>
Bordo: : (Nessun bordo)		
<b>Pagina 65: [40] Formattato</b>	<b>stefano federico</b>	<b>02/02/19 19:23:00</b>
Bordo: : (Nessun bordo)		

<b>Pagina 65: [41] Formattato</b>	<b>stefano federico</b>	<b>02/02/19 19:23:00</b>
Bordo: : (Nessun bordo)		
<b>Pagina 65: [42] Formattato</b>	<b>stefano federico</b>	<b>02/02/19 19:23:00</b>
Bordo: : (Nessun bordo)		
<b>Pagina 65: [43] Formattato</b>	<b>stefano federico</b>	<b>02/02/19 19:23:00</b>
Bordo: : (Nessun bordo)		
<b>Pagina 65: [44] Formattato</b>	<b>stefano federico</b>	<b>02/02/19 19:23:00</b>
Bordo: : (Nessun bordo)		
<b>Pagina 65: [45] Formattato</b>	<b>stefano federico</b>	<b>02/02/19 19:23:00</b>
Bordo: : (Nessun bordo)		
<b>Pagina 65: [46] Formattato</b>	<b>stefano federico</b>	<b>02/02/19 19:23:00</b>
Bordo: : (Nessun bordo)		
<b>Pagina 65: [47] Formattato</b>	<b>stefano federico</b>	<b>02/02/19 19:23:00</b>
Bordo: : (Nessun bordo)		
<b>Pagina 65: [48] Formattato</b>	<b>stefano federico</b>	<b>02/02/19 19:23:00</b>
Bordo: : (Nessun bordo)		
<b>Pagina 65: [49] Formattato</b>	<b>stefano federico</b>	<b>02/02/19 19:23:00</b>
Bordo: : (Nessun bordo)		
<b>Pagina 65: [50] Formattato</b>	<b>stefano federico</b>	<b>02/02/19 19:23:00</b>
Bordo: : (Nessun bordo)		
<b>Pagina 65: [51] Formattato</b>	<b>stefano federico</b>	<b>02/02/19 19:23:00</b>
Bordo: : (Nessun bordo)		
<b>Pagina 65: [52] Formattato</b>	<b>stefano federico</b>	<b>02/02/19 19:23:00</b>
Bordo: : (Nessun bordo)		
<b>Pagina 65: [53] Formattato</b>	<b>stefano federico</b>	<b>02/02/19 19:23:00</b>
Bordo: : (Nessun bordo)		
<b>Pagina 65: [54] Formattato</b>	<b>stefano federico</b>	<b>02/02/19 19:23:00</b>
Bordo: : (Nessun bordo)		
<b>Pagina 65: [55] Formattato</b>	<b>stefano federico</b>	<b>02/02/19 19:23:00</b>
Bordo: : (Nessun bordo)		
<b>Pagina 65: [56] Formattato</b>	<b>stefano federico</b>	<b>02/02/19 19:23:00</b>
Bordo: : (Nessun bordo)		
<b>Pagina 65: [57] Formattato</b>	<b>stefano federico</b>	<b>02/02/19 19:23:00</b>
Bordo: : (Nessun bordo)		
<b>Pagina 65: [58] Formattato</b>	<b>stefano federico</b>	<b>02/02/19 19:23:00</b>
Bordo: : (Nessun bordo)		
<b>Pagina 65: [59] Formattato</b>	<b>stefano federico</b>	<b>02/02/19 19:23:00</b>
Bordo: : (Nessun bordo)		
<b>Pagina 65: [60] Formattato</b>	<b>stefano federico</b>	<b>02/02/19 19:23:00</b>
Bordo: : (Nessun bordo)		

<b>Pagina 65: [61] Formattato</b>	<b>stefano federico</b>	<b>02/02/19 19:23:00</b>
Bordo: : (Nessun bordo)		
<b>Pagina 65: [62] Formattato</b>	<b>stefano federico</b>	<b>02/02/19 19:23:00</b>
Bordo: : (Nessun bordo)		
<b>Pagina 65: [63] Formattato</b>	<b>stefano federico</b>	<b>02/02/19 19:23:00</b>
Bordo: : (Nessun bordo)		
<b>Pagina 65: [64] Formattato</b>	<b>stefano federico</b>	<b>02/02/19 19:23:00</b>
Bordo: : (Nessun bordo)		
<b>Pagina 65: [65] Formattato</b>	<b>stefano federico</b>	<b>02/02/19 19:23:00</b>
Bordo: : (Nessun bordo)		
<b>Pagina 65: [66] Formattato</b>	<b>stefano federico</b>	<b>02/02/19 19:23:00</b>
Bordo: : (Nessun bordo)		
<b>Pagina 65: [67] Formattato</b>	<b>stefano federico</b>	<b>02/02/19 19:23:00</b>
Bordo: : (Nessun bordo)		
<b>Pagina 65: [68] Formattato</b>	<b>stefano federico</b>	<b>02/02/19 19:23:00</b>
Bordo: : (Nessun bordo)		
<b>Pagina 65: [69] Formattato</b>	<b>stefano federico</b>	<b>02/02/19 19:23:00</b>
Bordo: : (Nessun bordo)		
<b>Pagina 65: [70] Formattato</b>	<b>stefano federico</b>	<b>02/02/19 19:23:00</b>
Bordo: : (Nessun bordo)		
<b>Pagina 65: [71] Formattato</b>	<b>stefano federico</b>	<b>02/02/19 19:23:00</b>
Bordo: : (Nessun bordo)		
<b>Pagina 65: [72] Formattato</b>	<b>stefano federico</b>	<b>02/02/19 19:23:00</b>
Bordo: : (Nessun bordo)		
<b>Pagina 65: [73] Formattato</b>	<b>stefano federico</b>	<b>02/02/19 19:23:00</b>
Bordo: : (Nessun bordo)		
<b>Pagina 65: [74] Formattato</b>	<b>stefano federico</b>	<b>02/02/19 19:23:00</b>
Bordo: : (Nessun bordo)		
<b>Pagina 65: [75] Formattato</b>	<b>stefano federico</b>	<b>02/02/19 19:23:00</b>
Bordo: : (Nessun bordo)		
<b>Pagina 65: [76] Formattato</b>	<b>stefano federico</b>	<b>02/02/19 19:23:00</b>
Bordo: : (Nessun bordo)		
<b>Pagina 65: [77] Formattato</b>	<b>stefano federico</b>	<b>02/02/19 19:23:00</b>
Bordo: : (Nessun bordo)		
<b>Pagina 65: [78] Formattato</b>	<b>stefano federico</b>	<b>02/02/19 19:23:00</b>
Bordo: : (Nessun bordo)		
<b>Pagina 65: [79] Formattato</b>	<b>stefano federico</b>	<b>02/02/19 19:23:00</b>
Bordo: : (Nessun bordo)		
<b>Pagina 65: [80] Formattato</b>	<b>stefano federico</b>	<b>02/02/19 19:23:00</b>
Bordo: : (Nessun bordo)		

<b>Pagina 65: [81] Formattato</b>	<b>stefano federico</b>	<b>02/02/19 19:23:00</b>
Bordo: : (Nessun bordo)		
<b>Pagina 65: [82] Formattato</b>	<b>stefano federico</b>	<b>02/02/19 19:23:00</b>
Bordo: : (Nessun bordo)		
<b>Pagina 65: [83] Formattato</b>	<b>stefano federico</b>	<b>02/02/19 19:23:00</b>
Bordo: : (Nessun bordo)		
<b>Pagina 65: [84] Formattato</b>	<b>stefano federico</b>	<b>02/02/19 19:23:00</b>
Bordo: : (Nessun bordo)		
<b>Pagina 65: [85] Formattato</b>	<b>stefano federico</b>	<b>02/02/19 19:23:00</b>
Bordo: : (Nessun bordo)		
<b>Pagina 65: [86] Formattato</b>	<b>stefano federico</b>	<b>02/02/19 19:23:00</b>
Bordo: : (Nessun bordo)		
<b>Pagina 65: [87] Formattato</b>	<b>stefano federico</b>	<b>02/02/19 19:23:00</b>
Bordo: : (Nessun bordo)		
<b>Pagina 65: [88] Formattato</b>	<b>stefano federico</b>	<b>02/02/19 19:23:00</b>
Bordo: : (Nessun bordo)		
<b>Pagina 65: [89] Formattato</b>	<b>stefano federico</b>	<b>02/02/19 19:23:00</b>
Bordo: : (Nessun bordo)		
<b>Pagina 65: [90] Formattato</b>	<b>stefano federico</b>	<b>02/02/19 19:23:00</b>
Bordo: : (Nessun bordo)		
<b>Pagina 65: [91] Formattato</b>	<b>stefano federico</b>	<b>02/02/19 19:23:00</b>
Bordo: : (Nessun bordo)		
<b>Pagina 65: [92] Formattato</b>	<b>stefano federico</b>	<b>02/02/19 19:23:00</b>
Bordo: : (Nessun bordo)		
<b>Pagina 65: [93] Formattato</b>	<b>stefano federico</b>	<b>02/02/19 19:23:00</b>
Bordo: : (Nessun bordo)		
<b>Pagina 65: [94] Formattato</b>	<b>stefano federico</b>	<b>02/02/19 19:23:00</b>
Bordo: : (Nessun bordo)		
<b>Pagina 65: [95] Formattato</b>	<b>stefano federico</b>	<b>02/02/19 19:23:00</b>
Bordo: : (Nessun bordo)		
<b>Pagina 65: [96] Formattato</b>	<b>stefano federico</b>	<b>02/02/19 19:23:00</b>
Bordo: : (Nessun bordo)		
<b>Pagina 65: [97] Formattato</b>	<b>stefano federico</b>	<b>02/02/19 19:23:00</b>
Bordo: : (Nessun bordo)		
<b>Pagina 65: [98] Formattato</b>	<b>stefano federico</b>	<b>02/02/19 19:23:00</b>
Bordo: : (Nessun bordo)		
<b>Pagina 66: [99] Formattato</b>	<b>stefano federico</b>	<b>02/02/19 19:23:00</b>
Bordo: : (Nessun bordo)		
<b>Pagina 66: [100] Formattato</b>	<b>stefano federico</b>	<b>02/02/19 19:23:00</b>
Bordo: : (Nessun bordo)		

<b>Pagina 66: [101] Formattato</b>	<b>stefano federico</b>	<b>02/02/19 19:23:00</b>
Bordo: : (Nessun bordo)		
<b>Pagina 66: [102] Formattato</b>	<b>stefano federico</b>	<b>02/02/19 19:23:00</b>
Bordo: : (Nessun bordo)		
<b>Pagina 66: [103] Formattato</b>	<b>stefano federico</b>	<b>02/02/19 19:23:00</b>
Bordo: : (Nessun bordo)		
<b>Pagina 66: [104] Formattato</b>	<b>stefano federico</b>	<b>02/02/19 19:23:00</b>
Bordo: : (Nessun bordo)		
<b>Pagina 66: [105] Formattato</b>	<b>stefano federico</b>	<b>02/02/19 19:23:00</b>
Bordo: : (Nessun bordo)		
<b>Pagina 66: [106] Formattato</b>	<b>stefano federico</b>	<b>02/02/19 19:23:00</b>
Bordo: : (Nessun bordo)		
<b>Pagina 66: [107] Formattato</b>	<b>stefano federico</b>	<b>02/02/19 19:23:00</b>
Bordo: : (Nessun bordo)		
<b>Pagina 66: [108] Formattato</b>	<b>stefano federico</b>	<b>02/02/19 19:23:00</b>
Bordo: : (Nessun bordo)		
<b>Pagina 66: [109] Formattato</b>	<b>stefano federico</b>	<b>02/02/19 19:23:00</b>
Bordo: : (Nessun bordo)		
<b>Pagina 66: [110] Formattato</b>	<b>stefano federico</b>	<b>02/02/19 19:23:00</b>
Bordo: : (Nessun bordo)		
<b>Pagina 66: [111] Formattato</b>	<b>stefano federico</b>	<b>02/02/19 19:23:00</b>
Bordo: : (Nessun bordo)		
<b>Pagina 66: [112] Formattato</b>	<b>stefano federico</b>	<b>02/02/19 19:23:00</b>
Bordo: : (Nessun bordo)		
<b>Pagina 66: [113] Formattato</b>	<b>stefano federico</b>	<b>02/02/19 19:23:00</b>
Bordo: : (Nessun bordo)		
<b>Pagina 66: [114] Formattato</b>	<b>stefano federico</b>	<b>02/02/19 19:23:00</b>
Bordo: : (Nessun bordo)		
<b>Pagina 66: [115] Formattato</b>	<b>stefano federico</b>	<b>02/02/19 19:23:00</b>
Bordo: : (Nessun bordo)		
<b>Pagina 66: [116] Formattato</b>	<b>stefano federico</b>	<b>02/02/19 19:23:00</b>
Bordo: : (Nessun bordo)		
<b>Pagina 66: [117] Formattato</b>	<b>stefano federico</b>	<b>02/02/19 19:23:00</b>
Bordo: : (Nessun bordo)		
<b>Pagina 66: [118] Formattato</b>	<b>stefano federico</b>	<b>02/02/19 19:23:00</b>
Bordo: : (Nessun bordo)		
<b>Pagina 66: [119] Formattato</b>	<b>stefano federico</b>	<b>02/02/19 19:23:00</b>
Bordo: : (Nessun bordo)		
<b>Pagina 66: [120] Formattato</b>	<b>stefano federico</b>	<b>02/02/19 19:23:00</b>
Bordo: : (Nessun bordo)		

<b>Pagina 66: [121] Formattato</b>	<b>stefano federico</b>	<b>02/02/19 19:23:00</b>
Bordo: : (Nessun bordo)		
<b>Pagina 66: [122] Formattato</b>	<b>stefano federico</b>	<b>02/02/19 19:23:00</b>
Bordo: : (Nessun bordo)		
<b>Pagina 66: [123] Formattato</b>	<b>stefano federico</b>	<b>02/02/19 19:23:00</b>
Bordo: : (Nessun bordo)		
<b>Pagina 66: [124] Formattato</b>	<b>stefano federico</b>	<b>02/02/19 19:23:00</b>
Bordo: : (Nessun bordo)		
<b>Pagina 66: [125] Formattato</b>	<b>stefano federico</b>	<b>02/02/19 19:23:00</b>
Bordo: : (Nessun bordo)		
<b>Pagina 66: [126] Formattato</b>	<b>stefano federico</b>	<b>02/02/19 19:23:00</b>
Bordo: : (Nessun bordo)		
<b>Pagina 66: [127] Formattato</b>	<b>stefano federico</b>	<b>02/02/19 19:23:00</b>
Bordo: : (Nessun bordo)		
<b>Pagina 66: [128] Formattato</b>	<b>stefano federico</b>	<b>02/02/19 19:23:00</b>
Bordo: : (Nessun bordo)		
<b>Pagina 66: [129] Formattato</b>	<b>stefano federico</b>	<b>02/02/19 19:23:00</b>
Bordo: : (Nessun bordo)		
<b>Pagina 66: [130] Formattato</b>	<b>stefano federico</b>	<b>02/02/19 19:23:00</b>
Bordo: : (Nessun bordo)		
<b>Pagina 66: [131] Formattato</b>	<b>stefano federico</b>	<b>02/02/19 19:23:00</b>
Bordo: : (Nessun bordo)		
<b>Pagina 66: [132] Formattato</b>	<b>stefano federico</b>	<b>02/02/19 19:23:00</b>
Bordo: : (Nessun bordo)		
<b>Pagina 66: [133] Formattato</b>	<b>stefano federico</b>	<b>02/02/19 19:23:00</b>
Bordo: : (Nessun bordo)		
<b>Pagina 66: [134] Formattato</b>	<b>stefano federico</b>	<b>02/02/19 19:23:00</b>
Bordo: : (Nessun bordo)		
<b>Pagina 66: [135] Formattato</b>	<b>stefano federico</b>	<b>02/02/19 19:23:00</b>
Bordo: : (Nessun bordo)		
<b>Pagina 66: [136] Formattato</b>	<b>stefano federico</b>	<b>02/02/19 19:23:00</b>
Bordo: : (Nessun bordo)		
<b>Pagina 66: [137] Formattato</b>	<b>stefano federico</b>	<b>02/02/19 19:23:00</b>
Bordo: : (Nessun bordo)		
<b>Pagina 66: [138] Formattato</b>	<b>stefano federico</b>	<b>02/02/19 19:23:00</b>
Bordo: : (Nessun bordo)		
<b>Pagina 66: [139] Formattato</b>	<b>stefano federico</b>	<b>02/02/19 19:23:00</b>
Bordo: : (Nessun bordo)		
<b>Pagina 66: [140] Formattato</b>	<b>stefano federico</b>	<b>02/02/19 19:23:00</b>
Bordo: : (Nessun bordo)		





▼  
**Pagina 84: [155] Eliminato stefano federico 25/01/19 06:06:00**

▼  
**Pagina 84: [155] Eliminato stefano federico 25/01/19 06:06:00**

▼  
**Pagina 84: [155] Eliminato stefano federico 25/01/19 06:06:00**

▼  
**Pagina 84: [155] Eliminato stefano federico 25/01/19 06:06:00**

▼  
**Pagina 87: [156] Eliminato stefano federico 14/01/19 14:31:00**

▼